

Dear Editor,

Enclosed is a copy of the revised manuscript, “Spring net community production and its coupling with the CO₂ dynamics in the surface water of the northern Gulf of Mexico” by Jiang et al. In this revision, we have fully considered the comments and suggestions from both reviewers. A point-to-point response to the reviews is in the enclosure and a changes-tracked manuscript is also included.

With the agreement of all co-authors of the previous version of the manuscript, we added Najid Hussain, Michael K. Scaboo, Junxiao Zhang, and Yuanyuan Xu to the author list in the revised manuscript. They all attended the Gulf of Mexico cruise for data collection and also contributed to the preparation and revision of this manuscript. Najid measured the spectrophotometric DO onboard. Michael, Junxiao and Yuanyuan participated in collection and analysis of DIC and TA samples (see the author contributions section in the revised manuscript).

We thank you again for your consideration of this manuscript.

Sincerely,

A handwritten signature in black ink that reads "Zong-Pei Jiang". The signature is written in a cursive, slightly slanted style.

Zong-Pei Jiang

Ocean College, Zhejiang University

Zhoushan Campus, Zheda Road 1, Zhoushan, Zhejiang, China. 316021

Email: zpjiang@zju.edu.cn

Reviewer 1:

Major comments:

1. This manuscript contains a lot of data that a priori looks very good. Good comparison of the different methods can be done only in a particular area, while the rest of the data, mainly the pCO₂ and NCP from O₂/Ar, would be a good data set. In the section Methods there are a lot of explanation of how to arrive to the NCP calculations that can be found in the literature but very little is explained about replicates, average, and data quality controls or transformations (e.g. PQ to change from O₂ units to C units is missed)

Response: In the revised manuscript, the Methods section has been shortened by citing literatures for established NCP calculations and by removing unnecessary explanations. Relevant information has been added to explain the replicates, average, standard deviation, and data quality controls of the measurements. The transformations of the NCP units were described in the original manuscript (page 9, lines 17-18) and in the revised manuscript (page 9, line 20 to page 10, line 4).
2. The manuscript needs a little bit of more order to be able to read it fluid. Suggestions are made in the pdf attached.

Response: We sincerely thank the reviewer for the very detailed comments and suggestions which significantly improve our manuscript. Please see our responses to minor comments below.
3. Part of the discussion is based in differences between methods due to different stratified or mixed column states. I think the writer is interchanging "mixed layer" and "mixing column" concepts and making therefore wrong assumptions.

Response: In order to clearly show the different stratified or mixed water column states (as well as the different turbidity conditions), the vertical profiles at typical stations have been presented in the revised manuscript as the newly added figures in the supplement. In the nGOM, stratification was observed in the lower Mississippi river channel (Fig. S2) and in plume and offshore regions (Fig. S3) while well-mixed water column was observed in certain Atchafalaya coastal regions (Fig. S4).

We also discuss the influences of physical processes (vertical mixing and the lateral transport of the strongly net heterotrophic Mississippi and Atchafalaya river water) on NCP_{O₂Ar} estimation under different mixing conditions (section 4.1, Fig. 8). Depending on the different mixing conditions, NCP_{O₂Ar} reflected: 1) the combined result of NCP in the mixed layer (NCP_{M_LD}) and the lateral transportation of heterotrophic signal carried by the river water (NCP_{adv}) in the stratified river channel (Fig. 9a); 2) the combined result of water column production (NCP_{water}), benthic metabolisms (NCP_{benthic}), and NCP_{adv} in the well-mixed nearshore waters (Fig. 9b); 3) NCP_{M_LD} in the offshore stratified regions where the riverine influence was minor (Fig. 9c). We have revised the results and discussion sections to make these points clear to the readers.

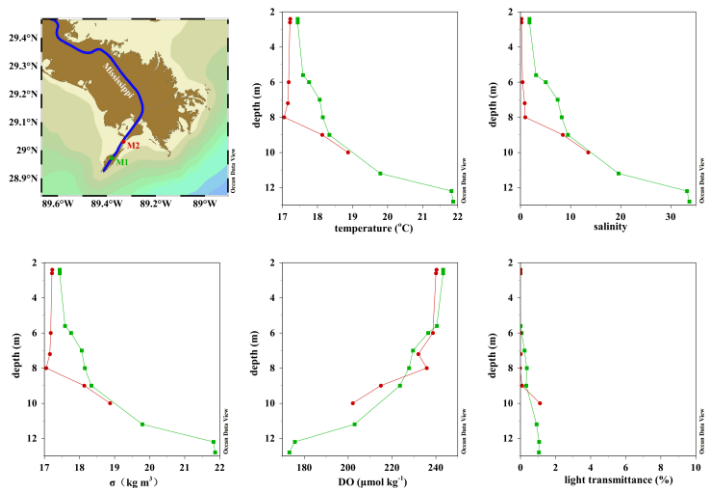


Fig. S2. Vertical profiles of (a) temperature, (b) salinity, (c) density anomaly, $\sigma = \text{density (kg m}^{-3}) - 1000$, (d) DO, (e) light transmittance in the lower Mississippi River channel. The different symbols correspond to the measurements from different sites shown in the map in the upper left corner.

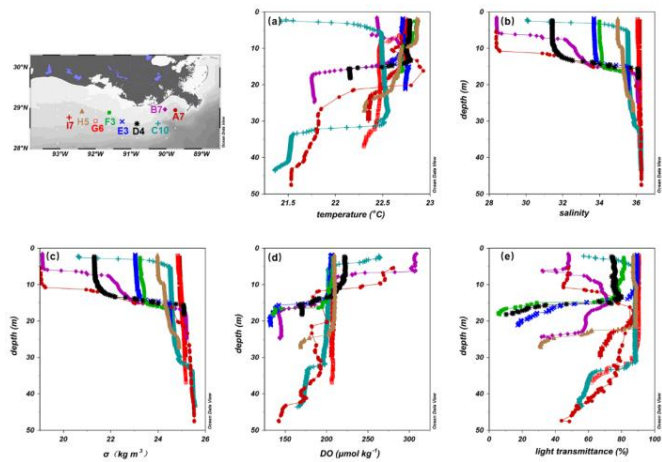


Fig. S3. Vertical profiles of (a) temperature, (b) salinity, (c) density anomaly, $\sigma = \text{density (kg m}^{-3}) - 1000$, (d) DO, (e) light transmittance at the stratified offshore region. The different symbols correspond to the measurements from different sites shown in the map in the upper left corner.

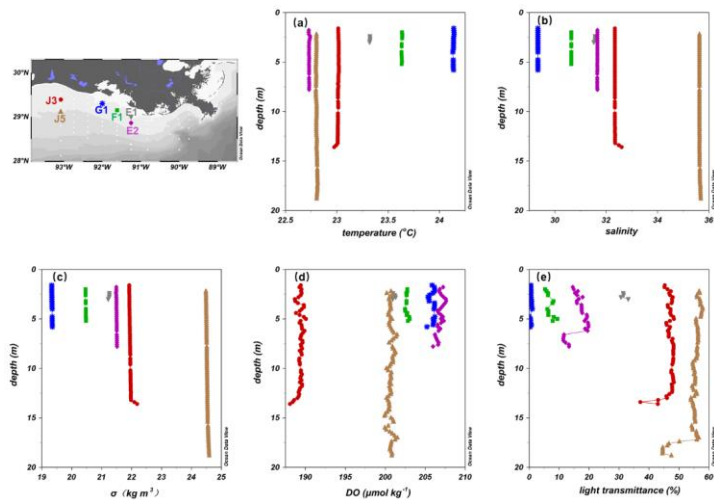


Fig. S4. Vertical profiles of (a) temperature, (b) salinity, (c) density anomaly, $\sigma = \text{density (kg m}^{-3}) - 1000$, (d) DO, (e) light transmittance in the well-mixed Atchafalaya coastal region. The different symbols correspond to the measurements from different sites shown in the map in the upper left corner.

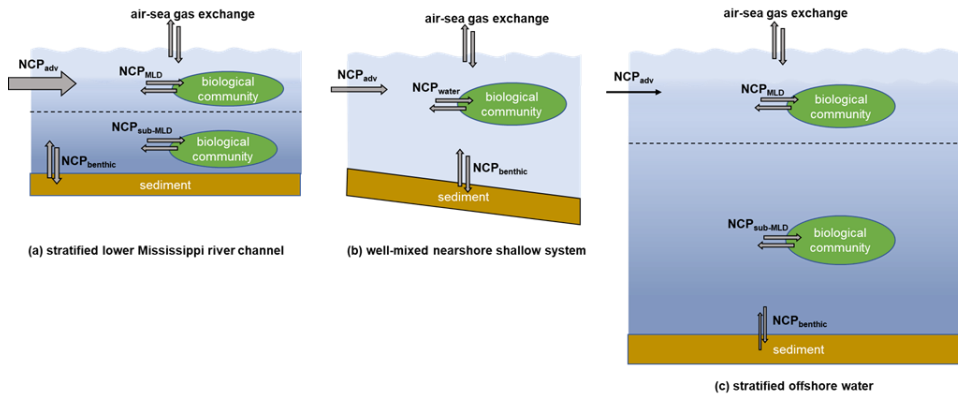


Fig. 9. The differences in water column mixing conditions in the nGOM and their influences on NCP estimation. The dotted lines in panels (a) and (c) indicate the mixed layer depth. In the stratified lower Mississippi River channel (a) and the offshore stratified system (c), $NCP_{DO-incub}$ equals the *in situ* community production in the mixed layer (NCP_{MLD}), while NCP_{O_2Ar} reflects the combined result of the NCP_{MLD} and the influence of lateral advection of the river water (NCP_{adv}). In the nearshore well-mixed shallow system (b), $NCP_{DO-incub}$ equals the water column community production (NCP_{water}), while NCP_{O_2Ar} reflects the combined result of NCP_{water} , $NCP_{benthic}$, and NCP_{adv} . Note that the influence of NCP_{adv} decreases offshore with the increasing water residence time.

4. Uncoupled O_2 and CO_2 fluxes and definition of sink or source of CO_2 can be the result of smoothing CO_2 values to a mean, but I cannot really tell without knowing the raw data. Also comments attached.
 Response: The O_2 and CO_2 fluxes were both calculated from high-resolution pCO_2 and DO data (1-minute average) from the continuous underway measurements. There was no smoothing of CO_2 values when discussing the uncoupled O_2 and CO_2 fluxes. These points have now been clearly stated in the Methods section in the revised manuscript.
5. Supplementary material of Figure S1. Is the data from the webpage only for the river discharge? This graph doesn't have x axis label. It should use dates instead and change consecutive numbers 1-12 to meaningful dates.
 Response: Both the river discharge and NO_x flux data were from the USGS (now explained in the figure caption of Fig. S1). The x axis label "month" has been added and the numbers 1-12 have been replaced by the meaningful dates "Jan, Feb, ...Dec" as suggested.
6. Supplementary material of Figure S2 (a,b) shows regression lines to show tendencies forced by few data points in the river. R^2 is not shown but is expected to be very low to use it.
 Response: This figure has now been moved to the main text as suggested by minor comment 44 below. The lines in this figure are conservative mixing lines (not regression lines) which demonstrate the changes of concentrations of DIC and

NO_x responding to the conservative mixing between river end member and seawater end member. We have clarified this in the revised figure caption as: “The end member concentrations of the Mississippi river, the Atchafalaya River, and offshore gulf surface water are shown in panels (a) and (b) together with the conservative mixing lines.”

Please also note the supplement to this comment:

<https://www.biogeosciences-discuss.net/bg-2019-88/bg-2019-88-RC1-supplement.pdf>

Minor comments:

1. Page 1, line 23 “use the same number of decimals for each number”
Response: Corrected as suggested.
2. Page 1, lines 27-28: “need to talk in the discussion about the “slow” air-sea gas exchange”
Response: In the revised manuscript, we now demonstrate the slow air-sea CO₂ exchange rate (compared to that of O₂) in the model simulation by calculating the re-equilibrium time for CO₂ and O₂ following a biological perturbation (Fig. S5). Both for the autotrophy and heterotrophy simulations, the re-equilibrium time for pCO₂ (more than one month) is significantly longer than that of O₂ (a few days). Because the slow air-sea CO₂ exchange rate is well-known in the carbonate system, we remove the original Figure 10 and add this new figure to the supplement according to the suggestion from reviewer 2 (minor comment 44).

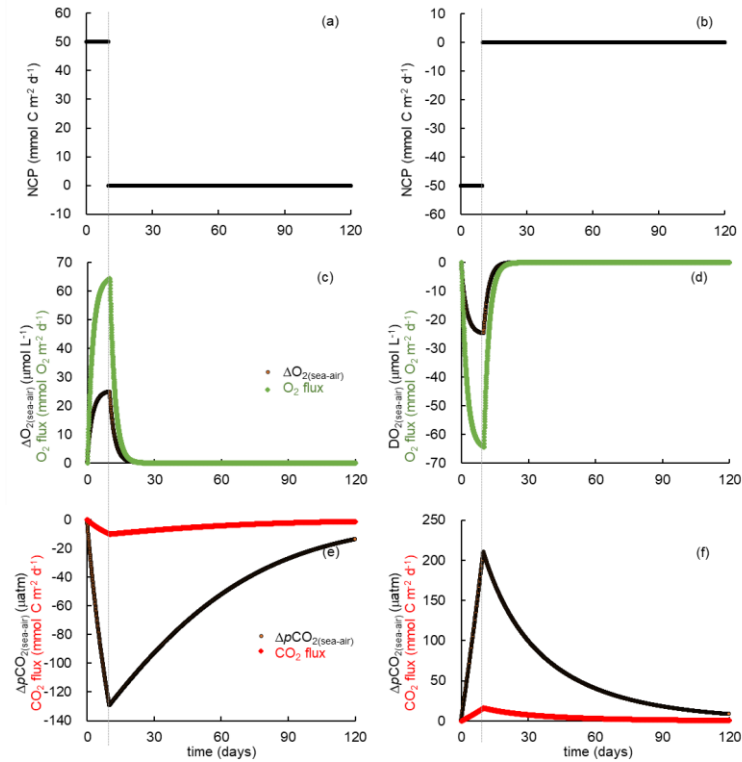


Fig. S5. Simulation of carbon and oxygen dynamics responding to NCP and gas exchange using a 1-D model. The system is assumed to be in equilibrium with the atmosphere on day 0, which is followed by a 10-day (a) autotrophic or (b) heterotrophic production. The variations in (c, d) O₂ flux and air-sea O₂ difference ($\Delta O_{2(\text{sea-air})}$) and (e, f) CO₂ flux and air-sea $p\text{CO}_2$ difference ($\Delta p\text{CO}_{2(\text{sea-air})}$).

3. Page 2, line 2: “reference”

Response: Corrected.

4. Page 3, line 14: “if it is the first time you use an acronym, define it”

Response: Corrected.

5. Page 3, line 19: AND SLOW air-sea exchange

Response: Revised as suggested.

6. Page 3, line 22: “I am struggling to place the sampling site on a map. Give reference context area in the map. show where the river is. From this map it doesn't seem to have a river but just coast line.”

Response: We have modified Figure 1 and its caption to better show the sampling sites as well as to highlight the Mississippi and Atchafalaya River.

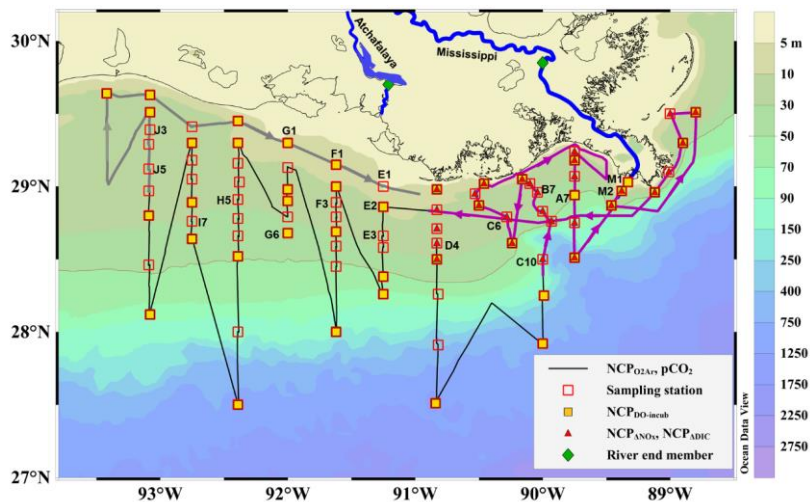


Fig. 1. Map and sampling sites in the northern Gulf of Mexico during the April 2017 cruise. The black dotted line is the cruise track along which the high-resolution underway measurements were made. The track in the Mississippi plume (purple line, 8-11 April) and in the Atchafalaya coastal regions (grey line, 15-17 April) are highlighted. Also shown are the 83 CTD sampling stations (hollow red squares), the 43 stations where light/dark bottle DO incubations were conducted (solid yellow squares), the 30 stations where non-conservative changes in DIC and NO_x were used to estimate NCP rates (solid red triangles), and the 2 stations where the properties of river end members were measured (solid green diamonds). The vertical CTD profiles of the labelled stations were shown in the supplement.

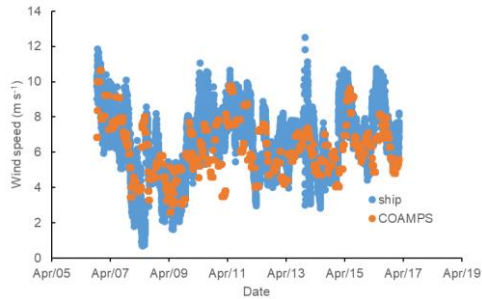
7. Page 3, line 23: “rephrase: ”at 83 sampling stations” at the end of the sentence”

Response: Revised as suggested.

8. Page 3, line 24: “active”

Response: Corrected.

9. Page 4, lines 1-2: “of what?”; “change and for a ”; “profiles or water column profiles”, “remove, you said the brand already in the sentence above”.
Response: This sentence has been revised to now state “Discrete water samples for DIC, TA, DO, and nutrients were collected from 3-12 depths depending on the bottom depth and vertical profiles of temperature, salinity and DO.”
10. Page 4, lines 7-8: “precision and accuracy are not the same thing, you can not give one value for both”, “? why do you cite? did you measure you own accuracy?”
Response: These sentences have been revised to now state “The precision of DIC and TA measurements were both 2 $\mu\text{mol kg}^{-1}$. DIC and TA measurements were calibrated, both with accuracy better than 0.1%, with certified reference materials provided by A. G. Dickson, Scripps Institution of Oceanography.”
11. Page 4, line 10: “include this two points in the map”
Response: These two sampling points have been included in the updated Fig. 1.
12. Page 5, line 11: “why air and not water equilibrated with air? Give reference of who does calibration with air.”; “the instrument precision needs to be calculated for your instrument, as it may differ from Cassar's equipment”
Response: The calibration of the O₂/Ar instrument was carried out according to an established method by measuring air as the atmospheric O₂/Ar is essentially constant (Cassar et al., 2009). We have added the reference for the calibration procedure and described the instrument precision as “As the atmospheric O₂/Ar is essentially constant relative to that in the surface water, calibrations of the O₂/Ar ion current ratio were conducted by sampling the ambient air every 3 hours through a second capillary (Cassar et al., 2009). The instrument precision estimated from the repeated measurements of atmospheric O₂/Ar ratio was 0.3%.”
13. Page 5, line 13: “Merge 2.3 and 2.4 and use subheadings for the different calculations.”
Response: As the NCP estimates involved several different methods and unit conversion, we think it is better to describe NCP in a separated section.
14. Page 5, line 20, “probably because COAMPS use the buoys data as well. What about the wind measured from the ship?”
Response: The COAMPS wind speed also agreed well with the ship measurement (see the figure below). As wind measured from the ship refers to instantaneous speed while biogeochemistry signals and air-sea flux change on a longer time scale, the daily averaged COAMPS wind speed is preferred in our study. Because the O₂ and CO₂ fluxes were calculated from the same wind speed, using COAMPS data or ship measurement won't affect the discussion on the relationship between O₂ and CO₂ fluxes.



Comparison between COAMPS wind speed and ship wind measurements

15. Page 5, line 23: “why? and what happen when sea values are close to 405? what % of the sea values where close to 405?”

Response: Paired $p\text{CO}_{2\text{seas}}$ and $p\text{CO}_{2\text{air}}$ are needed for the calculation of air-sea CO_2 flux (Eq. 1). In our study, the underway $p\text{CO}_2$ measuring system switched between the measurements of $p\text{CO}_{2\text{seas}}$ and $p\text{CO}_{2\text{air}}$. $p\text{CO}_{2\text{air}}$ was only measured every 3 hours in order to better capture the variability of $p\text{CO}_{2\text{seas}}$ and as $p\text{CO}_{2\text{air}}$ is not expected to change rapidly. “Comparing to the large variations in $p\text{CO}_{2\text{seas}}$ (110-1800 μatm), the variability of $p\text{CO}_{2\text{air}}$ was minor ($405 \pm 4 \mu\text{atm}$) so the $p\text{CO}_{2\text{air}}$ was set at the cruise average value of 405 μatm for the flux calculation.” This is a common practice for CO_2 flux calculation in the CO_2 community. When $p\text{CO}_{2\text{seas}}$ value is close to 405 μatm , the seawater is close to be equilibrium with the atmosphere and the CO_2 flux is close to zero.

16. Page 6, line 1: “define the term before saying how it was calculated”

Response: The definition of γ_{DIC} is “the $p\text{CO}_2$ buffer factor response to change in DIC”, so it has already been defined in this sentence. However, this variable (shown in the original Fig. 10) is not very useful in our discussion. It has now been removed from the revised manuscript as the original Fig. 10 (now Fig. 11) was revised without showing this variable.

17. Page 6, line 4: “it is not clear if you calculate oxygen fluxes from the optode, incubations?”

Response: The oxygen fluxes were calculated from the high resolution optode measurements (not from incubations). We have clarified this in the revised manuscript as: “ $\Delta\text{O}_{2(\text{sea-air})}$ is the difference between the seawater DO concentration from the calibrated underway optode measurement ($[\text{O}_2]_{\text{meas}}$) and the saturated DO concentration ($[\text{O}_2]_{\text{sat}}$) calculated from the measured sea surface temperature and salinity (Garcia and Gordon, 1992).”.

18. Page 6, line 8: “This section can be reduced by removing the majority of the explanatory equation, leaving only the main ones and citing the authors or papers where the equations are explained.”

Response: We have shortened this section as suggested.

19. Page 6, line 10: “you can simplify the subindex, no need to say write incub, it has been already explained.”
 Response: In order to make these variables readily understood in figure legend, we have chosen to keep the subindexes as they were originally described.
20. Page 6, line 13: “cite Craig and Hayward [1987]”; “you give details bellow. remove this part of the sence.”
 Response: Revised as suggested.
21. Page 6, line 14: “dissolved oxygen concentration in the surface water is affected by physical (e.g., changes in temperature, salinity and atmospheric pressure, bubble dissolution and/or injection) and biological processes (photosynthesis and respiration) (Fig 2).”
 Response: Revised as suggested.
22. Page 7, line 1: “how did you arrive to the equation? say something.”
 Response: This sentence has been revised to now state: “By measuring the biologically mediated oxygen supersaturation $\Delta(O_2/Ar)$ (Cassar et al., 2011; Craig and Hayward, 1987; Jonsson et al., 2013; Kaiser et al., 2005)...”
23. Page 7, line 4: “double check this this equation with Kaiser 2005 and Cassar 2011, I do not think it is totally correct.”
 Response: We confirmed that this equation is correct (see equations 1 and 3 in Cassar, 2011). According to minor comment 18, this explanatory equation has been removed and only one main equation is now presented in the revised manuscript: $NCP_{O_2Ar} = \text{bioflux} = k_{O_2} [O_2]_{\text{sat}} \Delta(O_2/Ar)$
24. Page 7, line 17: “you have to explain here how you passed from O2 units to C.”
 Response: The unit conversions of NCP estimates were described in the original manuscript (page 9, lines 17-18) and in the revised manuscript (page 9, line 20 to page 10, line 4).
25. Page 7, line 23: “what did you do with the dark ones?”
 Page 8, line 7: “you do not say how this samples where incubated.”
 Response: Change text to: “Clear and dark bottles were placed into a deck incubator screened at 50% of ambient sunlight for 24 hours. The deck incubator was plumbed with flowing seawater from the MIDAS system in order to maintain surface water temperatures.”
26. Page 8, line 3: “how many samples? SD of the spectrophotometric method etc?”
 Response: Clarified by adding the following “DO concentrations obtained from the LDO probe were verified by comparison to DO concentrations measured by the spectrophotometric method of Pai et al., (1993) in a subset of samples (n = 14). The mean difference between the two methods of $\pm 5\%$ was consistent with previous comparisons of probe measured versus Winkler measured DO based on several hundred comparisons (Murrell et al. 2013).”

27. Page 8, line 7: “Did you do it as somebody else who publish before? cite. $GPP=NCP-R$, not sure how you calculated GPP ”
Response: In our study, gross primary production ($\text{mmol O}_2 \text{ m}^{-3} \text{ d}^{-1}$) was calculated as $GPP = R_{D\text{Olight}} + |R_{D\text{Odark}}|$, where $R_{D\text{Olight}}$ is the change in DO in the light bottles during the 24-h incubation and is equivalent to NCP in these bottles, and $R_{D\text{Odark}}$ is the 24-h respiration-induced change in DO in the dark bottles. As $R_{D\text{Odark}}$ is negative, our equation $GPP = R_{D\text{Olight}} + |R_{D\text{Odark}}|$ is equivalent to $GPP = NCP - R$.
28. Page 8, line 15: “Integration calculation is different than for respiration. Need to justify it better or cite.”
Response: In our study, the respiration rate was assumed to be uniform in the mixed layer and the integrated respiration over the MLD (Resp_{int} , $\text{mmol O}_2 \text{ m}^{-2} \text{ d}^{-1}$) was calculated as $\text{Resp}_{\text{int}} = R_{\text{dark}} * \text{MLD}$. However, the gross primary production (GPP) varied with depth due to the reduction in light availability with increasing depth. To calculate the integrated GPP in the mixed layer (GPP_{int} , $\text{mmol O}_2 \text{ m}^{-2} \text{ d}^{-1}$), the GPP was scaled by the light environment in the MLD. We have clarified our calculation in the revised manuscript (page 8, lines 3-21).
29. Page 8, line 10: “NOT sure about this equation, please CITE does it comes from BEER-LAMBERT? PIERSON 2008?”
Response: Reference (Lohrenz et al., 1999) has been cited.
Lohrenz, S.E., Fahnenstiel, G.L., Redalje, D.G., Lang, G.A., Dagg, M.J., Whitedge, T.E. and Dortch, Q., 1999. Nutrients, irradiance, and mixing as factors regulating primary production in coastal waters impacted by the Mississippi River plume. *Continental Shelf Research*, 19(9), pp.1113-1141.
30. Page 9, line 17: “I couldn't access to the whole paper but looks like there are extensive studies of this river that may provide tau, for example: Lane, Robert R., et al. “Seasonal and Spatial Water Quality Changes in the Outflow Plume of the Atchafalaya River, Louisiana, USA.” *Estuaries*, vol. 25, no. 1, 2002, pp. 30–42. JSTOR, www.jstor.org/stable/1352905.”
Response: Although there were some previous studies on the Atchafalaya River (including the one provided by the reviewer), plume resident time for different salinity ranges were currently not available from the literature.
31. Page 10, line 2: “this figure needs to improve x axis”
Response: The x axis label “month” has been added and the numbers 1-12 have been replaced by the meaningful dates “Jan, Feb, ...Dec”.
32. Page 10, line 19: “the reader doesn't have to know where is Texas and you already said westward, remove Texas”
Response: Corrected.
33. Page 10, line 19: “from when is this data?”

Response: This sentence has been revised to state “The pattern of the Mississippi and Atchafalaya freshwater transport agreed well with the multiple-year average (2005-2010) condition in April by numerical simulation (Zhang et al., 2012).”

34. Page 11, line 1: “remove this”

Response: The repetitive word has been removed.

35. Page 11, line 4: “remove brand name”

Response: Corrected.

36. Page 11, line 8: “this should go up much earlier in the text! just before speaking about figure 5”

Response: Revised as suggested.

37. Page 11, line 24: “this can be due to sedimentation, more light than insitu”

Response: We fully agreed with the reviewer. In the revised manuscript, we have added vertical profiles of light transmittance in different regions (Figs. S2-S4) and discuss the potential bias in light/dark incubation method: “More importantly, for high-turbidity water samples (e.g., samples collected in the Mississippi River channel and in the HTACW), the incubated samples were not mixed in the same way as that in the natural environment and the sedimentation of particles in incubation bottles could alleviate the light limitation for phytoplankton. As a result, the gross primary production (GPP_m in Eq. 8) could be overestimated and $NCP_{DO-incub}$ would not represent the true *in situ* NCP in but high-turbidity waters but as an overestimation.” (page 14, lines 9-13).

38. Page 12, line 1: “subplots of figure 7 and 8 show the same information several times. It is confusing for the reader have to look at both. Choose one represent better what you are explaining and cite only one per time.”

Response: The original Fig. 7 (now Fig. 6) is chosen to present the Mississippi results.

39. Page 12, line 1: “instead of calling region 1 2 3 in the text and the graphs, call it by this headaings names, both in the text and in the graphs. remove the regions words

Response: Revised as suggested.

40. Page 12, line 2-3: “Fig 7a”; “give values in brackets”; “Fig 8a”;

Response: Revised as suggested.

41. Page 12, line 7: “only 8c”

Response: Revised as suggested.

42. Page 12, line 9: “choose”

Response: Corrected.

43. Page 12, line 8: “minus”
Response: Corrected.
44. Page 12, lines 16-18: “you have to explain this figure first. If it is important it should be a main figure and not as supplementary plot”; “number doesnt agree with figure”
Response: This figure has been moved to the main text and explained. Note that the numbers here are the deviations of DIC and NO_x from the conservative mixing lines but not the absolute concentrations. To clarify this, these sentences have been revised to now state “For both the Mississippi and Atchafalaya plume regions, the three end-member mixing model suggests that the enhanced biological production resulted in significant deviations of DIC and NO_x from their conservative mixing lines (Fig. 8). The amplitudes of the non-conservative biological removal of nutrients (up to 35 μmol kg⁻¹ in ΔNO_{xNCP}, Fig. 8a) and DIC (up to 250 μmol kg⁻¹ in ΔDIC_{NCP}, Fig. 8b) are similar to the findings of previous studies in the nGOM (Cai, 2003; Guo et al., 2012; Huang et al., 2012).”. Please also see the response to major comment 6.
45. Page 12, line 22: “you said before that chla was low in the Missisipi region. Here you say that Atchafalaya region is characterized by elevated Chla, but the values are lower than Missisipi region. You have to correct this.”
Response: Here we compared the observation results in the Atchafalaya plume with those in the Mississippi plume (both with elevated Chl-a concentrations in mid-salinity range). Note that low Chl-a concentrations were only observed in the lower Mississippi river channel.
46. Page 13, lines 2-6: “together”; “give numbers”
Response: Revised as suggested.
47. Page 13, line 22: “this graphs shows the MLD but without the sea bed depth we cannot know if there is stratification or not”
Page 13, line 25: “You just said above that the water column was stratified”; “if you said that it is mixed until the bottom, there is no separation between mixed layer and below, do not understand this sentence.”
Page 14, line 1: “I do not see why that would be add uncertainty. Mixed layer represent better fluxes because in contact with the atmosphere, but if the whole water column is mixed, then all water column is in contact with the atmosphere and that is not a bias”
Page 14, line 14: “if it is mixed layer what you sampled, everything is mixed, cannot be heterogeneity inside the mixed layer. You can test this from chla profiles for examples”
Response: Please see our responses to major comment 3.
48. Page 14, line 15: “I think one of the bias here may be the turbidity. If the incubated samples are not mixed in the same

way as natural water, the majority of the sediment probably sink to the bottom of the bottle and the light availability is bigger than in natural waters overestimating NCP.”

Response: Please see our response to minor comment 37.

49. Page 14, line 22: “Why are there errors when calculating MLD?”

Response: This sentence has been revised to now read “errors in estimating water residence time and the changes in MLD over the transit time of the plume water lead to proportional errors in the calculation of NCP_{ADIC} and NCP_{ANox} (Eq. 13 and Eq. 14)”.

50. Page 14, line 23: “IS THE CO_2 flux fast enough to cause this?”

Response: No, the CO_2 flux is generally small compared to NCP (< 10% in most reports); but O_2 flux is nearly the same as NCP. In the revised manuscript, the DIC changes induced by air-sea CO_2 exchange has been considered in calculating the biological-induced changes in DIC (Eq. 8).

51. Page 15, line 3: “here is the only place were you have the four methods. Why in figure 4 seems to agree better than in figure 8? why there are more data point in this figures than sampling point?”

Response: The NCP data presented in the original Fig. 4 and Fig. 8 were the same dataset and the numbers of data points in these two figures were identical to the sampling sites shown in Fig. 1 ($n = 43$ for $NCP_{DO-incub}$, $n = 30$ for NCP_{ADIC} and NCP_{ANox}). These data were more evenly distributed along with time in Fig. 4 but were clustered in the salinity range of 25-30 in Fig. 8.

52. Page 15, line 10: “this can be due to the bottle incubation method that may have exclude grazers. Did you do replicates? how was your standar deviation? if big that would be a reason”

Response: Grazers might be a factor which affected the bottle incubation. “The standard errors of $NCP_{DO-incub}$ from triplicate bottle incubations across all sites were on average about 16 % of the mean.” (page 8, line 21)

53. Page 15, line 11: “you are contradicting again yourself here. If the water column is well mixed, there is not stratification and therefore no mixed layer and pycnocline.”

Response: This comment has been taken. In the well-mixed water column, there is no stratification and mixed layer and our measurements reflect the water column NCP rate (Fig. 9b). We have corrected this throughout the manuscript.

54. Page 15, line 16: “there can be understimation if euphotic depth is deeper than mixed layer, but if you took all your four methods at the same depths, there is no bias in the comparison of the methods”

Response: We agree with this comment. As the samples for the four methods were all collected in the surface water, the production beneath the pycnocline did not result in bias in the comparison if no upwelling occurred. This sentence has been deleted.

55. Page 15, line 24: “that could be a result of”
Response: Corrected.
56. Page 16, line 7: “Did you explained anywhere that the values has been averaged? and why?”
Response: There is an ecological gradient along the river-ocean mixing continuum in the Mississippi plume: from high nutrient and turbid freshwater to clear, oligotrophic offshore oceanic waters. Data were averaged over increments of two salinity units in Figure 7 to better present the variations along the increasing salinity. We now explain this both in the main text and in the figure caption.
57. Page 16, lines 11-15: “I do not understand this sentence. Do you mean it was heterotrophic in the river and autotrophic at higher salinities? “; “could be. You didnt measured benthic respiration so you can only use hypotheses”
Response: As the water column in the lower Mississippi River channel was stratified (Fig. S2), benthic respiration had minor contribution to affect the NCP_{O_2Ar} in the mixed layer. Whereas, the advection could play a significant role influencing the surface NCP_{O_2Ar} signal in the Mississippi River channel due to the short water residence times. In the revised manuscript, the heterotrophy in the lower Mississippi River channel suggested by the negative NCP_{O_2Ar} were discussed in Section 4.1. “In the stratified lower Mississippi River channel (Fig. 9a), the influence of lateral transportation of the heterotrophic river water from the upper river channel was significant because of the short water residence time (~1 day, Green et al., 2006). Therefore, the heterotrophic condition in the lower Mississippi River channel could be attributed to the dominant influence of the heterotrophic NCP_{adv} over the local biological production.” (page 16, lines 4-15).
58. Page 16, line 11: “minus”
Response: Corrected.
59. Page 16, line 23: “You can find this explained in Seguro et al 2015 (The presence of a chl a peak in the middle of the inner part, after the salt wedge, is a typical feature of stratified and partially stratified estuaries (Voorhis et al., 1983; Collins and Williams, 1981; Humborg et al., 1997; Cloern et al., 2013). This happens because the decrease in turbidity allows a deeper photic layer than the mixing layer in the middle of the estuary (Sverdrup, 1953) where high concentrations of inorganic nutrients are still available (Figs. 3 and 5).)”
Response: Thanks for pointing out this. These references have been added.
60. Page 17, line 17: “you have to explain this graph first, what is the meaning of each quadrant”
Page 17, lines 17-21: there is a blue shadow in the text...which is coincident with an statement that said that both plumes have opposite patterns. I disagree, opposite patterns would be one plume in quadrant 4 and another in quadrant 2 or 3 and 1”; “this sentence is not clear”; “I think the author was trying to speak about Mississippi plume and HTACW?”
Response: We do agree with the reviewer that quadrant 4 and 2 (or 3 and 1) show the opposite pattern. This figure is explained and discussed in the revised manuscript as: “When plotting the paired CO_2 flux and NCP_{O_2Ar} data (Fig. 10),

most data collected in the lower Mississippi River channel fall in quadrant 2 suggesting net heterotrophy coupled with CO₂ outgassing to the atmosphere. The Mississippi plume and Atchafalaya plume exhibited opposite patterns with most data in these regions being in quadrant 4 (net autotrophy coupled with CO₂ uptake from the atmosphere). However, the data in quadrant 1 (autotrophic water as a CO₂ source observed near the Mississippi estuary) and quadrant 3 (heterotrophic water as a CO₂ sink in the HTACW) suggest decoupling between NCP_{O₂Ar} and CO₂ flux.” (page 18, lines 17-22)

61. Page 18, line 2: “i THINK THIS DISCUSSION would benefit from including the different residence times of CO₂ and O₂, as degassing would not occur at the same speed because of different solubilities of o₂ and co₂.”
Response: Please see the response to minor comment 2.
62. Page 18, line 10: “I would add this to the M & M section”
Response: The model description has been moved to the Methods section as suggested.
63. Page 19, line 17: “As explained abpve, I do not agree with this”
Response: See the response to major comment 3.
64. Page 25, line 20: “several typos”
Response: Corrected.
65. Page 27, line 9: “purple line”; “blue line”
Response: Corrected.
66. Page 31, line 2: “It is not clear how figure a and b has been created. Why region 3 is close to 0 in one plot but high numbers in the other? and the same happen with regions 1 and 2. If there is no data, the regions should be white colour.”
Response: This figure presented the results of the three end-member mixing model showing the composition of the surface water. Panel (a) showed the fractional contribution of the Mississippi River end member and higher values indicated more significant influence of the Mississippi plume. The same applied to panel (b) for the Atchafalaya River end member. In the revised manuscript, we removed the original panels (c) and (d) according to the major comment 8 by reviewer 2. Instead, we presented the fractional contribution of the offshore surface water end member in the updated panel (c) to better show the results of the three end-member mixing model (see the figure below).

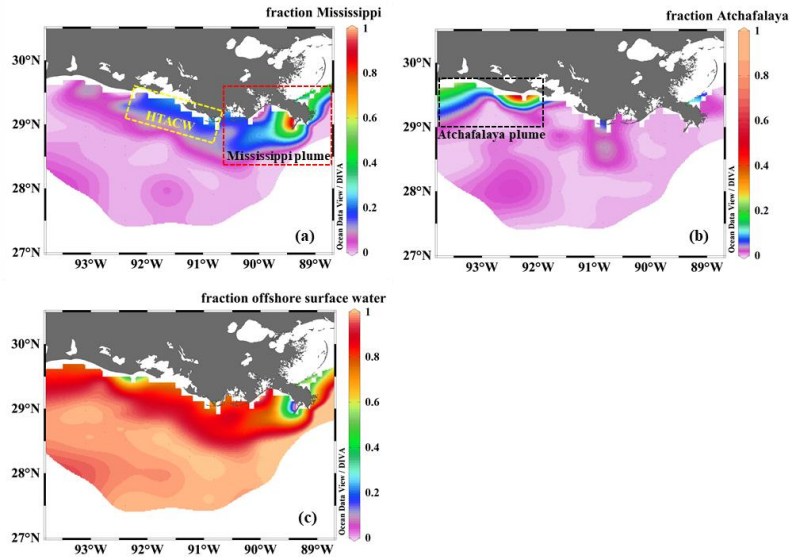


Fig. 4. The fractional contribution of (a) the Mississippi River, (b) the Atchafalaya River, and (c) offshore surface water to the surface water of the nGOM estimated from the three end-member mixing model. The sub-regions shown in panels (a) and (b) are the Mississippi plume, the high-turbidity Atchafalaya coastal water (HTACW), and the Atchafalaya plume.

67. Page 34, line 2: “would it be possible to put the coloured boxed underneath? if not, just finish the box before covering the labels at the bottom, at the end of the y axis.”

Response: Revised as suggested.

68. Page 34, line 2: “, CO2 flux and NCP O2/Ar”

Response: Corrected.

69. Page 34, line 4: “why?”

Response: See the response to minor comment 56.

70. Trying to be consistent in the symbols and colours of Figure 7, seems that you accidentally exchanged the colour and symbol of two regions.

Response: The figure legend has been corrected.

References Cited:

- Cai, W. J. 2003. Riverine inorganic carbon flux and rate of biological uptake in the Mississippi River plume. *Geophysical Research Letters* **30**(2).
- Cassar, N., B. A. Barnett, M. L. Bender, J. Kaiser, R. C. Hamme, and B. Tilbrook. 2009. Continuous high-frequency dissolved O₂/Ar measurements by equilibrator inlet mass spectrometry. *Analytical Chemistry* **81**: 1855-1864.
- Cassar, N., P. J. Difiore, B. A. Barnett, M. L. Bender, A. R. Bowie, B. Tilbrook, K. Petrou, K. J. Westwood, S. W. Wright, and D. Lefevre. 2011. The influence of iron and light on net community production in the Subantarctic and Polar Frontal Zones. *Biogeosciences* **8**: 227-237.
- Guo, X., W.-J. Cai, W.-J. Huang, Y. Wang, F. Chen, M. C. Murrell, S. E. Lohrenz, L.-Q. Jiang, M. Dai, J. Hartmann, Q. Lin, and R. Culp. 2012. Carbon dynamics and community production in the Mississippi River plume. *Limnology and Oceanography* **57**: 1-17.
- Huang, W. J., W. J. Cai, R. T. Powell, S. E. Lohrenz, Y. Wang, L. Q. Jiang, and C. S. Hopkinson. 2012. The stoichiometry of inorganic carbon and nutrient removal in the Mississippi River plume and adjacent continental shelf. *Biogeosciences* **9**: 2781-2792.
- Jonsson, B. F., S. C. Doney, J. Dunne, and M. Bender. 2013. Evaluation of the Southern Ocean O₂/Ar-based NCP estimates in a model framework. *Journal of Geophysical Research-Biogeosciences* **118**: 385-399.
- Kaiser, J., M. K. Reuer, B. Barnett, and M. L. Bender. 2005. Marine productivity estimates from continuous O₂/Ar ratio measurements by membrane inlet mass spectrometry. *Geophysical Research Letters* **32**.
- Lohrenz, S.E., Fahnenstiel, G.L. and Redalje, D.G., 1994. Spatial and temporal variations of photosynthetic parameters in relation to environmental conditions in coastal waters of the northern Gulf of Mexico. *Estuaries*, 17(4), pp.779-795.
- Lohrenz, S.E., Fahnenstiel, G.L., Redalje, D.G., Lang, G.A., Dagg, M.J., Whitledge, T.E. and Dortch, Q., 1999. Nutrients, irradiance, and mixing as factors regulating primary production in coastal waters impacted by the Mississippi River plume. *Continental Shelf Research*, 19(9), pp.1113-1141.
- Murrell, M. C., and Lehrter, J. C. 2011. Sediment and lower water column oxygen consumption in the seasonally hypoxic region of the Louisiana Continental Shelf. *Estuaries and Coasts*, 34, 912-924.
- Murrell, M. C., Stanley, R. S., Lehrter, J. C., and Hagy, J. D. 2013. Plankton community respiration, net ecosystem metabolism, and oxygen dynamics on the Louisiana continental shelf: Implications for hypoxia, *Cont. Shelf Res.*, 52, 27-38, <https://doi.org/10.1016/j.csr.2012.10.010>.
- Zhang, X. Q., R. D. Hetland, M. Marta-Almeida, and S. F. Dimarco. 2012. A numerical investigation of the Mississippi and Atchafalaya freshwater transport, filling and flushing times on the Texas-Louisiana Shelf. *Journal of Geophysical Research-Oceans* **117**(C11).

Reviewer 2:**General comment:**

The authors present results of Net Community Production (NCP) in waters of the northern Gulf of Mexico system which includes a portion of the downstream Mississippi and Atchafalaya rivers, and the continental shelf where these rivers discharge in the Gulf of Mexico. The NCP was estimated through four different methods: continuous O₂/Ar measurements, light/dark bottle incubations, DIC and NO_x measurements. The authors also analyzed the relation between the NCP and pCO₂ measurements to complete a picture in the metabolic state of the northern Gulf of Mexico (nGOM). The measurements were done during spring and summer in 2017 at an extensive network of stations sampled in vertical profiles and in continuous underway measurements along the ship track. The authors discuss the difference between the results from the different methods to estimate NCP. Their results show that during the sampling period and along the surveyed areas, the river headwaters are heterotrophic, while autotrophy (signaled by the highest measured NCP) characterized the continental shelf. With a 1-D model, the authors demonstrated a temporal mismatch between the estimated gas exchange and biological production, i.e. due to a decoupling between CO₂ fluxes and NCP, at the time of the measurements, and this could be related to the presence of pCO₂ transported from headwaters identified in areas where local productivity hints to dominant heterotrophy. The results of this work are interesting because the authors combine the traditional pCO₂ measurements to NCP values to better understand the metabolism of the Gulf of Mexico shelf system.

Unfortunately, I find that the quality of the presentation of results, as well as the text itself lacks scientific rigor. The authors make a big effort on trying to explain the results and make use of assumptions that were not really proven by their results (such as the presence of benthic respiration to justify NCP-water column integrated heterotrophy) and make no effort to investigate further the role of physical factors. At this stage, I cannot recommend this manuscript for publication in Biogeosciences. I list major and minor comments in a supplementary pdf aiming to provide a more detailed review. I recommend the authors to consider these comments if they think they might be useful to improve their work.

Please also note the supplement to this comment: <https://www.biogeosciences-discuss.net/bg-2019-88/bg-2019-88-RC2-supplement.pdf>

Response: We sincerely thank the reviewer for pointing out the weaknesses of our original manuscript and providing constructive comments and suggestions, which significantly improve the quality of this manuscript. In the revised manuscript, we present vertical profiles at typical stations (the newly added Figs. S2-S4 in the supplement) to better describe the different stratified or well-mixed mixing conditions. The influences of physical processes including vertical mixing and lateral advection on the NCP estimated from different methods are discussed (see the response to major comment 5 and section 4.1 in the revised manuscript). Aside from the uncertainties and errors of different methods, we showed that the contrasting results of different methods can be mainly explained by the different spatial and temporal scales associated with these methods responding to the mixing conditions. In addition, we have revised the manuscript throughout to improve English and scientific rigor according to the detailed suggestions from both reviewers.

Review for manuscript bg-2019-88

“Spring net community production and its coupling with the CO₂ dynamics in the surface water of the northern Gulf of Mexico” by Jiang et al.

Major comments:

1. The manuscript will benefit greatly by going through a thorough revision on the English language. I am myself not a native speaker, but I can still identify many mistakes in the wording, spelling mistakes, punctuation, etc. I list some examples in the minor comments, but the mistakes are so many that it is impossible to correct all through this review. In this context, the authors also make use several times of subjective terms without giving quantities to justify, e.g. “moderate”, “rapid”, “deeper”, “higher”. These words should be avoided or accompanied by a quantity to reference the use of the adjective.

Response: A thorough revision on the English language has been done by our coauthors who are native English speakers. Subjective terms have been avoided or accompanied by quantities as suggested.

2. The aims of the manuscript are not clearly stated. On the one hand, they aim to compare NCP estimates from four different methods, and on the other hand, they aim also to compare the relation NCP vs. pCO₂ in the area of study. But I think before aiming the second, they should clearly state early in the manuscript what is the purpose of comparing NCP from different methods? What is the gain and need of doing so?

Response: The main purpose of this manuscript is to better understand the spatial variability of NCP and pCO₂ in the nGOM and to investigate the relationship between NCP and CO₂ flux. Previous NCP studies in our study region have been mainly based on the light/dark incubation and non-conservative changes in DIC and NO_x. However, the detailed relationship between NCP and CO₂ dynamics remains unclear because of the low spatial resolution of the conventional NCP measurements based on discrete samples. To our knowledge, this work is the first attempt to obtain high-resolution NCP_{O₂/Ar} estimates from continuous O₂/Ar measurement in the nGOM. We thus compared the O₂/Ar result to those from the existing methods to evaluate the consistency of NCP estimates from various methods. Meanwhile, each of the methods have different advantages and shortcomings. By making NCP estimates using the different methods we can get a more robust understanding of the overall metabolism of the system. In the revised manuscript, the purpose of comparing NCP from different methods has been better described in the introduction section and improved method comparisons have been presented in section 4.1.

3. The authors list in the discussion section (Pag. 13-14), mostly the disadvantages of applying the different methods for NCP determination. After reading all these disadvantages and limitations in each method, I see difficult to justify a comparison between these methods at all and making this as one of the main aims for this study. Further, the comparison between the four methods for NCP estimates was also done in only few stations. The authors finally compare the NCP_{O₂/Ar} vs pCO₂ because both have high spatial resolution, hence proving that the methods comparison done in this work does not contribute substantially to the results presented in this work.

Response: As previous estimates of NCP for this shelf have mainly been based on light/dark incubations and non-conservative changes in DIC or nutrients, we think it is important to understand how the high spatial resolution NCP_{O₂/Ar} and the existing methods compare. Similar comparison of NCP estimated from multiple approaches has been carried out by Ulfsbo et al., (2014) in the central Arctic Ocean. Although uncertainties are associated with different approaches and

there was a high variability in NCP over our studied area, we found encouraging agreement among these methods showing elevated NCP rates in the plume regions. In the revised manuscript, we further discussed how different mixing conditions affected the NCP rates estimated from different methods. The DO incubation method represents the NCP by the local plankton community while the O₂/Ar method reflects the metabolic state of the water relating to both biological and physical processes. The comparison of different methods provides us with additional information about the metabolism of the system that is greater than the sum of the individual methods, especially for the regions where their results contrasted (e.g., in the lower Mississippi river channel and in the high-turbidity Atchafalaya water). Please see the revised section 4.1 for details.

4. The methods section lacks of detail and scientific rigor in many parts:

a) the authors do not show the vertical resolution of the sampled profiles, why they were not done at the same standard depths within each max. depth of the water column?

Response: Bottom depth varied significantly in our study region from nearshore (a few meters) to offshore (a few thousand meters). As a result, discrete water samples were taken from 3-12 depths depending on the bottom depth and the vertical structures of temperature, salinity and O₂. We sampled standard depths at offshore stations with bottom depth deeper than 200 m. In the nearshore and shelf region, standard depths were preferred but sometime we collected samples at non-standard depths to better characterize the vertical variability. Meanwhile, this study focused on the surface water and the samples for NCP and pCO₂ were all collected within the MLD: samples for NCP_{O₂Ar} and pCO₂ were collected from the underway system at a depth of ~2.5 m, while the discrete samples used to derive NCP_{DO-incub.}, NCP_{ADIC} and NCP_{ANO_x} were collected from the Niskin bottles at ~1.5 m.

b) No mention of duplicate or uncertainties analysis.

Response: Information on precision and uncertainties analysis has now been added.

c) How often were the pCO₂ measurements calibrated? (it is only stated regularly)

Response: Clarified as “The pCO₂ measurement was calibrated **twice daily** against 3 certified gas standards (150.62, 404.72, and 992.54 ppm) and has a precision of 0.1 μatm and an accuracy of 2 μatm.”

d) Overall the way they are written are all over the place and not rigorously written

Response: We have revised the methods section thoroughly to improve scientific rigor.

e) There is no sufficient rigor on writing the equations, e.g. one should not include the units in the equation itself but rather in the text when explaining the variables.

Response: Equations have been revised as suggested.

5. The authors did not show vertical profiles to evidence their claim that most of the sampled water columns were well mixed. Also, they mention that there is a strong stratification due to buoyancy of the fresher river water plume above the oceanic shelf water. I find hard to believe that it is justifiable to assume steady state in the NCP_{O₂Ar} determination. At least, the contribution of horizontal processes into the shelf O₂ budget should have been investigated. I think the authors fall short here by simply assuming steady state, particularly after several works have proven in the past that physical contributions during this method must be considered at best. A great scientific contribution would be for the authors to

provide an effort on quantifying the influence of horizontal processes into the NCP by O₂/Ar measurements.

Response: We sincerely thank the reviewer for pointing out the importance of physical influences on the NCP

estimation. The typical vertical profiles for well-mixed and stratified systems have now been added as supplemental figures (Figs. S2-S4). Most of our study regions were characterized by stratification (in the lower Mississippi river channel, Fig. S2 and in the plume and offshore regions, Fig. S3), while well-mixed water column was observed in limited nearshore waters in the Atchafalaya coastal region (Fig. S4).

In the revised manuscript, we present a new figure (Fig. 9) to show the differences in water column mixing conditions in the nGOM and their influences on NCP estimation. The influences of physical processes (lateral advection and vertical mixing) have now been discussed in section 4.1 in the revised manuscript and are briefly summarized as follow:

The DO incubation method is a direct measurement of NCP by plankton community and this method is free from the influences of lateral advection and sediment metabolism. The NCP_{DO-incub} thus equals the MLD-integrated NCP in the stratified regions (NCP_{MLD} in Fig. 9a, c) or the water column-integrated NCP in the well-mixed regions (NCP_{water} in Fig. 9b). In the stratified regions, the influences of sub-pycnocline (NCP_{sub-MLD} in Fig. 9a, c) and benthic metabolisms (NCP_{benthic} in Fig. 9a, c) on the surface O₂/Ar ratio were expected to be minor. On the contrary, the surface O₂/Ar ratio in the well-mixed nearshore regions (e.g., the HTACW, Fig. S4) was affected by the water column NCP_{water} as well as the NCP_{benthic} contributed by benthic metabolism (Fig. 9b). Moreover, both Mississippi and Atchafalaya river end members were highly heterotrophic and the lateral transportation of heterotrophic signal carried by the river water (NCP_{adv} in Fig. 9) should be considered. Therefore, NCP_{O₂Ar} reflects the combined result of the NCP_{MLD} and NCP_{adv} in the stratified region, and it reflects the combined result of NCP_{water}, NCP_{benthic}, and NCP_{adv} in the nearshore well-mixed shallow system. As NCP_{benthic} only affected a small portion of the nearshore water in the Atchafalaya coastal region, the NCP_{O₂Ar} measured in this study was mainly modulated by NCP_{MLD} and NCP_{adv}. Considering the nGOM as a whole, lateral advection of NCP_{adv} can be considered as internal transport within the system given that the NCP_{O₂Ar} was measured with adequate spatial coverage. As a result, the NCP_{O₂Ar} measured in this study well represented the overall metabolic state of the surface water of the nGOM.

We also explained why NCP_{DO-incub} and NCP_{O₂Ar} provided contrasting results in the Mississippi River channel and in the HTACW (see our responses to major comment 7 below).

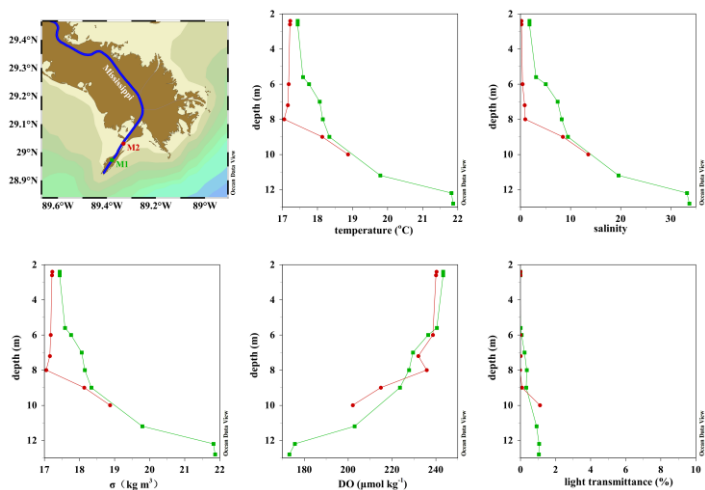


Fig. S2. Vertical profiles of (a) temperature, (b) salinity, (c) density anomaly, $\sigma = \text{density} (\text{kg m}^{-3}) - 1000$, (d) DO, (e) light transmittance in the lower Mississippi River channel. The different symbols correspond to the measurements from different sites shown in the map in the upper left corner.

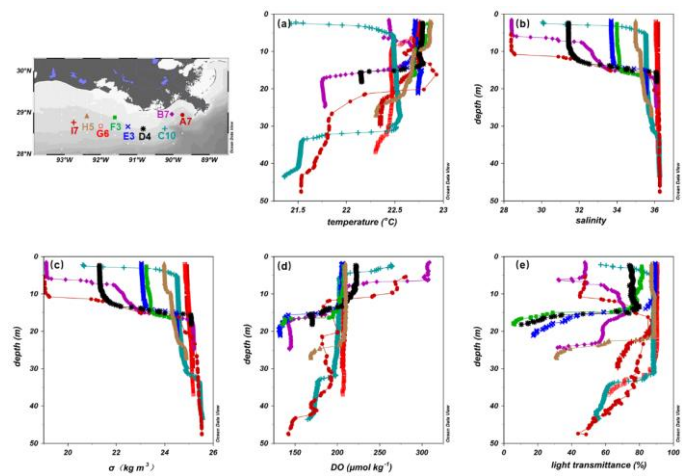


Fig. S3. Vertical profiles of (a) temperature, (b) salinity, (c) density anomaly, $\sigma = \text{density (kg m}^{-3}) - 1000$, (d) DO, (e) light transmittance at the stratified offshore region. The different symbols correspond to the measurements from different sites shown in the map in the upper left corner.

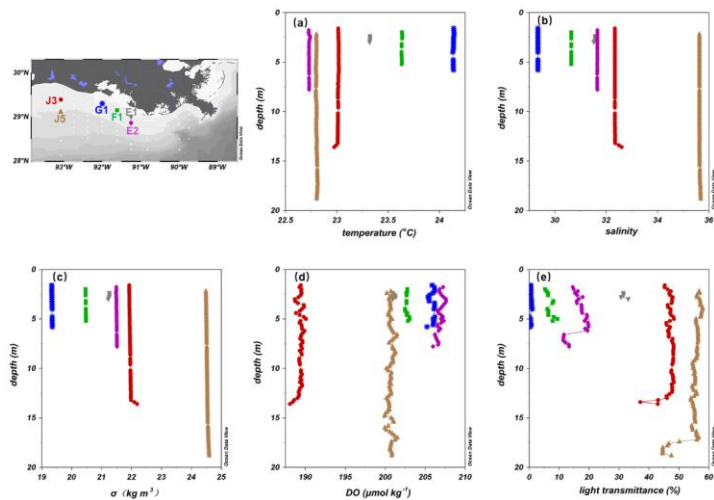


Fig. S4. Vertical profiles of (a) temperature, (b) salinity, (c) density anomaly, $\sigma = \text{density (kg m}^{-3}) - 1000$, (d) DO, (e) light transmittance in the well-mixed Atchafalaya coastal region. The different symbols correspond to the measurements from different sites shown in the map in the upper left corner.

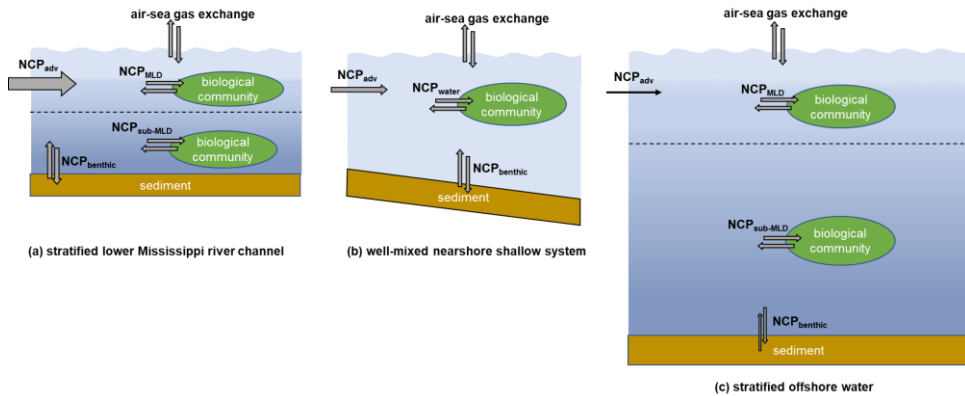


Fig. 9. The differences in water column mixing conditions in the nGOM and their influences on NCP estimation. The dotted lines in panels (a) and (c) indicate the mixed layer depth. In the stratified lower Mississippi River channel (a) and the offshore stratified system (c), $NCP_{DO-incub}$ equals the *in situ* community production in the mixed layer (NCP_{MLD}), while NCP_{O2Ar} reflects the combined result of the NCP_{MLD} and the influence of lateral advection of the river water (NCP_{adv}). In the nearshore well-mixed shallow system (b), $NCP_{DO-incub}$ equals the water column community production (NCP_{water}), while NCP_{O2Ar} reflects the combined result of NCP_{water} , $NCP_{benthic}$, and NCP_{adv} . Note that the influence of NCP_{adv} decreases offshore with the increasing water residence time.

- During the preparation of samples for the $NCP_{DO-incub}$, the authors mention that after initial measurement of DO, there was a compensation of volume in the incubation bottle by adding an extra volume of water. I find this problematic, by doing this there is introduction of DO from the new added water volume to the sample, hence it will change the initial measured DO conditions. By looking at the results of those 3 stations in the Mississippi river channel (results mentioned in P11, L21-23), it looks like while NCP_{O2Ar} resulted in negative values, the $NCP_{DO-incub}$ showed positive values, and I wonder how much of that difference is rather the influence of the addition of DO by the volume compensation? Are those the same three points shown in Fig. 4c of the Mississippi plume with high $NCP_{DO-incub}$ values? Also, consistently $NCP_{DO-incub}$ is higher than NCP_{O2Ar} also for the Atchafalaya plume. Indeed, incubation methods tend to bias the result due to a lack of homogeneity in the collected sample, and the authors should discuss these differences in the context of methods comparison. However, the introduction of a volume of water has another connotation, hence, I have no reason to trust the $NCP_{DO-incub}$ results and believe in these differences and going further discussing potential heterotrophy and autotrophy.

Response: The addition of DO was not corrected because the replacement volume (~ 3 ml) represents on average about 1% of the incubation volume (300 ml) and the addition of any O_2 in the replacement water was negligible. Even in an extreme case, for example a DO concentration of 0 in the bottle and 200 mmol m^{-3} in the replacement volume, the addition of the replacement water would change the DO in the bottle by 2 mmol m^{-3} , which is near the detection limit for this method of $\sim 2 \text{ mmol m}^{-3} \text{ d}^{-1}$ (Murrell et al. 2013). Another previous study with this method also found the correction was negligible (Murrell et al., 2009). The high values of $NCP_{DO-incub}$ reported in Fig. 4c are much greater

than the potential bias introduced by the replacement volume. We have revised the method description to clarify this: “The addition of DO to the bottle from the replacement water was considered small, on the order of the method detection limit of approximately $2 \text{ mmol m}^{-3} \text{ d}^{-1}$ (Murrell et al. 2009; 2013)”.

7. Further, they argue that in the Mississippi river channel the $\text{NCP}_{\text{O}_2/\text{Ar}}$ showed heterotrophy which is dominated by benthic respiration, and results of $\text{NCP}_{\text{DO-incub}}$ showed autotrophy. While it is true that the method with O_2/Ar measurements integrates the results in the mixed layer, it is based in surface measurements (one point in the vertical column), just as in the $\text{NCP}_{\text{DO-incub}}$. Unless benthic respiration is truly proven, the negative NCP values can well be the result of turbulent horizontal or vertical mixing, hence encouraging the method to include physical factors.
- Response: Many thanks to the reviewer for pointing out this mistake. A detailed examination of the data in the lower Mississippi river channel suggests that the water column was stratified rather than well-mixed (Fig. S4). The measured community respiration rates in the lower Mississippi River channel ($14.0 \pm 0.8 \text{ mmol C m}^{-2} \text{ d}^{-1}$) and in the HTACW (30.5 ± 10.7 and $\text{mmol C m}^{-2} \text{ d}^{-1}$) were not able to fully account for the heterotrophy suggested by $\text{NCP}_{\text{O}_2/\text{Ar}}$ ($-51.3 \pm 11.9 \text{ mmol C m}^{-2} \text{ d}^{-1}$) even when the GPP was not taken into account (assuming $\text{GPP}_{\text{lit}} = 0$ in Eq. 9). This indicates sources of heterotrophic signal other than the local community respiration. Because of the surface stratification, benthic respiration didn't contribute to the heterotrophy in the surface water indicated by the negative $\text{NCP}_{\text{O}_2/\text{Ar}}$. The light/dark incubation experiment at stations M1 and M2 suggested that the low O_2 concentration cannot be explained by in situ community mechanisms (low respiration rates and positive $\text{NCP}_{\text{DO-incub}}$ values). However, the Mississippi fresh water in the upper river channel was strongly heterotrophic and the advection of river water could play a significant role influencing the surface $\text{NCP}_{\text{O}_2/\text{Ar}}$ signal in the river channel because of the short water residence time (~1 day, Green et al., 2006). In the revised manuscript, the heterotrophy in the lower Mississippi River channel were discussed in Section 4.1. “In the stratified lower Mississippi River channel (Fig. 9a), the influence of lateral transportation of the heterotrophic river water from the upper river channel was significant because of the short water residence time (~1 day, Green et al., 2006). Therefore, the overall heterotrophic condition in the lower Mississippi River channel ($\text{NCP}_{\text{O}_2/\text{Ar}}$, $-51.2 \text{ mmol C m}^{-2} \text{ d}^{-1}$) can be attributed to the overwhelming influence of the heterotrophic NCP_{adv} over the autotrophic local biological production ($\text{NCP}_{\text{MLD}} = \text{NCP}_{\text{DO-incub}}$, $94.5 \text{ mmol C m}^{-2} \text{ d}^{-1}$).” (page 16, lines 5-18). In the stratified lower Mississippi River channel (Fig. 9a), the heterotrophic condition in the lower Mississippi River channel could be attributed to the dominant influence of the heterotrophic NCP_{adv} over the local biological production. In the vertically well-mixed HTACW (Fig. 9b), $\text{NCP}_{\text{O}_2/\text{Ar}}$ reflected the combined result of the water column community production, the lateral advection of CO_2 -rich Atchafalaya river water (NCP_{adv}), and sediment metabolism ($\text{NCP}_{\text{benthic}}$). Although we didn't measure the benthic respiration rates in our study, high sediment oxygen consumption and bottom water community respiration rates were reported in the Atchafalaya River Delta Estuary (Roberts and Doty, 2015) and on the Louisiana continental shelf (Murrell and Lehrter, 2011; Murrell et al., 2013). These studies suggested that the total below-pycnocline respiration rates show low variability over a large geographic and temporal range in the nGOM (46.4 to $104.5 \text{ mmol O}_2 \text{ m}^{-2} \text{ d}^{-1}$). The negative $\text{NCP}_{\text{O}_2/\text{Ar}}$ observed in the HTACW by our study ($-39.2 \pm 14.0 \text{ mmol C m}^{-2}$

d¹) agreed with the finding of Murrell et al., (2013) which showed shelf-scale net water column heterotrophy on the Louisiana shelf. This water column heterotrophy can be well explained by the combined results of NCP_{water} , $NCP_{benthic}$ and NCP_{adv} .

8. Figure 5 – Did you plot yourself panels c and d? It looks like those are a plain zoomed copy of panels in a figure published in the work by Zahng et al. (2012), which is referenced correctly. The authors should only cite this reference and refer the reader to that citation, and specifically to that figure, for further details. It is not ok to plainly copy and paste here those previously published figures. This does not mean to reproduce a figure with previous data, which instead would mean that you use the original data and produce the figure again. As those panels seem to be a plain copy this action breaches copyrights and authors must avoid doing this. Hence, panels c and d on this figure should be completely removed. Also, Figure 5 is mentioned before than Figure 4, why not switching the order of these figures?

Response: This comment has been taken and we apologize for this mistake. The panels (c) and (d) in the original Fig. 5 (now Fig. 4) have been removed. Instead, we presented the fractional contribution of the offshore surface water end member in the updated panel (c) to better show the results of the three end-member mixing model (see the figure below). We have also adjusted the order of figures as suggested.

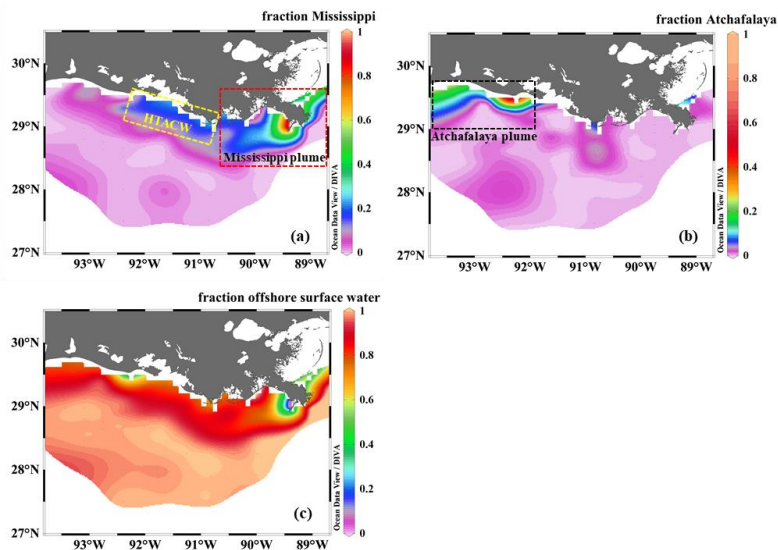


Fig. 4. The fractional contribution of (a) the Mississippi River, (b) the Atchafalaya River, and (c) offshore surface water to the surface water of the nGOM estimated from the three end-member mixing model. The sub-regions shown in panels (a) and (b) are the Mississippi plume, the high-turbidity Atchafalaya coastal water (HTACW), and the Atchafalaya plume.

9. Figure 6 – The spatial interpolation shown in panels a to d is quite bias. Showing a map with only the transect results of the NCP_{O_2Ar} , or the spatial interpolation for this result and NCP_{ADIC} and NCP_{ANOX} at best, but not a spatial interpolation for the very scarce $NCP_{DO-incub}$, where some structures in the spatial distribution of many places seem to be only an artifact of the interpolation, such as the large extent of the high NCP values in the Mississippi plume.

Response: The $NCP_{DO-incub}$, NCP_{ADIC} , NCP_{ANOX} in the original Fig. 6 (Fig. 5 in the revised manuscript) are now shown as colored dots to avoid bias and artifact from interpolation. We kept the contour plot of NCP_{O_2Ar} as the underway measurement provide NCP_{O_2Ar} with the same resolution as those data presented in Fig. 2.

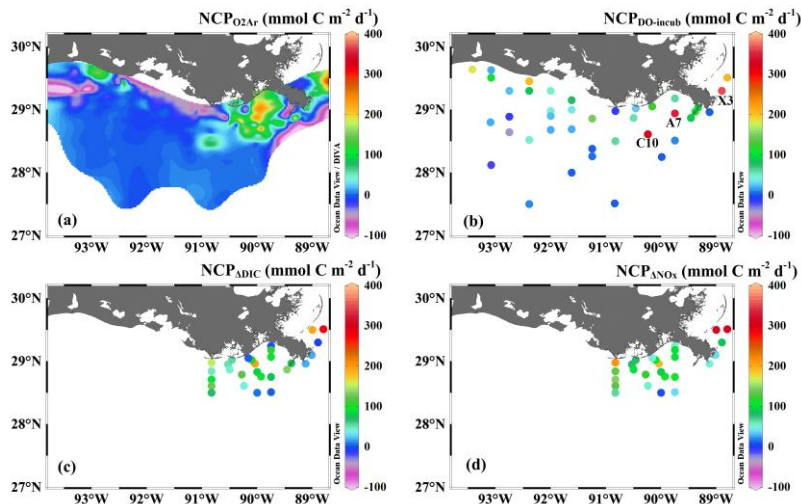


Fig. 5. The spatial variability of (a) NCP_{O_2Ar} , (b) $NCP_{DO-incub}$, (c) NCP_{ADIC} , and (d) NCP_{ANOX} . Noted that NCP_{ADIC} and NCP_{ANOX} were only estimated in the Mississippi plume (panel c, d).

Minor comments:

1. Between a quantity and its units there must be always a blank space, please revise this, especially for a number in percentage (e.g. 180 %, 10 m, 40 km, 28.5o N).

Response: Corrected as suggested.

Abstract (P1)

2. L23 – remove “the spring season” and change to “during spring in 2017”

Response: Corrected.

3. L23 – use same number of decimals in the degrees

Response: Corrected.

Pag. 3

4. L1 – how much is “moderate salinities”
Response: Corrected as “intermediate salinities (15 to 30 during this cruise)”.
5. L4 – Photosynthetically Active Radiation
Response: Corrected.
6. L18-19 this last sentence should be removed from here
Response: Corrected as suggested.

Pag. 4

7. L8 – Precision AND accuracy?
Response: These sentences have been revised to now state “The precisions of DIC and TA measurements were both 2 $\mu\text{mol kg}^{-1}$. DIC and TA measurements were calibrated, both with accuracy better than 0.1%, with certified reference materials provided by A. G. Dickson, Scripps Institution of Oceanography.”
8. L9 – mark this location in Fig. 1
Response: These two sampling stations are now marked and more information is presented in the updated Figure 1. We have also modified Figure 1 and its caption to better show the sampling sites as well as to highlight the Mississippi and Atchafalaya River.

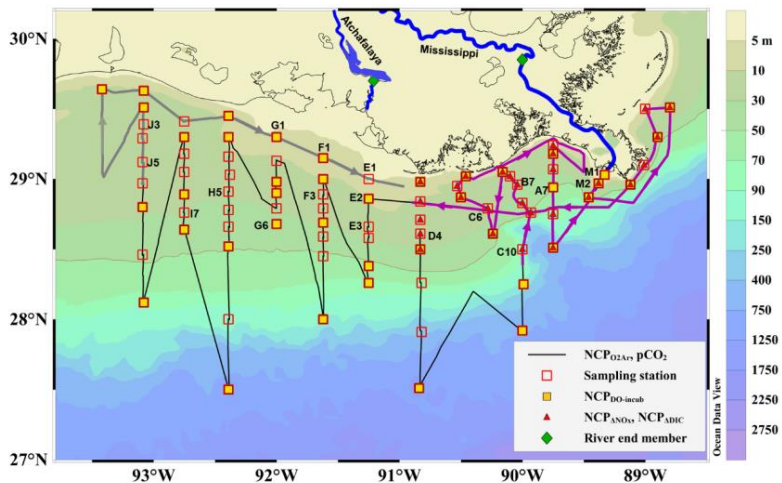


Fig. 1. Map and sampling sites in the northern Gulf of Mexico during the April 2017 cruise. The black dotted line is the cruise track along which the high-resolution underway measurements were made. The track in the Mississippi plume (purple line, Apr. 8-11) and in the Atchafalaya coastal regions (grey line, Apr. 15-17) are highlighted. Also shown are the 83 CTD sampling stations (hollow red squares), the 43 stations where light/dark bottle DO incubations were conducted (solid yellow squares), the 30 stations where non-conservative changes in DIC and NO_x were used to estimate NCP rates (solid red triangles), and the 2 stations where the properties of river end members were measured (solid green diamonds). The vertical CTD profiles of the named stations were shown in the supplement.

9. L10 – DO in discrete samples was measured by a

Response: Revised as suggested.

10. L18 – either you use the tilde symbol or explicitly write approximate

Response: The tilde symbol has been removed.

Pag. 5

11. L5 – against the **surface** discrete

Response: Revised as suggested.

12. L20 – where is this comparison of wind speeds shown?

Response: This sentence has been revised to now state “The COAMPS daily wind speed agreed well (mean difference = 0.4 m s⁻¹, **figure not shown**) with the measurements from the buoys in our study region”. Because the O₂ and CO₂ fluxes were calculated from the same wind speed, using COAMPS data or buoy measurement didn’t affect the discussion on the relationship between O₂ and CO₂ fluxes. Therefore, the comparison of wind speeds was not critical for our discussion and its figure was not shown in the manuscript.

13. L16, L20 and L25 – variables should be consistently written in italics (here and elsewhere)

Response: Corrected as suggested.

Pag. 6

14. L4 – why not referring to O_{2meas} instead of O_{2sea}? You also measure in river waters! And also to keep consistency with O_{2sat}.

L20 – in Eq. 3 again there is no consistency on the way the concentration of gases are expressed, while in Eq. 2 it was simply O_{2sat} and O_{2sea}, here it is [O₂]_{sat} and [O₂], respectively. Please keep consistency.

Response: [O₂]_{meas} and [O₂]_{sat} are now consistently used in the revised manuscript.

15. L6 – instead of “observed seawater DO” change to “measured surface water DO”

Response: Revised as suggested.

16. L7 – which T and S were used to calculate O_{2sat}?

Response: This sentence has been revised so that it now states: “ $\Delta O_{2(\text{sea-air})}$ is the difference between the seawater DO concentration from the calibrated underway optode measurement ([O₂]_{meas}) and the saturated DO concentration ([O₂]_{sat}) calculated from the measured sea surface temperature and salinity (Garcia and Gordon, 1992).”.

17. L20 – Current Eq. 4 should be shifted to be Eq. 3

Response: Corrected.

Pag. 7

18. L2 – here the authors need to better justify why in this region it is possible to neglect vertical mixing and lateral advection. They are important physical factors and later in the manuscript they claim it should be relevant to consider them. At least an effort should be done on explaining further why they were neglected.

Response: We now discuss how physical processes including vertical mixing and lateral advection affect the NCP estimation under different mixing conditions. Please see our responses to the general comment and major comments 5 and 7.

19. L4 - Equation 5 is of little use and is also wrong, the first term NCP should be removed because you are calculating NCP with the second term. I will completely remove it from the manuscript and use the term of the left in Eq. 6.

Response: Although Eq. 5 was correct (NCP in Eq. 6 was calculated from Eq. 5 assuming $MLD \frac{d[O_2]_{\text{net}}}{dt} = 0$ and $\frac{[Ar]}{[Ar]_{\text{sat}}} = 1$) (Cassar et al. 2011; Jonsson et al. 2013; Kaiser et al. 2005), this explanatory equation has been now removed to make the method section more concise as suggested by both reviewers.

20. L15 – Is Eq. 9 correct? If you reduce GPP this equation is rather adding a factor to the high GPP value calculated in Eq. 8. Please check it.

Response: The percent signs were absent in these equations and they have been corrected as now read:

if %PAR \geq 50 %, $GPP_{\text{int}} = GPP * MLD$

if %PAR < 50 %, $GPP_{\text{int}} = 2 * \%PAR * GPP * MLD$

21. L18 – in which depths the BOD bottles were collected?

Response: The depth information has been added as: “Surface water samples (~1.5 m) were collected from Niskin bottles into triplicate clear and black 300-ml BOD bottles (Wheaton).”

22. L22 – filtered seawater also introduces DO into the sample, see my major comment above.

Response: Please see the response to major comment 6.

Pag. 8

23. L3 – it is not sufficient to claim that there was no bias between the two methods, some values should be presented here.

Response: Clarified as “The mean difference between DO obtained by the probe and the spectrophotometric method of ± 5 % was consistent with previous comparisons of probe measured versus Winkler measured DO based on several hundred comparisons (Murrell et al. 2013).”

24. L4 – the units of the DO rate of change are wrong

Response: The units were correct here as the DO change rates during the incubation experiments ($\text{mmol m}^{-3} \text{d}^{-1}$). These rates were then integrated over the MLD to produce the NCP rates ($\text{mmol m}^{-2} \text{d}^{-1}$).

25. L16 – why it was chosen 50 % of light?

Response: The text has been changed to answer this question: “In our study, we assumed that GPP was linearly dependent on light up to a maximum GPP_{max} occurred when %PAR = 50 %. This assumption is based on previous measurements from this shelf that indicate photosynthesis begins to saturate at light level of $\sim 200 \mu\text{mol quanta m}^{-2} \text{s}^{-1}$ (Lohrenz et al., 1994), which is roughly 50 % of light in the surface mixed layer (Lohrenz et al., 1999).”

Pag. 9

26. L18 – “To facilitate the comparison, we converted NCP estimates from the different...”

Response: Corrected.

Pag. 10

27. L5 – the lower discharge in 2017 is also observed in previous months, not only in April

Response: This sentence has been revised to now state “These peaks in spring 2017 occurred later than the average condition during 1997-2017 and the monthly mean values of discharge and NO_x loading in April 2017 were slightly lower than the long-term mean values (Fig. S1).”.

28. L5 – “light”? please complete this to light transmittance

Response: Corrected.

29. L9 – The authors claim a correlation between MLD and salinity, however by looking at Fig. 5 panels b and c, this is not evident. If the authors define MLD based on a potential density criterion, they should make a comparison to density (i.e. incl. temperature which has more structure in surface waters) and not only to salinity.

Response: We agree with the reviewer that both temperature and salinity should be considered when discussing stratification. We have revised this sentence to now state “The Mississippi plume and most offshore regions were characterized by surface stratification, which was mainly caused by the buoyancy of fresher surface water in the plume and vertical temperature gradient in the offshore region (Fig. S3).”

30. L15 – remove “in”

Response: Corrected.

31. L17 – 19 this sentence will benefit by adding the correct punctuation

Response: This sentence has been revised to now state “In spring when river discharge is high and wind is typically downwelling-favourable, the Mississippi River freshwater generally flows westward in a contained nearshore current”.

Pag. 11

32. L2-4 too many subjective words without quantities or comparison in reference to something else (lower, deeper, higher?)

Response: Corrected. Quantities now have been added.

33. L2-4 Whereas I agree in the observations made regarding the HTACW in the Atchafalaya Bay in Fig. 3, I disagree in the MLD which does not look homogeneously deeper in that region. From Fig. 3c, the surface water does not look well mixed as the authors claim in the following sentence (and vertical profiles are not presented). Therefore, this needs more investigation.

Response: We appreciate the reviewer highlighting the need to display the vertical profiles. The HTACW region was, in fact, well-mixed as can be seen in the vertical profiles now provided in supplemental Fig. S4 in the revised manuscript.

34. L7-8 The authors define three sub-regions in Fig. 5 a and b based on the identified water characteristics, but they define them only by in their longitude limits and they should also include the latitude limits.

Response: In the revised manuscript, we divided the coastal region into four sub-regions: 1) the lower Mississippi River channel (Fig. S2, salinity < 2); 2) the Mississippi plume (Fig. 4a, to the east of 90.75° W, to the north of 28.30° N); 3) the high-turbidity Atchafalaya coastal water (Fig. 4a and Fig. 2d, 90.75-92.35° W, light transmittance < 20%, named as HTACW hereafter); and 4) the Atchafalaya plume (Fig. 4b, 92.35-93.50° W, to the north of 29.00° N).” In addition to longitude or latitude limits, we presented salinity limits for the lower Mississippi River channel and light transmittance limits for the high-turbidity Atchafalaya coastal water to better characterize these sub-regions.

Pag. 13

35. L9 – “spatial” instead of space
Response: Corrected.

Pag. 15

36. L1- associated with “the” different
Response: Corrected.

37. L7 – what inherent averaging the authors refer here? If they have continuous highly resolved data at least episodic extreme events would be better captured than discrete sampling.
Response: The modeling study by Teeter et al., (2018) suggested that the NCP_{O_2Ar} represents the exponentially weighted NCP over the past several residence times of O_2 (stated in the Methods section). The original expression of “episodic extreme events” was not appropriate and this sentence has been revised to now state “As NCP_{O_2Ar} is an exponentially weighted average rate, it is less able to capture high NCP values due to the inherent averaging of the O_2/Ar approach.”

38. L12-14 this assumption of integrating vertically the NCP_{O_2Ar} can be avoided by considering vertical processes if the authors suspect this is the case (as mentioned in L17 same page).
L12 – also, the authors contradict themselves in the structure of the water column, it is well mixed or not?
Response: The influences of vertical mixing on NCP_{O_2Ar} have now been better explained according to different mixing conditions. Please see the response to general comment and major comment 5.

39. L15 – “fraction”
Response: Corrected.

Pag. 16

40. L1 – vertical or horizontal mixing?
Response: As our study focused on the surface water, the mixing here was mainly horizontal mixing between the river water and seawater.

41. L10 – space between “community were”

Response: Corrected.

Pag. 17

42. L17 – before explaining the results in Fig. 9, please explain what it is plotted there.

Response: This figure is explained and discussed in the revised manuscript as: “When plotting the paired CO₂ flux and NCP_{O₂A_r} data (Fig. 10), most data collected in the lower Mississippi River channel fall in quadrant 2 suggesting net heterotrophy coupled with CO₂ outgassing to the atmosphere. The Mississippi plume and Atchafalaya plume exhibited opposite patterns with most data in these regions being in quadrant 4 (net autotrophy coupled with CO₂ uptake from the atmosphere). However, the data in quadrant 1 (autotrophic water as a CO₂ source observed near the Mississippi estuary) and quadrant 3 (heterotrophic water as a CO₂ sink in the HTACW) suggest decoupling between NCP_{O₂A_r} and CO₂ flux.”

Pag. 18

43. L3-10 these lines should be part of a methods section where the 1-D model is introduced to the reader

Response: The model description has now been moved to the Methods section as suggested.

44. L11-25 I am not surprised by the results presented in Fig. 10, they are only showing the wellknown changes in the carbonate system, and this figure can only be seen as a proof of their model performance under standard defined initial conditions. I would place this figure in supplement.

Response: We agree with the reviewer that the results shown in this figure are well-known and this figure has been moved to the supplement. According to the suggestion from reviewer 1, we have updated this figure to show the differences in gas exchange rate and equilibrium time of O₂ and CO₂. Please see our response to minor comment 2 by reviewer 1 for details.

Pag. 19

45. L23 – “ has the advantage of being “

Response: Corrected.

Pag. 20

46. L3 – I miss the results on the distribution of nutrients. From the way the results were presented, this conclusion is not clearly supported

Response: In the revised manuscript, the distributions of NO_x, light transmittance, Chl-a, and NCP were presented in Fig. 7a and the relationship between NCP-induced uptake of nutrients and DIC were presented in Fig. 8. These results supports the conclusion of “In the river plume, the light availability generally determined the onset of the biological growth and the river-borne nutrient loading set the magnitude of the biological production (Fig. 7, Fig. 8)”. This sentence has been moved to page 17, lines 17-20.

Figures

47. Figure 1 – I miss some labels in the map. For people that is not familiar with this study region, it will be useful to add directly in the map the labels of the location of the main features that are mentioned throughout the manuscript, e.g., Mississippi and Atchafalaya deltas, Mississippi South Pass, Atchafalaya Bay. Also, add numbers to the stations and remove the units to all of the depths in the color bar, and rather add “m” above the bar as in Figure 3. The figure caption needs to be improved.

Response: We have modified Fig. 1 to add more features accordingly. Also see the response to minor comment 8.

48. Figure 2 – This schematic contains extra information that is not a central part of the manuscript. If you are not talking about the actual biological pump and its components, I will remove it from the figure. I would also invert the order with the CO₂ and carbonate system on the left and the O₂ part on and the O₂ part on the right of the figure.

Response: We agree with the reviewer that this schematic didn't contribute much and it has been removed from the revised manuscript.

49. Figure 4 – This figure needs to be georeferenced, or provide more information in Figure 1, where was the start of the continuous transect? Also, you could add number of stations so it is clearer the geographical position of the points in panel c.

Response: Arrows have been now added in Fig. 1 to better show the direction of the transect and labels have been added for some key stations. In panel c, we heighthed three stations with high NCP_{PO₂-incub} values and their positions were given in Fig. 5.

50. Figure S1 – add labels to the x-axis

Response: The label “month” has been added to the x-axis.

References

51. - The authors should carefully revise the guidelines for authors before submitting a manuscript to a journal. In this case, for the presentation of references, in the text they are always lacking of a comma between the authors and the year of the publication. Also, the format of the presentation of references at the end of the manuscript, should be also carefully checked (e.g. the year of the publication must precede the doi).

Response: Corrected.

References Cited:

- Craig, H., and T. Hayward. 1987. Oxygen supersaturation in the ocean: Biological versus physical contributions. *Science* 235: 199-202.
- Castro-Morales, K., N. Cassar, D. R. Shoosmith, and J. Kaiser. 2013. Biological production in the Bellingshausen Sea from oxygen-to-argon ratios and oxygen triple isotopes. *Biogeosciences* **10**: 2273-2291.
- Garcia, H. E., and L. I. Gordon. 1992. Oxygen solubility in seawater: Better fitting equations. *Limnology and Oceanography* 37: 1307-1312.
- Jonsson, B. F., S. C. Doney, J. Dunne, and M. Bender. 2013. Evaluation of the Southern Ocean O₂/Ar-based NCP estimates in a model framework. *Journal of Geophysical Research-Biogeosciences* 118: 385-399.
- Kaiser, J., M. K. Reuer, B. Barnett, and M. L. Bender. 2005. Marine productivity estimates from continuous O₂/Ar ratio measurements by membrane inlet mass spectrometry. *Geophysical Research Letters* 32.

- Murrell, M. C., J. G. Campbell, J. D. Hagy III, and J. M. Caffrey. 2009. Effects of irradiance on benthic and water column processes in a Gulf of Mexico estuary: Pensacola Bay, Florida, USA. *Estuarine, Coastal and Shelf Science* 81: 501–512.
- Murrell, M. C., and J. C. Lehrter, 2011. Sediment and lower water column oxygen consumption in the seasonally hypoxic region of the Louisiana Continental Shelf. *Estuaries and Coasts*, 34, 912-924.
- Murrell, M. C., Stanley, R. S., Lehrter, J. C., and Hagy, J. D. 2013. Plankton community respiration, net ecosystem metabolism, and oxygen dynamics on the Louisiana continental shelf: Implications for hypoxia, *Cont. Shelf Res.*, 52, 27-38, <https://doi.org/10.1016/j.csr.2012.10.010>.
- Nicholson, D. P., R. H. R. Stanley, E. Barkan, D. M. Karl, B. Luz, P. D. Quay, and S. C. Doney. 2012. Evaluating triple oxygen isotope estimates of gross primary production at the Hawaii Ocean Time-series and Bermuda Atlantic Time-series Study sites. *Journal of Geophysical Research-Oceans* 117.
- Shadwick, E. H., B. Tilbrook, N. Cassar, T. W. Trull, and S. R. Rintoul. 2015. Summertime physical and biological controls on O₂ and CO₂ in the Australian Sector of the Southern Ocean. *Journal of Marine Systems* 147: 21-28.
- Teeter, L., Hamme, R. C., Ianson, D., and Bianucci, L. 2018. Accurate estimation of net community production from O₂/Ar measurements. *Global Biogeochemical Cycles*, 32, 1163–1181.
- Ulfsbo, A., Cassar, N., Korhonen, M., van Heuven, S. Hoppema, M., Kattner, G., and Anderson, L. G. 2014. Late summer net community production in the central Arctic Ocean using multiple approaches, *Global Biogeochem. Cycles*, 28, 1129-1148.

Spring net community production and its coupling with the CO₂ dynamics in the surface water of the northern Gulf of Mexico

Zong-Pei Jiang^{1,2}, Wei-Jun Cai^{2*}, John Lehrter³, Baoshan Chen², Zhangxian Ouyang², Chenfeng Le¹, Brian J. Roberts⁴, Najid Hussain², Michael K. Scaboo², Junxiao Zhang⁵, Yuanyuan Xu²

¹Ocean College, Zhejiang University, Zhoushan, Zhejiang, China

²School of Marine Science and Policy, University of Delaware, Newark, Delaware, USA

³University of South Alabama, Alabama, USA

⁴Louisiana Universities Marine Consortium, Louisiana, USA

⁵South China Sea Marine Survey and Technology Center, State Oceanic Administration, Guangzhou, Guangdong, China

Correspondence to: Wei-Jun Cai (wcai@udel.edu)

Abstract. Net community production (NCP) in the surface water of the northern Gulf of Mexico (nGOM) and its coupling with the CO₂ system were examined during the productive spring season. NCP was estimated using multiple approaches: 1) underway O₂ and Ar ratio, 2) oxygen changes during light/dark bottle oxygen incubations, and 3) non-conservative changes in dissolved inorganic carbon or nutrients. NCP rates derived from various methods displayed similar pattern along the river-ocean mixing gradient showing high production rates in the plume region. NCP_{O₂Ar} estimated from high-resolution O₂ and Ar underway measurement indicated heterotrophic condition at the high-nutrient and high-turbidity Mississippi river end (-51.3±11.9 mmol C m⁻² d⁻¹ when salinity < 2) resulting from the influence of terrestrial carbon input and light limitation on photosynthesis. High NCP_{O₂Ar} rates (105.0±59.2 mmol C m⁻² d⁻¹, up to 235.4 mmol C m⁻² d⁻¹) were observed in the Mississippi and Atchafalaya plume at intermediate salinities between 15 to 30 where light and nutrient were both favourable for phytoplankton production. NCP_{O₂Ar} rates observed in the high-salinity, oligotrophic offshore waters (salinity > 35.5) were close to zero due to nutrient limitation. Air-sea CO₂ fluxes generally showed corresponding changes from being a strong CO₂ source in the river channel (55.5±7.6 mmol C m⁻² d⁻¹), to a CO₂ sink in the plume (-13.4±5.5 mmol C m⁻² d⁻¹) and to be nearly in equilibrium with the atmosphere in offshore waters. Overall, the surface water of the nGOM was autotrophic during spring in 2017 with an area-weighted mean NCP_{O₂Ar} of 21.2 mmol C m⁻² d⁻¹ and as a CO₂ sink of -6.7 mmol C m⁻² d⁻¹. A temporal mismatch between *in situ* biological production and gas exchange of O₂ and CO₂ was shown through a 1-D model to result in decoupling between NCP_{O₂Ar} and CO₂ flux (e.g., autotrophic water as a CO₂ source outside the Mississippi river mouth and heterotrophic water as a CO₂ sink in the Atchafalaya coastal water). This decoupling was a result of *in situ* biological production superimposed on the lingering background pCO₂ from the source water because of the slow air-sea CO₂ exchange rate and the buffering effect of the carbonate system.

设置了格式

设置了格式

删除了: mixed layer

设置了格式: 字体: (默认) Times New Roman, (中文) Times New Roman

删除了: and or nutrients; in order to assess uncertainties and

删除了: the spring season ...n spring

删除了: NCP rate ...f 21.2 mmol C m⁻² d⁻¹ and as a CO₂ sink of -6

设置了格式: 字体: 倾斜

删除了: could was shown through a 1-D model to result in

设置了格式: 字体: 倾斜

1 Introduction

The continental shelf is among the most biologically active areas of the biosphere and plays a significant role in global biogeochemical cycles (Chen and Borges, 2009; Chen and Swaney, 2012; Gattuso et al., 1998; Muller-Karger et al., 2005). Despite its moderate surface area (~7%), the continental shelf accounts for 14-30% of net ecosystem production (Gattuso et al., 1998), 80% of organic matter burial (Gattuso et al., 1998), and 15-21% of the CO₂ uptake of the global ocean (Cai, 2011; Cai et al., 2006; Chen and Borges, 2009; Laruelle et al., 2010). Moreover, anthropogenic impacts have substantially changed the nutrient and carbon loads delivered to the coastal oceans (Bauer et al., 2013; Regnier et al., 2013; Yang et al., 2018), with associated development of a series of environmental problems, e.g., coastal eutrophication, hypoxia, and acidification (Cai et al., 2011; Diaz and Rosenberg, 2008; Rabalais et al., 2014; Wallace et al., 2014). Understanding and quantifying how these impacts affect the metabolic balance and CO₂ fluxes of coastal systems is of critical interest to scientists and policy-makers. However, the substantial heterogeneity resulting from physical and biogeochemical interactions makes assessing metabolic state and carbon flux a challenging task in dynamic coastal environments.

Net community production (NCP) is defined as the difference between gross primary production and community respiration (Eppley and Peterson, 1979; Sarmiento and Gruber, 2006) and indicates whether the ecosystem is a net source or sink of organic matter (Eppley and Peterson, 1979; Sarmiento and Gruber, 2006). NCP in the mixed layer plays an important role in regulating the surface CO₂ and O₂ dynamics. It also represents the amount of organic carbon available for export to the subsurface, which is closely related to bottom water biogeochemical processes, e.g., the development and maintenance of hypoxia.

The northern Gulf of Mexico (nGOM) is a river-dominated continental shelf (Mckee et al., 2004) with NCP and CO₂ dynamics affected by the terrestrial inputs of carbon and nutrients from the Mississippi-Atchafalaya River system (Lohrenz et al., 2014). The CO₂ variability in the nGOM has been extensively investigated by high-resolution underway measurement of the partial pressure of CO₂ (pCO₂) (Huang et al., 2015). High terrestrial inorganic and organic carbon loading results in CO₂ oversaturation and net CO₂ efflux to the atmosphere in the river channel and estuary of the Mississippi River (Cai, 2003; Guo et al., 2012; Huang et al., 2015; Lohrenz et al., 2010). On the continental shelf, reduced pCO₂ observed in the Mississippi plume (sink for atmospheric CO₂) was attributed to strong primary production supported by the excessive

设置了格式: 字体颜色: 自动设置

设置了格式: 字体颜色: 自动设置

删除了: trophic

设置了格式: 字体颜色: 自动设置

删除了: . NCP reflects the trophic state of the aquatic ecosystem indicating whether the ecosystem is a net source or sink of organic

设置了格式: 字体: (默认) Times New Roman

设置了格式: 字体颜色: 自动设置

设置了格式: 字体颜色: 自动设置

设置了格式: 字体颜色: 自动设置

删除了: which

设置了格式: 字体颜色: 自动设置

删除了: receives a large amount of carbon and nutrient inputs from

设置了格式: 字体颜色: 自动设置

删除了: NCP and CO₂ dynamics in the nGOM are significantly affected by the concurrent terrestrial inputs of nutrients and carbon loadings. The

删除了: and air-sea CO₂ flux

删除了: have

删除了: high

设置了格式: 字体颜色: 自动设置

设置了格式: 字体颜色: 自动设置

删除了: -

删除了: lower

删除了: at moderate salinities

设置了格式: 字体颜色: 自动设置

设置了格式: 字体颜色: 自动设置

riverine nutrient loads (Guo et al., 2012; Huang et al., 2015; Lohrenz et al., 1990; 1999; 2014). With the enhanced surface production and subsequently subsurface respiration of the sinking organic matter, recurring bottom hypoxia that covers large portions of the Louisiana-Texas shelf has been observed in summer when stratification limits O₂ replenishment (Bianchi et al., 2010; Obenour et al., 2013; Rabalais et al., 2002). Springtime riverine nutrient flux and subsequent biological production in surface water play a critical role in determining the size of the summertime bottom-water hypoxia area in the nGOM (Justić et al., 1993; Turner et al., 2012). The rapid subsurface respiration also leads to a significant decrease in pH and a weakening of acid-base buffer capacity, which leads to the enhanced coastal ocean acidification problem (Cai et al., 2011). Previous NCP studies in the nGOM have been mainly based on the oxygen changes during light/dark bottle oxygen incubations and non-conservative removal of dissolved inorganic carbon or nutrients (Cai, 2003; Huang et al., 2012; Guo et al., 2012; Murrell et al., 2009; 2013). However, the detailed relationship between NCP and CO₂ dynamics remains unclear because of the low spatial resolution of the conventional NCP measurements based on discrete samples. In this study, we present the first attempt to obtain high-resolution NCP_{O₂/Ar} estimates from continuous underway measurement of oxygen to argon ratio (O₂/Ar) in the nGOM in spring 2017. The NCP_{O₂/Ar} result was compared to those derived from traditional approaches to evaluate the consistency of NCP estimates from various methods. Meanwhile, these NCP methods are associated with different temporal and spatial scales and are affected by different biological and physical processes. By making NCP estimates using the different methods we can get a more robust understanding of the overall metabolism of the system. The simultaneous underway determination of NCP_{O₂/Ar} and pCO₂, together with measurements of dissolved oxygen (DO), dissolved inorganic carbon (DIC), total alkalinity (TA), nutrients, and other environmental parameters, allow us to better constrain the variability and controls of the metabolic balance and CO₂ flux in the nGOM. We also use a 1-D model to investigate the relationship between NCP and air-sea fluxes of O₂ and CO₂.

2 Methods

2.1 Sample collection and measurements

The cruise was conducted onboard RV Pelican during 6-16 April 2017. The study region covered the Mississippi and Atchafalaya estuary and the adjacent Louisiana continental shelf (Fig. 1). Vertical water column profiles of temperature,

设置了格式: 字体颜色: 自动设置

删除了: Springtime riverine nutrient flux and subsequent biological production in surface waters play a critical role in determining the size of the summertime bottom-water hypoxia area in the nGOM

设置了格式: 字体颜色: 自动设置

设置了格式: 字体颜色: 自动设置

删除了: Guo et al., 2012, Huang et al., 2012

设置了格式: 字体颜色: 自动设置

设置了格式: 非突出显示

移动了(插入) [1]

删除了: (

设置了格式: 非突出显示

删除了: in the surface water in the nGOM

设置了格式: 字体颜色: 自动设置

设置了格式: 字体: 10 磅, 检查拼写和语法

删除了: Cai, 2003

设置了格式: 突出显示

设置了格式: 字体颜色: 自动设置

上移了 [1]: (Guo et al., 2012, Huang et al., 2012, Cai, 2003)

设置了格式: 字体颜色: 自动设置

删除了: high

删除了: NCP

删除了: O₂

删除了: Ar

设置了格式: 下标

删除了:

删除了: These

删除了: rates were

删除了: NCP estimates

设置了格式: 字体颜色: 自动设置

删除了: (light/dark bottle oxygen incubation and non-conservative

设置了格式: 字体: (中文) Times New Roman, 10 磅

删除了: DIC

设置了格式: 字体颜色: 自动设置

删除了: In particular, we demonstrate that there is a time lag

设置了格式: 突出显示

删除了: .

设置了格式: 字体颜色: 自动设置

删除了: The study region covers the Mississippi and Atchafalaya

删除了: the

删除了: At 83 sampling stations v

salinity, DO, chlorophyll fluorescence (Chl-a), and photosynthetically active radiation (PAR) were measured by a SeaBird CTD system (SBE 911plus) at 83 sampling stations (Fig. 1). Discrete water samples for DIC, TA, DO, and nutrients were collected from 3-12 depths depending on the bottom depth and vertical profiles of temperature, salinity and DO. River water samples of the Mississippi (89.98° W, 29.85° N) and Atchafalaya (91.21° W, 29.70° N, Fig. 1) were taken on 5 April, one day prior to the cruise, to identify the DIC and TA concentrations of the river end members. Samples for DIC and TA were collected in 250 mL borosilicate glass bottles and preserved with 50 µl of saturated HgCl₂ solution (Dickson et al., 2007). DIC was measured by non-dispersive infrared measurement on the CO₂ stripped from the acidified sample (AS-C3, Apollo SciTech). TA titrations were conducted with a ROSS™ combination electrode 8102 (Thermo Fisher Scientific) on an automated titrator (AS-ALK2, Apollo SciTech). The precision of DIC and TA measurements were both 2 µmol kg⁻¹. DIC and TA measurements were calibrated, both with accuracy better than 0.1 %, with certified reference materials provided by A. G. Dickson, Scripps Institution of Oceanography. DO in discrete samples was measured by a Shimadzu UV-1700 at 25 °C using the spectrophotometric method following Pai et al., (1993) with an accuracy of 0.2 %. For nutrient analysis, water from each Niskin bottle was immediately filtered through 0.22 µm, sterile, polyethersulfone syringe filters and stored frozen for subsequent nutrient characterization. Samples were analyzed in duplicate for dissolved NO_x (NO₃⁻ + NO₂⁻) by Cu-Cd reduction followed by azo dye colorimetry using a Lachat Instruments QuikChem® FIA+ 8000 Series Automated Ion Analyzer at the Louisiana Universities Marine Consortium as described previously (Roberts and Doty, 2015). Standard curves were prepared using standard NO₃-N and NO₂-N stock solutions (Hach, Loveland CO) and yielded r² values of > 0.999.

2.2 Underway measurements

The underway system was fed by the ship's seawater supply from an inlet located at an approximate depth of 2.5 m. The flow-through system and the Multiple Instrument Data Acquisition System (MIDAS) provided measurements on sea surface temperature, conductivity (Seabird SBE 21 Thermosalinograph), chlorophyll fluorescence (Turner Model 10 Series Fluorometers), and light transmittance (WETLabs 25-centimeter path length transmissometer). MIDAS also integrated data from the ship's meteorological suite: wind, barometric pressure, temperature and relative humidity (R.M. Young) and PAR (LI-COR LI-190SZ).

删除了: available

删除了: SeaBird

删除了: system

移动了(插入) [2]

删除了: Discrete water samples were collected 3-12 depths depending on the bottom depth and the vertical salinity and O₂ structures of the water reading from the SBE 911plus profiler.

删除了: . USA

上移了 [2]: River water samples of the Mississippi (89.98° W, 29.85° N) and Atchafalaya (91.21° W, 29.70° N) were taken on 5 April, one day prior to the cruise, to identify the DIC and TA concentrations of the river end members.

删除了: DIC and TA measurements were calibrated with certified reference materials provided by A. G. Dickson, Scripps Institution of Oceanography. The precision and accuracy of the DIC and TA measurements were better than 0.1% (~2 µmol kg⁻¹) (Huang et al. 2012).

设置了格式: 字体颜色: 自动设置

删除了: in discrete samples

设置了格式: 字体颜色: 自动设置

设置了格式: 字体颜色: 自动设置

删除了: (PES)

删除了: with an ASX-400 Series XYZ autosampler

设置了格式: 字体颜色: 自动设置

删除了: ~

删除了: 3

删除了: integrates

删除了: photosynthetically active radiation

Underway seawater $p\text{CO}_2$ was measured with a precision of 0.1 μatm by an automated flow-through $p\text{CO}_2$ measuring system (AS-P2, Apollo SciTech) with a shower head equilibrator and a non-dispersive infrared gas detector (LI-COR, LI-7000) (Huang et al., 2015). The $p\text{CO}_2$ measurement was calibrated twice daily against 3 certified gas standards (150.62, 404.72, and 992.54 ppm) and the accuracy was better than $\pm 2 \mu\text{atm}$. Underway $p\text{CO}_2$ system alternated measurements on a stream of seawater split from the same inlet for the MIDAS and a stream of outside air from the bow of the vessel away from chimney contamination. The atmospheric $p\text{CO}_2$ was measured every 3 hours, automatically. The underway DO was measured by an Aanderaa 4835 optode which was calibrated against discrete surface water values by spectrophotometric measurements. Underway high-resolution measurements of O_2/Ar were made by equilibrator inlet mass spectrometry as described by Cassar et al. (2009). Briefly, a fraction of underway seawater (the same supplied to the $p\text{CO}_2$ measuring system) was pumped through a gas-permeable membrane contactor cartridge at a flow rate of 100 mL min^{-1} . The cartridge was connected to a quadrupole mass spectrometer (Pfeiffer Prisma) through a fused-silica capillary which continuously sampled headspace gases for O_2/Ar measurement. As the atmospheric O_2/Ar is essentially constant relative to that in the surface water, calibrations of the O_2/Ar ion current ratio were conducted by sampling the ambient air every 3 hours through a second capillary (Cassar et al., 2009). The instrument precision estimated from the repeated measurements of atmospheric O_2/Ar was 0.3 %.

2.3 Calculations

The mixed layer depth (MLD) was defined as the depth at which the density changed by 0.03 kg m^{-3} relative to the surface value and was calculated according to the density profiles at sampling stations. Air-sea CO_2 flux was calculated as:

$$F_{\text{CO}_2} = k_{\text{CO}_2} K_0 \Delta p\text{CO}_{2(\text{sea-air})} = k_{\text{CO}_2} K_0 (p\text{CO}_{2\text{meas}} - p\text{CO}_{2\text{air}}) \quad (1)$$

where k_{CO_2} is the gas transfer velocity of CO_2 calculated using the daily mean wind speed from the three-dimensional Coupled Ocean/Atmosphere Mesoscale Prediction System (COAMPS) (Hodur, 1997) and the coefficients of Sweeney et al. (2007). The COAMPS daily wind speed agreed well (mean difference = 0.4 m s^{-1} , figure not shown) with buoy measurements in our study region (s42047, s8768094, FRWL1, MRSL1, LOPL1, GISL1, PSTL1, and PILL1, data from the National Data Buoy Center, <http://www.ndbc.noaa.gov/maps/WestGulf.shtml>). K_0 is the CO_2 solubility coefficient calculated

- 删除了: The u
- 删除了: alternates
- 删除了: the
- 删除了: h
- 删除了: The $p\text{CO}_2$ measurement was calibrated regularly against 3 certified gas standards (150.62, 404.72, 992.54 ppm) and has an accuracy of 2 μatm .
- 设置了格式: 字体颜色: 自动设置
- 删除了: s
- 删除了: oxygen to argon ratio (
- 删除了:)
- 删除了: were
- 删除了: an Equilibrator
- 删除了: Inlet
- 删除了: Mass
- 删除了: Spectrometry
- 删除了: is
- 删除了: samples
- 删除了: ratio
- 删除了: s
- 设置了格式: 字体颜色: 自动设置
- 设置了格式: 字体颜色: 自动设置, 下标
- 设置了格式: 字体颜色: 自动设置
- 设置了格式: 字体: 10 磅
- 删除了: C
- 设置了格式: 下标
- 删除了: is
- 删除了: \pm
- 删除了: or better (Cassar et al. 2009)
- 删除了: changes
- 删除了: , figure not shown
- 删除了: the
- 删除了: from the buoys
- 设置了格式: 字体颜色: 自动设置
- 域代码已更改
- 设置了格式: 字体颜色: 自动设置
- 设置了格式: 字体颜色: 自动设置

from the measured sea surface temperature and salinity (Weiss, 1974). $\Delta p\text{CO}_2(\text{sea-air})$ is the difference between the measured $p\text{CO}_2$ in the surface water ($p\text{CO}_{2\text{meas}}$) and in the atmosphere ($p\text{CO}_{2\text{air}}$). Comparing to the large variations in $p\text{CO}_{2\text{meas}}$ (110-1800 μatm), the variability of $p\text{CO}_{2\text{air}}$ was minor ($405 \pm 4 \mu\text{atm}$) so the $p\text{CO}_{2\text{air}}$ was set at the cruise average value of 405 μatm for the flux calculation. The negative F_{CO_2} corresponds to a net CO_2 uptake by the ocean (ocean as a CO_2 sink for the atmosphere). Air-sea O_2 flux was calculated as:

$$F_{\text{O}_2} = k_{\text{O}_2} \Delta\text{O}_{2(\text{sea-air})} = k_{\text{O}_2} ([\text{O}_2]_{\text{meas}} - [\text{O}_2]_{\text{sat}}) \quad (2)$$

where k_{O_2} is the gas exchange velocity of O_2 which was calculated in a similar way with that of k_{CO_2} . $\Delta\text{O}_{2(\text{sea-air})}$ is the difference between the seawater DO concentration from the calibrated underway optode measurement ($[\text{O}_2]_{\text{meas}}$) and the saturated DO concentration ($[\text{O}_2]_{\text{sat}}$) calculated from the measured sea surface temperature and salinity (Garcia and Gordon, 1992). The oxygen saturation percentage (DO%) is calculated as $\text{DO}\% = [\text{O}_2]_{\text{meas}}/[\text{O}_2]_{\text{sat}}$.

2.4 NCP estimates

In this study, NCP rates were estimated by three different approaches: underway O_2/Ar measurements ($\text{NCP}_{\text{O}_2/\text{Ar}}$), light/dark bottle DO incubations ($\text{NCP}_{\text{DO-incub}}$), and non-conservative changes in DIC (NCP_{ADIC}) or NO_x ($\text{NCP}_{\text{ANO}_x}$).

NCP from the O_2/Ar method: DO concentration in the surface water is affected by physical (e.g., changes in temperature, salinity, and atmospheric pressure, bubble dissolution and injection) and biological processes (photosynthesis and respiration). Ar and O_2 have similar responses to physical processes as they have similar solubility and temperature dependency (Garcia and Gordon, 1992; Hamme and Emerson, 2004). On the other hand, Ar is biologically inert and can be used to infer abiotic influences on oxygen. Contemporaneous measures of O_2 and Ar thus allow the biological-induced O_2 changes to be isolated (Craig and Hayward, 1987). By measuring the biologically mediated oxygen supersaturation $\Delta(\text{O}_2/\text{Ar})$ (Cassar et al., 2011; Craig and Hayward, 1987; Jonsson et al., 2013; Kaiser et al., 2005);

$$\Delta(\text{O}_2/\text{Ar}) = \frac{[\text{O}_2]/[\text{Ar}]}{[\text{O}_2]_{\text{sat}}/[\text{Ar}]_{\text{sat}}} - 1 \quad (3)$$

the surface NCP can be approximated by the net air-sea biological oxygen flux (bioflux, $\text{mmol O}_2 \text{ m}^{-2} \text{ d}^{-1}$) under a physically isolated mixed layer assumption (Jonsson et al. 2013):

删除了: the measured sea surface

删除了: $p\text{CO}_{2\text{meas}}$ and $p\text{CO}_{2\text{air}}$ are

设置了格式: 字体: Symbol

删除了: $p\text{CO}_{2\text{sea}}$

删除了: observed

删除了: measured measured $p\text{CO}_2$ concentrations

删除了: ocean

删除了: waterwater ($p\text{CO}_{2\text{meas}}$) and in the atmosphere

删除了: $p\text{CO}_{2\text{sea}}$

删除了: $p\text{CO}_{2\text{meas}}$... $\text{CO}_{2\text{meas}}$ (110-1800 μatm), the variability of

删除了: and so the $p\text{CO}_{2\text{air}}$ is ... as set at a ... he cruise average

删除了: is was calculated in a similar way with that of k_{CO_2} . The

删除了: $\text{O}_{2\text{sea meas}}$ is ... the observed ... seawater DO concentration fr

删除了: mixed layer average NCP rates were estimated by four

设置了格式: 字体颜色: 自动设置

删除了: and

设置了格式: 字体颜色: 自动设置

删除了: The surface NCP can be estimated from the O_2/Ar measurements through an oxygen mass balance in the mixed layer under a steady state assumption, refer to Kaiser et al. (2005) and Cassar et al. (2011) for details. As shown in Fig. 2.

设置了格式: 字体颜色: 自动设置

删除了: /or injection) and biological processes (photosynthesis an

删除了:

where $[\text{O}_2]$ and $[\text{Ar}]$ are the O_2 and Ar concentrations of the seawater sample, $[\text{O}_2]_{\text{sat}}$ and $[\text{Ar}]_{\text{sat}}$ are the equilibrium saturation concentrations (Garcia and Gordon 1992; Hamme and Emerson 2004), and $\Delta(\text{O}_2/\text{Ar})$ is the biologically mediated oxygen supersaturation (Cassar et al. 2011).

$$\Delta(\text{O}_2/\text{Ar}) = \frac{[\text{O}_2]/[\text{Ar}]}{[\text{O}_2]_{\text{sat}}/[\text{Ar}]_{\text{sat}}} - 1 \quad (4)$$

If the influences of vertical mixing and lateral advection are neglected, the budget of the $[\text{O}_2]_{\text{biol}}$ in mixed layer can be described as (Kaiser et al. 2005):

$$\text{MLD} \frac{d[\text{O}_2]_{\text{biol}}}{dt} \approx \text{NCP} - k_{\text{O}_2} [\text{O}_2]_{\text{sat}} \Delta(\text{O}_2/\text{Ar}) \quad (5)$$

where where $[\text{O}_2]$ and $[\text{Ar}]$ are the O_2 and Ar concentrations of the seawater sample, $[\text{O}_2]_{\text{sat}}$ and $[\text{Ar}]_{\text{sat}}$ are the equilibrium saturation

下移了 [6]: where $[\text{O}_2]$ and $[\text{Ar}]$ are the O_2 and Ar concentrations of

移动了 (插入) [6]

删除了: (Cassar et al. 2011).

删除了:

设置了格式: 字体颜色: 自动设置

删除了: the second term on the right represents O_2 gas exchange

设置了格式

$$NCP_{O_2Ar} = \text{bioflux} = k_{O_2} [O_2]_{\text{sat}} \Delta(O_2/Ar) \quad (4)$$

The modeling study by Teeter et al., (2018) suggested that the bioflux accurately represents the exponentially weighted NCP over the past several residence times of O₂. The residence times of O₂ (MLD/gas transfer velocity of O₂, ~2.3 days during our cruise) refers to the length of time required to exchange O₂ between the mixed layer and the atmosphere (Kaiser et al., 2005; Teeter et al., 2018). To account for the wind speed history prior to the arrival of the ship at each station, the weighting technique of Reuer et al., (2007) modified by Teeter et al., (2018) was applied to calculate the gas exchange velocity of O₂ in this study.

NCP from the DO incubation: NCP was estimated with light/dark bottle incubation method at 43 CTD stations (Fig. 1). Surface water samples (~1.5 m) were collected from Niskin bottles into triplicate clear and black 300-ml BOD bottles (Wheaton). The initial oxygen saturation percentage and temperature in each bottle was measured by inserting a luminescent/optical dissolved oxygen probe (Hach LDO101, Hach Hq40d meter) into the bottle. Care was taken to avoid introducing air bubbles during this step. After recording the initial oxygen saturation percentage value, the probe was removed and the small volume displaced by the probe (3-5 ml) was replaced with filtered seawater from an offshore, low nutrient site. The addition of DO to the bottle from the replacement water was considered small, on the order of the method detection limit of approximately 2 mmol m⁻³ d⁻¹ (Murrell et al. 2009; 2013). Clear and dark bottles were placed into a deck incubator screened at 50% of ambient sunlight for 24 hours. The deck incubator was plumbed with flowing seawater from the MIDAS in order to maintain surface water temperatures. After 24 hours, the oxygen saturation percentage and temperature were measured again with the oxygen probe. DO concentrations obtained from the LDO probe were verified by comparison to DO concentrations measured by the spectrophotometric method of Pai et al., (1993) in a subset of samples (n = 14). The mean difference between the two methods of ±5% was consistent with previous comparisons of probe measured versus Winkler measured DO based on several hundred comparisons (Murrell et al. 2013).

The respiration rate was calculated from the DO changes in the dark bottles (R_{dark}, mmol O₂ m⁻³ d⁻¹). The respiration rate was assumed to be uniform in the mixed layer, thus, the integrated respiration over the MLD (Resp_{int}, mmol O₂ m⁻² d⁻¹) was calculated as Resp_{int} = R_{dark}*MLD. The gross primary production (GPP) varied with depth due to the reduction in light

删除了: 6

删除了: where k₀₂ was calculated from the 10-m COAMPS wind speed (Hodur 1997) following the wind speed-dependent parameterization of Sweeney et al. (2007). The weighting technique of Reuer et al. (2007) modified by Teeter et al. (2018) was applied to account for the 30-day wind speed history prior to the arrival of ship. Here Ar is assumed to be at equilibrium saturation ([Ar]/[Ar]_{sat} = 1 in Eq. 5), which introduces an error of ~1% into NCP estimate (Cassar et al. 2011).

设置了格式: 字体: 非倾斜

设置了格式

设置了格式: 字体颜色: 自动设置

设置了格式: 字体颜色: 自动设置

删除了: incubationincubation methods...at 43 CTD stations (Fig. ...

设置了格式

删除了: (3-5 ml)

设置了格式: 上标

删除了:

设置了格式: 字体颜色: 自动设置

删除了: The bottles were then capped with glass stoppers and placed in a deck incubator plumbed with flowing sea water from the MIDAS system in order to maintain surface water temperatures.

设置了格式: 字体颜色: 自动设置

设置了格式

删除了: Clear bottles were placed into boxes screened at 50% of ambient sunlight.

设置了格式: 字体颜色: 自动设置

设置了格式: 字体颜色: 自动设置

删除了: O₂

删除了: method were verified by comparison to O₂ ...O

设置了格式: 字体颜色: 自动设置

删除了: The rate of DO change (mmol O₂ m⁻³ d⁻¹) during an incubation was calculated from the difference in DO concentrations between the final and initial measurement. The rR

设置了格式

删除了: rate in the dark bottles (R_{DO})

删除了: The

设置了格式: 字体颜色: 自动设置

删除了: DO

设置了格式

availability with increasing depth. The mean percentage of PAR (%PAR) in the water column in relation to surface PAR (E_0) was calculated at each station as:

$$\%PAR = \frac{E_0}{K_d \cdot MLD} (1 - e^{-(K_d \cdot MLD)}) \quad (5)$$

where E_0 is 100 %, light attenuation (K_d, m^{-1}) is the rate of exponential decline in PAR as a function of depth as measured by the CTD. In our study, we assumed that GPP was linearly dependent on light up to a maximum GPP_{max} occurred when %PAR = 50 %. This assumption is based on previous measurements from this shelf that indicate photosynthesis begins to saturate at light level of $\sim 200 \mu\text{mol quanta m}^{-2} \text{ s}^{-1}$ (Lohrenz et al., 1994), which is roughly 50 % of light in the surface mixed layer (Lohrenz et al., 1999). GPP_{max} was thus estimated as $GPP_{max} = R_{light} - R_{dark}$ where R_{light} is the DO change rate in the light bottles. To calculate the integrated GPP in the mixed layer ($GPP_{int}, \text{mmol O}_2 \text{ m}^{-2} \text{ d}^{-1}$), the GPP was scaled by the light environment in the MLD:

$$\text{if } \%PAR \geq 50\%, GPP_{int} = GPP \cdot MLD \quad (6)$$

$$\text{if } \%PAR < 50\%, GPP_{int} = 2 \cdot \%PAR \cdot GPP \cdot MLD \quad (7)$$

The coefficient 2 in Eq. 7 was used so that the product $2 \cdot \%PAR$ would scale from 0 to 1, i.e., GPP approaches GPP_{max} at %PAR = 50 %. Finally, the NCP integrated over the MLD ($NCP_{DO-incub}, \text{mmol O}_2 \text{ m}^{-2} \text{ d}^{-1}$) was estimated as:

$$NCP_{DO-incub} = (GPP_{int} - Resp_{int}) \quad (8)$$

The standard errors of $NCP_{DO-incub}$ from triplicate bottle incubations across all sites were on average about 16 % of the mean. NCP from the non-conservative changes in DIC or nutrients: NCP can also be estimated from the biological-induced deviations of DIC or nutrients from the conservative mixing. We applied a three end-member mixing model (Huang et al., 2012) to distinguish the contribution from conservative mixing (X_{mix}) and the biological-induced change (ΔX_{biol}). The X_{mix} was calculated from the fractions of gulf surface seawater (f_{sw}), the Mississippi River water (f_{MR}), and the Atchafalaya River water (f_{AR}) together with the corresponding end-member concentrations shown in Table 1:

$$1 = f_{sw} + f_{MR} + f_{AR} \quad (9)$$

$$X_{mix} = X_{sw} \cdot f_{sw} + X_{MR} \cdot f_{MR} + X_{AR} \cdot f_{AR} \quad (10)$$

We used salinity and potential alkalinity ($PTA = TA + NO_3^-$) (Brewer and Goldman, 1976) as the two conservative tracers to constrain f_{sw} , f_{MR} , and f_{AR} using a non-negative least square method (Lawson and Hanson, 1974). The concentrations of

设置了格式: 字体颜色: 自动设置

域代码已更改

设置了格式: 字体颜色: 自动设置

设置了格式

删除了: Gross primary production

设置了格式

删除了: was

设置了格式: 字体颜色: 自动设置

删除了: calculated

设置了格式

删除了: DO...light + |

设置了格式: 字体颜色: 自动设置

删除了: $R_{DO-dark}$... where $R_{DO-light}$ is the average ...O change ratein

设置了格式

删除了: 8

设置了格式: 字体颜色: 自动设置

设置了格式: 字体颜色: 自动设置

设置了格式: 字体颜色: 自动设置

删除了: 9

设置了格式: 字体颜色: 自动设置

删除了: The Eq. 9 assumed that GPP was linearly dependent on light up to a maximum GPP that occurred when %PAR = 50.

设置了格式

删除了:

设置了格式: 字体颜色: 自动设置

设置了格式: 字体颜色: 自动设置

删除了: , NCP unit: $\text{mmol O}_2 \text{ m}^{-2} \text{ d}^{-1}$

设置了格式: 字体颜色: 自动设置

删除了: 10

设置了格式

删除了: and or nutrients: NCP can also be estimated from the

删除了: 11

删除了: $X_{mix} \dots_{mix} = X_{sw} \cdot f_{sw} + X_{MR} \cdot f_{MR} + X_{AR} \cdot f_{AR}$ (12

删除了: Here wWe used salinity and potential alkalinity (PTA = T

ΔDIC_{mix} and ΔNO_{xmix} from conservative mixing can then be calculated from Eq. 10, and the biological-induced changes in DIC

(ΔDIC_{NCP}) and ΔNO_{x} (ΔNO_{xNCP}) were estimated as:

$$\Delta DIC_{NCP} = \Delta DIC_{meas} - \Delta DIC_{mix} - \Delta DIC_{gas} \quad (11)$$

$$\Delta NO_{xNCP} = \Delta NO_{xmeas} - \Delta NO_{xmix} \quad (12)$$

where ΔDIC_{meas} and ΔNO_{xmeas} are the observed concentrations of DIC and ΔNO_{x} , and ΔDIC_{gas} is the DIC changes induced by air-

sea CO_2 exchange. Note that ΔDIC_{NCP} ($mmol\ C\ m^{-3}$) and ΔNO_{xNCP} ($mmol\ N\ m^{-3}$) represent the cumulative NCP-induced

changes in the concentrations of DIC and ΔNO_{x} since the mixing of river water with oceanic water. In order to calculate the

NCP rates derived from DIC (NCP_{ADIC} , $mmol\ C\ m^{-2}\ d^{-1}$) or ΔNO_{x} (NCP_{ANox} , $mmol\ N\ m^{-2}\ d^{-1}$), the MLD and plume residence

time (τ) need to be considered (Cai, 2003):

$$NCP_{ADIC} = \Delta DIC_{NCP} * MLD / \tau \quad (13)$$

$$NCP_{ANox} = \Delta NO_{xNCP} * MLD / \tau \quad (14)$$

To facilitate comparison with previous studies (Guo et al., 2012, Huang et al., 2012, Cai, 2003), τ values for the Mississippi plume were taken from Green et al., (2006) as 1, 1.5, and 6 days for salinity range of 0-18, 18-27, and 27-34.5 respectively.

In our study, we only calculated NCP_{ADIC} and NCP_{ANox} for stations in the Mississippi plume, because τ for the Atchafalaya plume is not available.

NCP unit conversion: To facilitate the comparison of NCP estimates from the different approaches, NCP rates were

converted to the same carbon units ($mmol\ C\ m^{-2}\ d^{-1}$) using the Redfield ratio of C:N:O₂ = 106:16:138. The photosynthetic molar ratio of C:O₂ for new and recycled production may vary between 1.1 (NH₄⁺ as nitrogen source) and 1.4 (NO₃⁻ as nitrogen source) (Laws, 1991). In our study region, the riverine input of NO₃⁻ was the main nitrogen source for biological

uptake (Table 1) and we considered the average Redfield ratio of C:O₂ = 106:138 to be appropriate. Although biological C:N

uptake may differ from the Redfield stoichiometry (Geider and La Roche, 2002; Sambrotto et al., 1993), the applicability of

the Redfield C:N ratio has been previously demonstrated in our study region (Huang et al., 2012; Xue et al., 2015) and

confirmed in this study.

删除了: DIC_{Mix} ... IC_{mix} and ...nd NO_xMix ... O_xmix from conservati...

删除了: can be

删除了: DIC_{obs} ... IC_{meas} - ... DIC_{Mix}

设置了格式: 下标

删除了: 13

删除了: NO_xobs ... O_xmeas - ... NO_xMix ... O_xmix (14)

删除了: DIC_{obs} ... IC_{meas} and NO_xobs

设置了格式: 下标

删除了: .

设置了格式: 下标

删除了: , NCP unit: mmol C m² d⁻¹ ... (15)

删除了: , NCP unit: mmol N m² d⁻¹ ... (16)

删除了: In order (To facilitate comparison with previous studies

删除了: we converted NCPNCP estimates from different approach...

设置了格式: 非上标/下标

删除了: (Table 1) is

设置了格式: 非上标/下标

删除了: the stoichiometry of

设置了格式: 字体: (默认) Times New Roman, 10 磅, 字体颜色: 自动设置, 图案: 清除

删除了: ratio (Geider and La Roche, 2002; Sambrotto et al., 1993)

2.5 1-D model for NCP and gas exchange

A simple 1-D model was used to examine the relationship between NCP and air-sea fluxes of O_2 and CO_2 . The environmental settings of the model were taken from the averaged condition during our study period: temperature = 22 °C, salinity = 35, TA = 2400 $\mu\text{mol L}^{-1}$, $pCO_{2\text{air}} = 405 \mu\text{atm}$, MLD = 6 m, and wind speed = 6 m s^{-1} . The initial state of the seawater was set to be in equilibrium with the atmosphere, and the concentrations of DO and pCO_2 in the seawater were modulated by time-dependent NCP functions and air-sea gas exchange at hourly time steps. At each time step, the relative changes in concentrations of DIC, TA, and DO resulting from NCP were assumed to follow the ratio of 106:17:138 (Zeebe and Wolf-Gladrow, 2001). The pCO_2 was calculated from DIC and TA using the CO2SYS program (Pierrot and Wallace, 2006). The air-sea flux of O_2 and CO_2 were calculated following Eq. 1 and Eq. 2.

设置了格式: 检查拼写和语法

带格式的: 标题 2, 行距: 单倍行距

3 Results

3.1 General pattern

The Mississippi and Atchafalaya Rivers typically experience peak discharge and NO_x loading in spring (Fig. S1). The peaks in discharge and NO_x in spring 2017 occurred later than the average condition during 1997-2017 and the monthly mean values of discharge and NO_x loading in April 2017 were slightly lower than the long-term mean values (Fig. S1). Surface water parameters (temperature, salinity, light transmittance, Chl-a, DO%, pCO_2 , and $\Delta O_2/Ar$) showed high spatial variability on the inner and middle shelf (bottom depth < 50 m), with much lower variability observed on the outer shelf (bottom depth > 50 m) (Fig. 2). The highest physical and biogeochemical variations were observed in the Mississippi plume during 8-11 April and in the Atchafalaya coastal region during 15-17 April (Fig. 3). In spring when river discharge is high and the wind is typically downwelling-favourable, the Mississippi River freshwater generally flows westward in a contained nearshore current (Zhang et al., 2012; Lehrter et al., 2013). Our three end-member mixing model accurately reproduced the westward extension of the Mississippi freshwater on the Louisiana shelf from the Mississippi bird's foot delta (Fig. 2b and Fig. 4a). The model also suggested a westward Atchafalaya plume trajectory in a narrow band along the coast with little Atchafalaya freshwater was transported upcoast toward the Mississippi Delta (Fig. 4b). The pattern of the Mississippi and Atchafalaya freshwater transport agreed well with the multiple-year average condition (2005-2010) in April by numerical simulation

设置了格式: 字体颜色: 自动设置

设置了格式: 下标

删除了: The discharges and NO_x loadings of the Mississippi River and Atchafalaya River exhibit typical seasonality with peaks in spring (Fig. S1). The

删除了: April spring 2017 is ...occurred slightly ...ater lower ...ha...

设置了格式: 字体颜色: 自动设置

删除了: while with much lower spatial ...ariability was ...bserved

删除了: toward the Texas coast

删除了: Southwest Pass ...Fig. 3b, ...ig. 2b and Fig. 5a...a), which

设置了格式: 字体: (默认) Times New Roman, 字体颜色: 自动设置

删除了: Our The model also suggested a westward Atchafalaya

删除了: also ...greed well with the multiple-year average

设置了格式: 字体: (默认) Times New Roman, 字体颜色: 自动设置

删除了: April simulation result

(Zhang et al., 2012). To better investigate the variability of surface water parameters, we divided the coastal region into four sub-regions: 1) the lower Mississippi River channel (Fig. S2, salinity < 2); 2) the Mississippi plume (Fig. 4a, east of 90.75° W, north of 28.30° N); 3) the high-turbidity Atchafalaya coastal water (Fig. 4a and Fig. 2d, 90.75-92.35° W, light transmittance < 20%, named as HTACW hereafter); and 4) the Atchafalaya plume (Fig. 4b, 92.35-93.50° W, north of 29.00° N). Typical vertical CTD profiles are shown in the supplement (Figs. S2-S4) to demonstrate the different mixing conditions observed in the four sub-regions as well as other regions in the nGOM.

3.2 Estimates of NCP

In comparison to the discrete measurements of $NCP_{DO-incub}$, NCP_{ADIC} , and NCP_{ANox} , the underway O_2/Ar measurements provided NCP_{O2Ar} estimates with the highest resolution and most complete spatial coverage (Fig. 5). The $NCP_{DO-incub}$, NCP_{ADIC} , and NCP_{ANox} were mostly obtained at salinities higher than 20, while the NCP_{O2Ar} covered the whole salinity range (0 to 36.4) providing more information on the NCP variability in the dynamic estuary environments. All methods suggested high variability of NCP in the surface water of the nGOM (Fig. 3c, Fig. 5) and these methods display similar spatial patterns with high production rates in the plume region around the Mississippi bird's foot delta (Fig. 5). The results of NCP_{ADIC} (-19.0 to 274.9 mmol C m⁻² d⁻¹) and NCP_{ANox} (1.6 to 314.0 mmol C m⁻² d⁻¹) were close to each other (Fig. 5c, d), and their ranges were similar to that of NCP_{O2Ar} in the Mississippi plume (-99.6 to 235.4 mmol C m⁻² d⁻¹) (Fig. 3c). $NCP_{DO-incub}$ (-56.0 to 360.7 mmol C m⁻² d⁻¹) gave the maximum NCP estimates in the Mississippi plume (stations C10, A7, and X3 in Fig. 5b and Fig. 3c). As NCP_{O2Ar} is a backward exponentially weighted average rate (Teeter et al., 2018), it is less able to capture high NCP values due to the inherent averaging of the O_2/Ar approach. Moreover, NCP_{O2Ar} could be a poor estimate of daily production rate (e.g., $NCP_{DO-incub}$ in our study) when the mixed layer is not at steady state (Teeter et al., 2018). These could explain the observed difference between NCP_{O2Ar} and $NCP_{DO-incub}$ in the dynamic Mississippi plume. In the high-salinity offshore waters, NCP_{O2Ar} and $NCP_{DO-incub}$ both suggest low NCP rates close to zero (Fig. 5a, b). One major difference between NCP_{O2Ar} and $NCP_{DO-incub}$ is that the O_2/Ar method generated negative NCP estimates in the lower Mississippi River channel and in the HTACW while $NCP_{DO-incub}$ suggested positive NCP rates in these regions (Fig. 5a, b).

删除了: (see Fig. 5 in Zhang et al., (2012))

上移了 [5]: (see Fig. 5 in Zhang et al., (2012))

移动了 (插入) [5]

删除了: of Zhang et al. (2012) during non-summer seasons (Fig. 5d).

移动了 (插入) [7]

删除了: the distribution and variability of the

删除了: threefour sub-regions (Fig. 5a, b)

删除了: (1)

设置了格式: 字体: (默认) Times New Roman, (中文) Times New Roman

删除了: to the east of 90.75° W, north of 28.30° N)... (2)

删除了: HTACW

设置了格式: 字体: (默认) +西文标题 (Times New Roman)

删除了: 90.5-92.3

设置了格式

删除了: ,

删除了: (3)

删除了: along the coast

删除了: Although the HTACW coastal water outside the Atchafalaya Bay (90.5-92.3°W, region 2 in Fig. 5a) was affected by the Mississippi freshwater (Fig. 5a), its properties mixing condition and water chemistry in this region were significantly different from those of in the Mississippi plume around the Mississippi Delta (Fig. 3). In comparison to the Mississippi plume, (This high-turbidity Atchafalaya coastal water (named as HTACW hereafter) HTACW was characterized by well-mixed water column, higher temperature, deeper MLD, lower light transmittance, lower DO% and lower $\Delta O_2/Ar$ (Fig. 3). The vertical SBE 911plus profiles showed that the water column in the HTACW was well mixed. Therefore, the HTACW cannot be simply treated as an extension of the Mississippi plume. To better investigate the distribution and variability of the surface water parameters, we divided the coastal region into three sub-regions (Fig. 5a, b): (1) the Mississippi plume (to the east of 90.5°W), (2) the HTACW (90.5-92.3°W), and (3) the Atchafalaya plume (92.3-93.5°W along the coast).

上移了 [7]: To better investigate the distribution and variability of the surface water parameters, we divided the coastal region into three sub-regions (Fig. 5a, b): (1) the Mississippi plume (to the east of 90.5°W), (2) the HTACW (90.5-92.3°W), and (3) the Atchafalaya plume (92.3-93.5°W along the coast).

删除了: As shown in Fig. 1, NCP_{ADIC} and NCP_{ANox} were only available at 30 stations in the Mississippi plume; $NCP_{DO-incub}$ estimates were generated via incubation experiments at 43 stations throughout the sampling region; while the underway O_2/Ar

设置了格式

删除了: Acknowledging the diverging estimates from different approaches (Fig. 4c), $NCP_{DO-incub}$, NCP_{ADIC} , NCP_{ANox} and NCP_{O2Ar} all displayed similar spatial pattern in the Mississippi plume with high production rates around the Mississippi bird's foot delta (Fig. 6a-

3.3 Mississippi River channel and plume

Vertical CTD profiles showed strong surface stratification in the lower Mississippi River channel (Fig. S2). The light transmittance in the surface water of the river channel was close to zero (Fig. 6a) and the Chl-a concentrations were low (Fig. 6b) despite the ample nutrient availability (NO_x up to $123 \mu\text{mol/kg}$, Table 1). Similar to most inner estuaries (Borges and Abril, 2011; Chen et al., 2012; Chen and Swaney, 2012), high $p\text{CO}_2$ (up to $1803.0 \mu\text{atm}$, Fig. 6c), undersaturated DO ($83.7 \pm 0.8\%$, Fig. 6d) and net CO_2 efflux ($55.5 \pm 7.6 \text{ mmol C m}^{-2} \text{ d}^{-1}$, Fig. 6e) was observed in the lower Mississippi River channel. The negative $\text{NCP}_{\text{O}_2\text{Ar}}$ ($-51.3 \pm 11.9 \text{ mmol C m}^{-2} \text{ d}^{-1}$, Fig. 6f) suggested net heterotrophic condition in the Mississippi River channel, which contrasts with the positive $\text{NCP}_{\text{DO-incub}}$ ($94.5 \pm 11.6 \text{ mmol C m}^{-2} \text{ d}^{-1}$, Fig. 7c) measured by the DO incubation method.

The Mississippi plume and most offshore regions were characterized by surface stratification, which was mainly caused by the buoyancy of fresher surface water in the plume and vertical temperature gradient in the offshore region (Fig. S3). With the increasing light transmittance (Fig. 6a) in conjunction with persistence of riverine-derived nutrient concentrations (Fig. 7a) along the Mississippi plume flow path, phytoplankton biomass reached high levels at intermediate salinities of 15–30 (Fig. 6b). The high Chl-a concentrations in the plume region corresponded to large decreases in $p\text{CO}_2$ (down to $113.9 \mu\text{atm}$, Fig. 6c) and strong oceanic CO_2 uptake (up to $42.7 \text{ mmol m}^{-2} \text{ d}^{-1}$, Fig. 6e), as well as elevated DO% (up to 180.1%, Fig. 6d) and NCP rates (Fig. 6f). The observed high NCP rates (e.g., up to $235.4 \text{ mmol C m}^{-2} \text{ d}^{-1}$ in $\text{NCP}_{\text{O}_2\text{Ar}}$, up to $360.7 \text{ mmol C m}^{-2} \text{ d}^{-1}$ in $\text{NCP}_{\text{DO-incub}}$, Fig. 7c) are within the range of prior estimates for this region during spring season (up to $624.0 \text{ mmol C m}^{-2} \text{ d}^{-1}$, Cai, 2003; Guo et al., 2012; Huang et al., 2012; Lohrenz et al., 1990, 1997, 1999), and are among the highest in large river estuarine and shelf waters (Cooley and Yager, 2006; Dagg et al., 2004; Ning et al., 1988; Terson et al., 2000).

3.4 Atchafalaya plume and HTACW

The Atchafalaya River discharges in a shallow broad, low-gradient shelf (10 m isobath doesn't occur until more than 40 km offshore of the delta, Fig. 1) which frequently experiences cross-shelf currents (Roberts and Doty, 2015). The Atchafalaya plume water, extended westward in a narrow band along the coast (Fig. 4b), generally showed similar biogeochemical variability to that observed in the Mississippi plume (Fig. 6). Within the Atchafalaya plume, elevated Chl-a, DO%, and $\text{NCP}_{\text{O}_2\text{Ar}}$ were observed together with a dropdown in $p\text{CO}_2$ and oceanic CO_2 uptake (Fig. 6). For both the Mississippi and

删除了:

删除了: In the shallow, well-mixed Mississippi river channel, ...

删除了: , 8b

删除了: ($55.5 \pm 7.6 \text{ mmol C m}^{-2} \text{ d}^{-1}$, Fig. 7e

删除了: , 8d

删除了: river River channel, ... which is similar to most inner

删除了: (Fig. 7a, 8a)... phytoplankton biomass reached high level

删除了: , 8b

删除了: ThisThe high Chl-a concentrations in the plume region

删除了: , 8b

删除了: 7f

删除了: , 8c

删除了: , up to 361

设置了格式: 非上标/下标

删除了: -238

删除了: Lohrenz et al. 1997; Lohrenz et al.

设置了格式: 字体颜色: 自动设置

删除了: The results of the three end-member mixing model suggested that the enhanced biological production also resulted in significant non-conservative removal of DIC (up to $250 \mu\text{mol kg}^{-1}$, Fig. S2a) and nutrients (up to $35 \mu\text{mol kg}^{-1}$ in NO_x , Fig. S2b) in the mid-salinity range of the Mississippi plumes, similar with the findings of previous studies (Cai, 2003; Guo et al., 2012; Huang et al., 2012). The biological uptake ratio of NO_x and DIC (0.14 in Fig. S2c) was close to the Redfield N:C ratio (16/106=0.15).

删除了: and HTACW

删除了: cross cross-shelf currents (Roberts and Doty, 2015). The

设置了格式: 字体颜色: 自动设置

删除了: NCP

设置了格式: 字体颜色: 自动设置

删除了: at intermediate salinities coupled

设置了格式

删除了: sink

设置了格式: 字体颜色: 自动设置

删除了: 7

删除了: The observation results in the Atchafalaya plume were characterized by elevated Chl-a, DO%, and NCP at intermediate salinities coupled with dropdown in $p\text{CO}_2$ and oceanic CO_2 sink (Fig. 7).

Atchafalaya plume regions, the three end-member mixing model suggests that the enhanced biological production resulted in significant deviations of DIC and NO_x from their conservative mixing lines (Fig. 8). The amplitudes of the non-conservative biological removal of nutrients (up to $35 \mu\text{mol kg}^{-1}$ in $\Delta\text{NO}_{3\text{NCP}}$, Fig. 8a) and DIC (up to $250 \mu\text{mol kg}^{-1}$ in $\Delta\text{DIC}_{\text{NCP}}$, Fig. 8b) are similar to the findings of previous studies in the nGOM (Cai, 2003; Guo et al., 2012; Huang et al., 2012). The biological uptake ratio of $\Delta\text{NO}_{3\text{NCP}}$ and $\Delta\text{DIC}_{\text{NCP}}$ (0.14 in Fig. 8c) was close to the Redfield N:C ratio (16/106). However, $\text{NCP}_{\text{O}_2\text{Ar}}$ suggested that the southwest part of the Atchafalaya plume was heterotrophic (around 29.30°N , 93.50°W , Fig. 5a). A detailed examination of the CTD profiles revealed that the water column in this area was vertically well-mixed (Fig. S4), which was different than the stratification condition observed in other plume regions.

The HTACW was characterized by a well-mixed water column and low light transmittance (Fig. S4). Although the Chl-a concentrations in the HTACW were similar to those in the Atchafalaya plume in the salinity range of 24 to 32 (Fig. 6b), the $\text{DO}\%$ was much lower and undersaturated in the HTACW (94.7%, Fig. 6d). The $p\text{CO}_2$ ($327.8 \pm 34.6 \mu\text{atm}$) in the HTACW was higher than that in the Atchafalaya plume ($288.7 \pm 43.7 \mu\text{atm}$) at the same salinities (Fig. 6c), but the HTACW still acted as a weak sink for atmospheric CO_2 ($-7.1 \pm 3.1 \text{ mmol C m}^{-2} \text{ d}^{-1}$, Fig. 6e). Similar to that in the Mississippi River channel, the two approaches for NCP estimation presented different results in the HTACW: the negative $\text{NCP}_{\text{O}_2\text{Ar}}$ ($-39.2 \pm 14.0 \text{ mmol C m}^{-2} \text{ d}^{-1}$, Fig. 5a) suggests net heterotrophic condition, while $\text{NCP}_{\text{DO-incub}}$ rates were positive ($62.6 \pm 23.3 \text{ mmol C m}^{-2} \text{ d}^{-1}$, Fig. 5b).

4. Discussion

4.1 Comparison of NCP estimations

A comparison of NCP estimated from various methods should be interpreted with caution as each approach has its independent assumptions and limitations and refers to different temporal and spatial scale (Ulfsbo et al., 2014). However, applying multiple methods provides complementary information to better understand the processes affecting the metabolism of the ecosystem.

NCP from the DO incubation method: The $\text{NCP}_{\text{DO-incub}}$ was estimated from the 24-hour DO changes in incubation bottles, which gives a daily NCP estimate for the plankton community at the sampling location. The DO incubation method is a direct measurement of NCP and this method is free from the influences of lateral advection and sediment metabolism. The

删除了: .

设置了格式: 字体颜色: 文字 1

删除了: 3.5 HTACW

删除了: (region 2 in Fig 5a)

删除了: 25

删除了: 30

删除了: 7b

删除了: undersaturated DO were observed in the HTACW together with low light transmittance

设置了格式: 字体: (默认) Times New Roman, (中文) Times New Roman

删除了: 7a

删除了: .

删除了: concentrations

删除了: numbers

设置了格式: 字体: Symbol

删除了: were

删除了: generally

删除了: those

删除了: 7c

删除了: the HTACW

删除了:

删除了: 7e

删除了: river

删除了: rates

删除了: heterotrophy

删除了: (numbers, Fig. 6a)

设置了格式: 突出显示

删除了: indicates net autotrophy (numbers, Fig. 6b)

删除了: .

设置了格式: 字体颜色: 自动设置

删除了: In our study, the NCP rates estimated from different independent approaches refer to different temporal and space scales. The $\text{NCP}_{\text{DO-incub}}$ was estimated from the 24-hour DO changes in incubation bottles, which gives a snapshot of daily estimate for the ecosystem in the water column at the sampling location. The NCP_{DIC} and NCP_{NO_x} in the Mississippi plume reflected the average community production rate along the flow path over the transit time of the plume water since the beginning of river-ocean mixing proc...

设置了格式: 字体颜色: 自动设置

设置了格式: 字体颜色: 自动设置

设置了格式: 字体颜色: 自动设置

删除了: .

$NCP_{DO-incub}$ thus equals the MLD-integrated NCP in the stratified regions (NCP_{MLD} in Fig. 9a, c) or the water column-integrated NCP in the well-mixed regions (NCP_{water} in Fig. 9b). However, there are uncertainties related to scaling from samples collected at discrete depths to integrated mixed layer NCP values. First, the scaling method used here assumes a homogenous distribution of respiration rate over the MLD. Second, we only measured GPP at one light level (50 %) and we assumed that the GPP below 50 % surface PAR was linearly scaled to %PAR (Eq. 6 and Eq. 7). Similar assumptions for the Louisiana shelf were tested previously by Murrell and Lehrter, (2011) who found that single point measurements (vs. multi-point measurements in a layer) provided robust estimates of integrated rates. However, in the current study, the assumption has been further applied to shallow nearshore sites (< 10 m depth), which may exhibit greater heterogeneity in vertical PAR distributions due to the high algal biomass and suspended sediment particle concentrations. More importantly, for high-turbidity water samples (e.g., samples collected in the Mississippi River channel and in the HTACW), the incubated samples were not mixed in the same way as that in the natural environment and the sedimentation of particles in incubation bottles could alleviate the light limitation for phytoplankton. As a result, the gross primary production (GPP_{int} in Eq. 8) could be overestimated and $NCP_{DO-incub}$ would not represent the true *in situ* NCP in but high-turbidity waters but as an overestimation.

NCP from the O₂/Ar method: NCP_{O_2Ar} is derived from the air-sea biological oxygen flux (Eq. 4), which represents the exponentially weighted NCP over the past several residence times of O₂ (Kaiser et al. 2005; Teeter et al. 2018). When using the O₂/Ar method to estimate NCP_{MLD} , a key assumption is the negligible physical inputs to the mixed layer. However, this assumption can be invalid in the dynamic coastal environments. Recent studies have shown that entrainment and upwelling processes (mixing with O₂-depleted subsurface water) can lead to significant underestimation in NCP_{MLD} using the O₂/Ar method, especially in coastal upwelling zones (Castro-Morales et al., 2013; Nicholson et al., 2012; Shadwick et al., 2015; Teeter et al., 2018). As most regions in our study were characterized by the persistent surface stratification (Fig. S2 and S3), the influences of sub-pycnocline ($NCP_{sub-MLD}$ in Fig. 9a, c) and benthic metabolisms ($NCP_{benthic}$ in Fig. 9a, c) on the surface O₂/Ar ratio were expected to be minor. On the contrary, the surface O₂/Ar ratio in the well-mixed nearshore regions (e.g., the HTACW, Fig. S4) was affected by both water column (NCP_{water}) and benthic metabolisms ($NCP_{benthic}$) (Fig. 9b). Moreover, both Mississippi and Atchafalaya river end members were highly heterotrophic and the lateral transportation of this heterotrophic signal carried by river water (NCP_{adv} in Fig. 9) should be considered. As it generally takes a few days for O₂ to

设置了格式: 字体颜色: 自动设置

带格式的: 左, 定义网格后不调整右缩进, 不调整西文与中文之间的空格, 不调整中文和数字之间的空格

删除了: A

设置了格式: 下标

设置了格式: 字体颜色: 自动设置

设置了格式: 字体颜色: 自动设置

删除了: of the O₂/Ar method

设置了格式: 字体颜色: 自动设置

删除了: physically isolated condition with

设置了格式: 字体颜色: 自动设置

设置了格式: 下标

删除了: NCP using the O₂ budget approach

删除了: areas with low biological production rates and in

设置了格式: 字体颜色: 自动设置

删除了: The

删除了: entrainment and upwelling

设置了格式: 下标

设置了格式: 下标

删除了: is

删除了: in most areas of our study region because of the persistent spring-summer halocline stratification (Fig. 3c). However, the contribution from benthic metabolism in the well-mixed Mississippi river channel and the HTACW adds an additional complexity to the O₂/Ar approach. In these well-mixed shallow waters, NCP_{O_2Ar} reflected not only the NCP in the mixed layer, but the NCP in the whole water column including the signals of benthic processes. An additional source of uncertainty in NCP_{O_2Ar} is associated with the calculation of the bioflux of O₂. Although the variable gas transfer velocity can be considered using a weighting technique for wind speed history (Reuer et al. 2007; Teeter et al. 2018), O₂ flux calculated from different wind speed parameterizations (Liss and Merlivat 1986; Nightingale et al. 2000; Sweeney et al. 2007; Wanninkhof 1992) could result in a relative variability of 15%.

设置了格式: 字体颜色: 自动设置

设置了格式: 字体颜色: 自动设置

设置了格式: 下标

设置了格式: 字体颜色: 自动设置

设置了格式: 字体颜色: 自动设置

设置了格式: 字体颜色: 自动设置

become in equilibrium with the atmosphere (see the discussion below), NCP_{adv} could play an important role affecting the O_2/Ar ratio in the river channel and estuary where water transport speed was rapid (Fig. 9a, b). The influence of NCP_{adv} decreased offshore and the impact of remote source water heterotrophy was negligible in most offshore regions where water residence time was sufficiently long (Fig. 9c). Therefore, NCP_{O_2Ar} represented the metabolic state of the water which was affected not only by local aquatic ecosystem (NCP_{MLD} or NCP_{water} in Fig. 9), but also by additional factors including $NCP_{benthic}$ and NCP_{adv} (Fig. 9). Depending on the different mixing conditions, NCP_{O_2Ar} reflected 1) the combined result of NCP_{MLD} and NCP_{adv} in the stratified river channel and plume region; 2) the combined result of NCP_{water} , $NCP_{benthic}$, and NCP_{adv} in the well-mixed nearshore waters (e.g., HTACW); 3) NCP_{MLD} in the offshore stratified regions where the riverine influence was minor. As $NCP_{benthic}$ only affected a small portion of the nearshore water in the Atchafalaya coastal region, the NCP_{O_2Ar} measured in this study was mainly modulated by NCP_{MLD} and NCP_{adv} . Considering the nGOM as a whole, lateral advection of NCP_{adv} can be considered as internal transport within the system given that the NCP_{O_2Ar} was measured with adequate spatial coverage. As a result, the NCP_{O_2Ar} measured in this study well represented the overall metabolic state of the surface water of the nGOM.

NCP from the non-conservative changes in DIC and nutrients: The NCP_{ADIC} and NCP_{ANox} in the Mississippi plume reflected the average community production rate along the flow path during the river-ocean mixing process. There are several sources of uncertainty associated with the NCP estimated from the non-conservative mixing change in DIC and nutrients. First, errors in estimating water residence time and the changes in MLD over the transit time of the plume water lead to proportional errors in the calculation of NCP_{ADIC} and NCP_{ANox} (Eq. 13 and Eq. 14). The plume water residence time is a function of river discharge and other physical conditions, it is therefore expected that using a set of past model-assessed τ values probably would introduce the largest uncertainty in the estimation of NCP_{ADIC} and NCP_{ANox} . Second, uncertainty may be caused by the changes in the concentrations of DIC and nutrients of the river end members. However, this uncertainty decreases with salinity (Huang et al., 2012) and was generally low in our study.

To better investigate the NCP rates estimated from different methods, we focused on the regions where NCP_{O_2Ar} and $NCP_{DO-incub}$ provided contrasting results: NCP_{O_2Ar} suggested heterotrophy in the Mississippi River channel and in the HTACW where positive $NCP_{DO-incub}$ rates were presented. The contrasting results of NCP_{O_2Ar} and $NCP_{DO-incub}$ can be mainly explained

设置了格式

设置了格式

设置了格式

上移了 [3]: In addition, the If the incubated samples are not mixed in the same way as natural water, the majority of the sediment probably sink to the bottom of the bottle and the light availability is bigger than in natural waters overestimating NCP.

删除了:
NCP from the DO incubation method: Although the DO incubation method is a direct measurement of NCP, there are uncertainties related to scaling from samples collected at discrete depths to integrated surface mixed layer values. First, the scaling method used here assumes a homogenous distribution of respiration rate over the MLD. Second, we only measured GPP at one light level (50%) and we assumed that the GPP at this level was maximal and that GPP below 50% surface PAR was linearly scaled to % PAR (Eqs. 8, 9). Similar assumptions for the Louisiana shelf were tested previously by Murrell and Lehrer (2011) who found that single point measurements (vs. multi-point measurements in a layer) provided robust estimates of integrated rates. However, in the current study, the assumption has been further applied to shallow nearshore sites (< 10 m depth), which may exhibit greater heterogeneity in vertical PAR distributions due to the very high biomass and suspended sediment particles. In addition, the If the incubated samples are not mixed in the same way as natural water, the majority of the sediment probably sink to the bottom of the bottle and the light availability is bigger than in natural waters overestimating NCP. More importantly, the bottle incubation method accounts for the NCP by plankton community but is not able to detect the impact of sediment metabolism (e.g., benthic respiration in the Mississippi river channel and the HTACW). In addition, the If the incubated samples are not mixed in the same way as natural water, the majority of the sediment probably sink to the bottom of the bottle and the light availability is bigger than in natural waters overestimating NCP.

设置了格式

设置了格式

设置了格式

移动了 (插入) [3]

设置了格式

删除了: First

删除了: s to proportional errors in the NCP

设置了格式: 字体颜色: 自动设置

删除了: estimation (Eqs... 15...3, ...and Eq. 16...4). The plume

设置了格式: 字体: (中文) Arial Unicode MS

删除了:
Considering the different temporal and spatial resolutions and uncertainties associated with different approaches, a comparison of

设置了格式: 字体: (中文)+中文正文(宋体),(中文)中文(中国)

下移了 [4]: In the Mississippi plume, all methods showed strong heterogeneity in the dynamics Mississippi plume regions (Fig. 6a-d,

移动了 (插入) [4]

删除了: river River channel and in the HTACW where positive

by the different spatial and temporal scales associated with the two methods responding to the mixing conditions. In the high-turbidity Mississippi River channel (light transmittance close to zero) and HTACW (light transmittance <20 %), the GPP was strongly limited by light availability and the DO incubation method could result in significant overestimation in the *in situ* GPP and NCP due to the improved light environment in the incubation bottles. However, the measured community respiration rates (Resp_{mt} in Eq. 8) in the lower Mississippi River channel (14.0±0.8 and mmol C m⁻² d⁻¹) and in the HTACW (30.5±10.7 and mmol C m⁻² d⁻¹) were not able to fully account for the heterotrophy suggested by NCP_{O₂A_r} (-51.3±11.9 and -39.2±14.0 mmol C m⁻² d⁻¹ in the lower Mississippi River channel and HTACW respectively) even when the GPP was not taken into account (assuming GPP_{mt} = 0 in Eq. 9). This indicates sources of heterotrophic signal other than the local community respiration in these two regions. In the stratified lower Mississippi River channel (Fig. 9a), the influence of lateral transportation of the heterotrophic river water from the upper river channel was significant because of the short water residence time (~1 day, Green et al., 2006). Therefore, the heterotrophic condition in the lower Mississippi River channel could be attributed to the dominant influence of the heterotrophic NCP_{adv} over the local biological production. In the vertically well-mixed HTACW (Fig. 9b), NCP_{O₂A_r} reflected the combined result of the water column community production, the lateral advection of CO₂-rich Atchafalaya river water (NCP_{adv}), and sediment metabolism (NCP_{benthic}). High sediment oxygen consumption and bottom water community respiration rates were observed in the Atchafalaya River Delta Estuary (Roberts and Doty, 2015) and on the Louisiana continental shelf (Murrell and Lehrter, 2011; Murrell et al., 2013). These studies suggested that the total below-pycnocline respiration rates show low variability over a large geographic and temporal range in the nGOM (46.4 to 104.5 mmol O₂ m⁻² d⁻¹). The negative NCP_{O₂A_r} observed in the HTACW by our study (-39.2±14.0 mmol C m⁻² d⁻¹) agreed with the finding of Murrell et al., (2013) which showed shelf-scale net water column heterotrophy on the Louisiana shelf. This water column heterotrophy can be well explained by the combined results of NCP_{water}, NCP_{benthic} and NCP_{adv}. The same logic can be applied to explain the net heterotrophy observed in the southwest part of the Atchafalaya plume with well-mixed water column (negative NCP_{O₂A_r} around 29.30° N, 93.50° W, Fig. 5a).

4.2 Controls on the surface NCP and CO₂ flux

设置了格式: 字体: 倾斜

设置了格式: 字体颜色: 自动设置

设置了格式: 字体颜色: 自动设置

设置了格式: 字体颜色: 自动设置

设置了格式: 字体颜色: 自动设置

设置了格式: 字体颜色: 自动设置

设置了格式: 字体颜色: 自动设置

设置了格式: 字体颜色: 自动设置

设置了格式: 字体颜色: 自动设置

设置了格式: 字体颜色: 自动设置

设置了格式: 下标

删除了: These nearshore waters were characterized by well-mixed water column which indicates that the surface O₂/A_r could be affected by vertical mixing with sub-pycnocline waters and benthic metabolism. In these well-mixed waters, the DO incubation approach accounted for the plankton production in the mixed layer while the NCP_{O₂A_r} approach reflected the NCP of the whole water column including the benthic signals. On one hand, production in the mixed layer only represented a fraction of the total production of the water column as the euphotic depth commonly extended below the pycnocline and sub-pycnocline chlorophyll maxima were frequently observed in the nGOM (Lehrter et al. 2009). The study by Lehrter et al. (2009) suggested a substantial fraction (25-50%) of phytoplankton production occurs beneath the pycnocline. On the other hand, high sediment oxygen consumption and bottom water plankton community respiration rates were observed on the Louisiana continental shelf (Murrell et al. 2013). By comparing rates of water column primary productivity and community respiration, Murrell et al. (2013) showed shelf scale net heterotrophy metabolism for the whole water column on the Louisiana shelf. Therefore, the different results from NCP_{DO-incub} and NCP_{O₂A_r} in the Mississippi river channel and the HTACW were not contradictory: NCP_{DO-incub} suggested autotrophic production of the plankton community in these nearshore waters while NCP_{O₂A_r} indicated net heterotrophy metabolism for the whole water column mainly resulting from benthic respiration. As the underway O₂/A_r method provides the highest resolution NCP estimation coupled with pCO₂ measurement, NCP_{O₂A_r} was presented together with the CO₂ variables in the following sections to investigate the variability and controls of the metabolic balance in the nGOM.

As the underway O₂/Ar method provided the highest resolution NCP estimation coupled with pCO₂ measurement, NCP_{O₂/Ar} was presented together with the CO₂ variables in the following sections to investigate the variability and controls of the metabolic balance. Nutrients, irradiance, and mixing were considered to be the major controlling factors of biological production in coastal waters of the nGOM (Lehrter et al., 2009; Lohrenz et al., 1999; Murrell et al., 2013; Turner and Rabalais, 2013). Here we use the results in the Mississippi plume (averaged over increments of two salinity units, Fig. 7) to demonstrate the controlling mechanisms of the changes in surface NCP and CO₂ flux along with the increasing salinity. There is an ecological gradient along the river-ocean mixing continuum: from turbid, eutrophic, freshwater to clear, oligotrophic offshore oceanic waters (Fig. 7a). The freshwater input from the Mississippi River was characterized by strong heterotrophy with high DIC and pCO₂, supported by the decomposition of terrestrial organic carbon (Bianchi et al., 2010). Meanwhile, phytoplankton growth and production was limited by light availability in the high-turbidity Mississippi River channel despite the high nutrient concentration (Fig. 7a-c). The net heterotrophy of the water at the low salinity end and the corresponding CO₂ release (Fig. 7d) were attributed to the terrestrial carbon input, light limitation on primary production, and short water residence time (Lehrter et al., 2009; Lohrenz et al., 1990; 1999; Roberts and Doty, 2015). While high CO₂ efflux was observed at low salinities, its contribution to the overall regional CO₂ flux was relatively small due to the limited spatial coverage of low salinity regions (Huang et al., 2015). Due to the alleviation of light limitation in conjunction with persistence of riverine nutrient concentrations, Chl-a, DO% and NCP_{O₂/Ar} all showed an increasing trend with salinity along the flow path of the Mississippi plume (Fig. 8). A positive correlation between the mean NCP_{O₂/Ar} rates and Chl-a concentrations (Fig. 7b, d) was observed in the Mississippi plume (r² = 0.75, figure not shown) where light availability generally determined the onset of the biological growth and the river-borne nutrient loading set the magnitude of biological production (Fig. 7, Fig. 8). At intermediate salinities (15 to 30) in the Mississippi plume, there existed an “optimal growth region”, where light and nutrient availability were both favourable for phytoplankton growth (Fig. 7) (Cloern et al., 2013; Demaster et al., 1996; Seguro et al., 2015). High NCP_{O₂/Ar} (114.8±54.6 mmol C m⁻² d⁻¹) was observed in this optimal growth region corresponding to an oceanic CO₂ uptake of -13.5±5.3 mmol C m⁻² d⁻¹ (Fig. 7d). In high-salinity offshore water, phytoplankton growth and production were primarily limited by depleted nutrient concentration (Lehrter et al. 2009; Lohrenz et al. 1990; Lohrenz et al. 1999). Because of the minor terrestrial

删除了: the nGOM coastal waters of the nGOM (Lehrter et al., 20...

删除了: As shown in Fig. 8a, t

删除了: high eutrophic nutrient... and turbid ... freshwater to clear, ...

设置了格式

删除了: (e.g., DIC = 2312 μmol kg⁻¹, Table 1) and

设置了格式: 字体颜色: 自动设置

删除了: organic carbon (Bianchi et al., 2010). ... Meanwhile, ...

设置了格式: 下标

删除了: at the low salinity end... were attributed to the terrestrial ...

设置了格式

删除了: we observed

设置了格式: 字体颜色: 自动设置

删除了: its

设置了格式

删除了: 3030) in the Mississippi plume, there exists ... existed an ...

删除了: are were both favorable... favourable for phytoplankton ...

influence and low biological production, DO and $p\text{CO}_2$ in the offshore gulf water were close to equilibrium with atmosphere and $\text{NCP}_{\text{O}_2\text{Ar}}$ and CO_2 flux were close to zero (Fig. 7).

The spatial variability of NCP and CO_2 flux in the nGOM are associated with the trajectory of the Mississippi and Atchafalaya plume as the surface biogeochemical variations are strongly affected by riverine influences. For instance, an unusually broad plume extension in the nGOM in March 2010, driven by upwelling favourable wind and high freshwater discharge, was associated with elevated chlorophyll concentrations and stronger biological CO_2 uptake (Huang et al., 2013). Modeling studies also suggested that NCP and CO_2 flux in the nGOM were susceptible to changes in river and wind forcing (Fennel et al., 2011; Xue et al., 2016). To better study the variability of surface NCP and CO_2 flux, further studies are needed to investigate how the seasonal and inter-annual variations in environmental conditions (freshwater discharge, riverine inputs of carbon and nutrients, wind forcing, coastal circulation etc.) affect the trajectory of the river plume and the biological processes therein.

4.3 Coupling between NCP and CO_2 flux

Overall, the surface water of the nGOM (93.00-89.25° W, 28.50-29.50° N) was estimated to be net autotrophic during our study period with an area-weighted mean $\text{NCP}_{\text{O}_2\text{Ar}}$ rate of $21.2 \text{ mmol C m}^{-2} \text{ d}^{-1}$ and as a CO_2 sink of $-6.7 \text{ mmol C m}^{-2} \text{ d}^{-1}$.

When plotting the paired CO_2 flux and $\text{NCP}_{\text{O}_2\text{Ar}}$ data (Fig. 10), most data collected in the lower Mississippi River channel fall in quadrant 2, suggesting net heterotrophy coupled with CO_2 outgassing to the atmosphere. The Mississippi plume and Atchafalaya plume exhibited opposite patterns with most data in these regions being in quadrant 4 (net autotrophy coupled with CO_2 uptake from the atmosphere). However, the data in quadrant 1 (autotrophic water as a CO_2 source observed near the Mississippi River mouth) and quadrant 3 (heterotrophic water as a CO_2 sink in the HTACW) suggest decoupling between $\text{NCP}_{\text{O}_2\text{Ar}}$ and CO_2 flux.

Here we use the 1-D model (Section 2.5) to investigate the relationship between NCP and air-sea gas fluxes of O_2 and CO_2 .

We calculated the re-equilibrium time for O_2 and CO_2 following the occurrence of 10 days biological modification; NCP was set as 50 (net autotrophy) or -50 (net heterotrophy) $\text{mmol C m}^{-2} \text{ d}^{-1}$ from days 0 to 10, and as zero after day 11 (Fig. S5). The air-sea O_2 flux rapidly reached a balance with the NCP-induced O_2 changes for both the autotrophy and heterotrophy simulations with the re-equilibrium time for O_2 for each estimation to be a few days (Fig. S5). Given the same environmental

- 删除了: concentrations
- 设置了格式
- 删除了: rates were close to zero (Fig. 3...7). Overall, the study
- 设置了格式
- 带格式的
- 删除了: patterns variability of NCP and CO_2 flux in the nGOM ar
- 设置了格式
- 删除了: would affect the trajectory of the river plumes
- 删除了: The NCP affects air-sea gas exchange through its influen
- 设置了格式
- 设置了格式
- 删除了: As shown in Fig. 9, m
- 设置了格式
- 删除了: $\text{NCP}_{\text{O}_2\text{Ar}}$ and CO_2 flux
- 设置了格式
- 删除了: with
- 设置了格式
- 删除了: negative NCP rates (net heterotrophy) associated with CO
- 设置了格式
- 删除了:
- 设置了格式
- 删除了: waters exhibited opposite patterns with most of the ...ata
- 设置了格式
- 删除了: Fig. 9), which had positive NCP rates and a CO_2 sink for
- 设置了格式
- 删除了: This indicates strong coupling between the elevated
- 设置了格式
- 删除了:
- 删除了: assumed
- 设置了格式
- 删除了: 3010-
- 设置了格式
- 删除了: net
- 设置了格式
- 删除了: autotrophic production...odification (
- 设置了格式
- 设置了格式
- 设置了格式
- 删除了: 100
- 设置了格式
- 删除了:)
- 设置了格式
- 删除了: 30 10, and as zero after day 11 (Fig. S5)as well as 30-day
- 设置了格式
- 删除了: Both for the autotrophy and heterotrophy simulations, the
- 设置了格式

settings, the re-equilibrium time for CO_2 was much longer (more than one month, Fig. S5). This is related to the relative slow air-sea CO_2 exchange rate, and, more importantly, the carbonate buffering system, i.e., the gas exchange-induced changes in aquatic CO_2 are buffered by a much larger carbon pool of HCO_3^- - CO_3^{2-} (Zeebe and Wolf-Gladrow, 2001). NCP affects air-sea gas exchange of CO_2 through its influence on $p\text{CO}_2$ in the surface water. Net autotrophy results in a net biological uptake of CO_2 from the seawater (decrease in $\Delta p\text{CO}_{2(\text{sea-air})}$ in Eq. 1) while net heterotrophy has the opposite effect. However, $\Delta p\text{CO}_{2(\text{sea-air})}$ is not only affected by the *in situ* NCP ($\Delta p\text{CO}_{2\text{NCP}}$), but also by the background level of $\Delta p\text{CO}_2$ which is related to the preceding mixing and biological processes ($\Delta p\text{CO}_{2\text{background}}$): $\Delta p\text{CO}_{2(\text{sea-air})} = \Delta p\text{CO}_{2\text{background}} + \Delta p\text{CO}_{2\text{NCP}}$. Therefore, local ecosystem net autotrophy (negative $\Delta p\text{CO}_{2\text{NCP}}$) does not necessarily result in CO_2 uptake from the atmosphere (negative $\Delta p\text{CO}_{2(\text{sea-air})}$) if the NCP-induced $p\text{CO}_2$ decrease occurs in a water with high heterotrophic background (highly positive $\Delta p\text{CO}_{2\text{background}}$). Similarly, net heterotrophy does not necessarily result in a CO_2 outgassing if the $\Delta p\text{CO}_{2\text{background}}$ of the source water is highly autotrophic.

In the simulation with time-dependent varying NCP rates (Fig. 11), we demonstrated how the preceding biological processes and the lingering background $p\text{CO}_2$ affect the relationship between NCP and CO_2 flux. The NCP rate in this simulation was set as 0 during days 0 to 30, changed to $-50 \text{ mmol C m}^{-2} \text{ d}^{-1}$ (net heterotrophy) during days 31 to 60, then to $100 \text{ mmol C m}^{-2} \text{ d}^{-1}$ (net autotrophy) during days 61 to 90, and to $-50 \text{ mmol C m}^{-2} \text{ d}^{-1}$ again during days 91 to 120 (Fig. 11a). Although NCP changed instantly, the backward exponentially weighted NCP derived from the bioflux of O_2 ($\text{NCP}_{\text{O}_2\text{A}_t}$ in Fig. 11a) lagged a few days behind NCP. After each change in NCP, the memory effect of the preceding NCP on DO tends to be small as the air-sea O_2 exchange quickly balanced the NCP-induced O_2 production or consumption within several days (Fig. 11b, c). On the contrary, the slow CO_2 gas exchange and long re-equilibrium time of CO_2 generated a significant memory effect of the preceding NCP on $\Delta p\text{CO}_{2(\text{sea-air})}$ (Fig. 11b, c). The combined result of *in situ* production and the lingering effect of background $p\text{CO}_2$ thus resulted in the decoupling between $\text{NCP}_{\text{O}_2\text{A}_t}$ and CO_2 flux (data in quadrant 1 and quadrant 3 in Fig. 11d). One typical example is the results during days 91 to 120 (data in quadrant 3 in Fig. 11d): the strong preceding autotrophic production during days 61 to 90 led to highly negative $\Delta p\text{CO}_{2\text{background}}$ ($-315.5 \text{ } \mu\text{atm}$ on day 90, Fig. 11c), which makes the water acted as a CO_2 sink during days 91 to 120 (Fig. 11b) when the *in situ* heterotrophic NCP increased $p\text{CO}_2$ during this time period (Fig. 11c).

- 删除了: combined effects of NCP and gas exchange resulted
- 删除了: 设置了格式
- 删除了: in constant decreases in DIC and $p\text{CO}_2$ during the
- 删除了: difference in their
- 删除了: 设置了格式
- 删除了: 设置了格式
- 删除了: s (Fig. 10f)... and, more importantly to
- 删除了: 设置了格式
- 删除了: 设置了格式
- 删除了: (Fig. 2).
- 删除了: 设置了格式
- 删除了: Run-2
- 删除了: 设置了格式
- 删除了: Run-2
- 删除了: 设置了格式
- 删除了: varied with time: NCP was
- 删除了: 设置了格式
- 删除了: ;
- 删除了: 设置了格式
- 删除了: ;
- 删除了: 设置了格式
- 删除了: ;
- 删除了: 设置了格式
- 删除了: T
- 删除了: 设置了格式
- 删除了: 设置了格式
- 删除了: NCP^{weighted}
- 删除了: 设置了格式
- 删除了: equals the O_2 bioflux ...lagged a few days behind
- 删除了: 设置了格式
- 删除了: ;
- 删除了: 设置了格式
- 删除了: Similar with Run-1, t
- 删除了: 设置了格式
- 删除了: flux
- 删除了: 设置了格式
- 删除了: changes with a time lag of a few days
- 删除了: 设置了格式
- 删除了: after each change in NCP
- 删除了: 设置了格式
- 删除了: 11c
- 删除了: 设置了格式
- 删除了: On the contrary, However,
- 删除了: 设置了格式
- 删除了: and the lingering background $p\text{CO}_2$
- 删除了: 设置了格式
- 删除了: NCP
- 删除了: 设置了格式

In summary, the decoupling between NCP and CO₂ flux can be the result of competing effect of $\Delta p\text{CO}_{2\text{background}}$ and $\Delta p\text{CO}_{2\text{NEP}}$. In our observation, surface waters with oversaturated $p\text{CO}_2$ and positive NCP_{O₂Ar} (data in quadrant 1 in Fig. 10) were observed directly outside of the Mississippi River mouth. This is the region where *in situ* autotrophic biological productivity began to increase due to the alleviated light limitation, but the highly heterotrophic, $\Delta p\text{CO}_{2\text{background}}$ from the river channel made the water still acted as a CO₂ source. Decoupling was also observed in the HTACW where CO₂ uptake occurred under heterotrophic condition (data in quadrant 3 in Fig. 10). As discussed above, this phenomenon can be explained by *in situ* heterotrophy superimposed on surface water with low background $p\text{CO}_2$ resulting from the preceding autotrophic biological production.

Conclusions

During a spring cruise in the northern Gulf of Mexico in April 2017, we found encouraging agreement among NCP estimates from multiple approaches despite the different temporal and spatial resolutions and uncertainties associated with each approach. Our study showed that the DO incubation method represents the daily NCP by the local plankton community while the O₂/Ar method reflects the metabolic state of the water relating to both biological and physical processes over longer time scales. The DO incubation method may significantly overestimate NCP rates for high-turbidity water samples due to the improved light environment in the incubation bottles resulting from the settling of particles. The O₂/Ar method has the advantage being able to provide high-resolution NCP estimates matching the underway $p\text{CO}_2$ measurement, which provides more accurate estimation of the overall metabolic condition of the surface water of the nGOM and also allows a better examination on the NCP and CO₂ dynamics. The NCP_{O₂Ar} and CO₂ flux showed higher spatial variability on the inner and middle shelf which was strongly influenced by the Mississippi-Atchafalaya River system. Along the river-ocean mixing gradient, NCP_{O₂Ar} and CO₂ flux were characterized by 1) heterotrophy and CO₂ release at low salinities resulting from the decomposition of terrestrial carbon and light limitation on photosynthesis, 2) strong autotrophy and CO₂ uptake at intermediate salinities of 15-30 where light and nutrient are both favourable for phytoplankton growth, 3) close-to-zero NCP rate and CO₂ flux in the offshore seawater resulting from nutrient limitation. This study also demonstrated that, due to the slow air-sea CO₂ exchange and the buffering effect of the carbonate system, decoupling between NCP and CO₂ flux could be

- 删除了: is a
- 删除了: the competing effect of $\Delta p\text{CO}_{2\text{background}}$ and $\Delta p\text{CO}_{2\text{NEP}}$ in F...
- 设置了格式
- 设置了格式
- 删除了:
- 设置了格式
- 删除了: offshore
- 设置了格式
- 删除了: Southwest PassRiver mouth (data in quadrant 1 in Fig. 9)
- 设置了格式
- 删除了: . However
- 设置了格式
- 删除了: background $p\text{CO}_2$
- 设置了格式
- 删除了: AnotherDecoupling case of decoupling between NCP and
- 设置了格式
- 删除了: s (data in quadrant 3 in Fig. 9
- 设置了格式
- 删除了: benthic respiration-induced
- 设置了格式
- 删除了: advection of
- 设置了格式
- 删除了: (indicated by the negative values of $\Delta\text{DIC}_{\text{NCP}}$ and ANO_s
- 删除了: norther
- 设置了格式
- 删除了: different each approaches
- 设置了格式
- 删除了: high high-resolution NCP NCP
- 设置了格式
- 删除了: coupling between NCP and CO₂ dynamics. ...he variabil
- 设置了格式
- 删除了: in
- 设置了格式
- 删除了: river River system. Along the river-ocean mixing gradien
- 设置了格式
- 删除了: availability of light generally determines the onset of the
- 设置了格式
- 删除了: . The surface NCP is characterized by l
- 设置了格式
- 删除了: ow ...CP rate and CO₂ flux rates ...n the at both low-
- 设置了格式
- 删除了: Due to the differences in the gas exchange rates of CO₂ a
- 设置了格式

observed as the competing result of *in situ* biological production and the lingering effect of background $p\text{CO}_2$ of the source water.

设置了格式: 字体: 倾斜

Acknowledgement

We thank the captain and crew of *RV Pelican* for their excellent work. We are grateful for the comments and suggestions from Isabel Seguro and the other anonymous reviewer which significantly improve the quality of this paper. This work was supported by the National Key Research and Development Program of China 2016YFA0601400, NSF OCE-1559279 and OCE-1760660. Zong-Pei Jiang and Junxiao Zhang acknowledge the support by China Scholar Council for supporting their one-year visit of the Cai laboratory during which the fieldwork was accomplished.

设置了格式: 字体颜色: 自动设置

带格式的: 标题 1, 行距: 单倍行距

设置了格式: 字体: 倾斜

设置了格式: 字体: (默认) Times New Roman, (中文) Times New Roman, 10 磅, 非加粗, 英语(英国)

References

- Álvarez, M., H. Sanleón-Bartolomé, T. Tanhua, L. Mintrop, A. Luchetta, C. Cantoni, K. Schroeder, and G. Civitarese. 2014. The CO_2 system in the Mediterranean Sea: a basin wide perspective, *Ocean Science*, **10**(1), 69-92.
- Bauer, J. E., W. J. Cai, P. A. Raymond, T. S. Bianchi, C. S. Hopkinson, and P. a. G. Regnier. 2013. The changing carbon cycle of the coastal ocean. *Nature* **504**: 61-70.
- Bianchi, T. S., S. F. Dimarco, J. H. Cowan, R. D. Hetland, P. Chapman, J. W. Day, and M. A. Allison. 2010. The science of hypoxia in the Northern Gulf of Mexico: A review. *Science of the Total Environment* **408**: 1471-1484.
- Borges, A. V., and G. Abril. 2011. Carbon dioxide and methane dynamics in estuaries, p. 119-161. *Treatise on estuarine and coastal science*. Academic Press.
- Brewer, P. G., and J. C. Goldman. 1976. Alkalinity changes generated by phytoplankton growth. *Limnology and Oceanography* **21**: 108-117.
- Cai, W. J. 2003. Riverine inorganic carbon flux and rate of biological uptake in the Mississippi River plume. *Geophysical Research Letters* **30**(2).
- Cai, W. J. 2011. Estuarine and coastal ocean carbon paradox: CO_2 sinks or sites of terrestrial carbon incineration? *Annual Review of Marine Science*, **3**: 123-145.
- Cai, W. J., M. H. Dai, and Y. C. Wang. 2006. Air-sea exchange of carbon dioxide in ocean margins: A province-based synthesis, *Geophysical Research Letters* **33**: L12603.
- Cai, W. J., X. P. Hu, W. J. Huang, M. C. Murrell, J. C. Lehrter, S. E. Lohrenz, W. C. Chou, W. D. Zhai, J. T. Hollibaugh, Y. C. Wang, P. S. Zhao, X. H. Guo, K. Gundersen, M. H. Dai, and G. C. Gong. 2011. Acidification of subsurface coastal

设置了格式: 字体颜色: 自动设置

删除了: (

删除了:),

删除了: , doi:10.5194/os-10-69-2014.

waters enhanced by eutrophication. *Nature Geoscience* **4**: 766-770.

Cassar, N., B. A. Barnett, M. L. Bender, J. Kaiser, R. C. Hamme, and B. Tilbrook. 2009. Continuous high-frequency dissolved O₂/Ar measurements by equilibrator inlet mass spectrometry. *Analytical Chemistry* **81**: 1855-1864.

Cassar, N., P. J. Difiore, B. A. Barnett, M. L. Bender, A. R. Bowie, B. Tilbrook, K. Petrou, K. J. Westwood, S. W. Wright, and D. Lefevre. 2011. The influence of iron and light on net community production in the Subantarctic and Polar Frontal Zones. *Biogeosciences* **8**: 227-237.

Cloern, J.E., Jassby, A.D., Patterns and scales of phytoplankton variability in estuarine-coastal ecosystems. *Estuaries Coasts* **33**, 230-241. 2010.

Castro-Morales, K., N. Cassar, D. R. Shoosmith, and J. Kaiser. 2013. Biological production in the Bellingshausen Sea from oxygen-to-argon ratios and oxygen triple isotopes. *Biogeosciences* **10**: 2273-2291.

Chen, C.-T. A., and A. V. Borges. 2009. Reconciling opposing views on carbon cycling in the coastal ocean: Continental shelves as sinks and near-shore ecosystems as sources of atmospheric CO₂. *Deep-Sea Research Part II-Topical Studies in Oceanography* **56**: 578-590.

Chen, C.-T. A., T.-H. Huang, Y.-H. Fu, Y. Bai, and X. He. 2012. Strong sources of CO₂ in upper estuaries become sinks of CO₂ in large river plumes. *Current Opinion in Environmental Sustainability* **4**: 179-185.

Chen, C. T. A., and D. P. Swaney. 2012. Terrestrial-ocean transfers of carbon and nutrient across the coastal boundary: Editorial overview. *Current Opinion in Environmental Sustainability* **4**: 159-161.

Chen, X., S. E. Lohrenz, and D. A. Wisenburg. 2000. Distribution and controlling mechanisms of primary production on the Louisiana–Texas continental shelf. *Journal of Marine Systems* **25**: 179-207.

Cooley, S. R., and P. L. Yager. 2006. Physical and biological contributions to the western tropical North Atlantic Ocean carbon sink formed by the Amazon River plume. *Journal of Geophysical Research-Oceans* **111**.

Craig, H., and T. Hayward. 1987. Oxygen supersaturation in the ocean: Biological versus physical contributions. *Science* **235**: 199-202.

Dagg, M., R. Benner, S. Lohrenz, and D. Lawrence. 2004. Transformation of dissolved and particulate materials on continental shelves influenced by large rivers: plume processes. *Continental Shelf Research* **24**: 833-858.

Demaster, D. J., W. O. Smith, D. M. Nelson, and J. Y. Aller. 1996. Biogeochemical processes in Amazon shelf waters: Chemical distributions and uptake rates of silicon, carbon and nitrogen. *Continental Shelf Research* **16**: 617-643.

Diaz, R. J., and R. Rosenberg. 2008. Spreading dead zones and consequences for marine ecosystems. *Science* **321**: 926-929.

Dickson, A. G., C. L. Sabine, and J. R. Christian. 2007. Guide to best practices for ocean CO₂ measurements. North Pacific Marine Science Organization (PICES).

Egleston, E. S., C. L. Sabine, and F. M. M. Morel. 2010. Revelle revisited: Buffer factors that quantify the response of ocean chemistry to changes in DIC and alkalinity. *Global Biogeochemical Cycles*, **24**.

Eppley, R. W., and B. J. Peterson. 1979. Particulate organic matter flux and planktonic new production in the deep ocean. *Nature* **282**: 677-680.

设置了格式: 字体:(默认) Times New Roman

设置了格式: 字体:(默认) Times New Roman, 加粗

设置了格式: 字体:(默认) Times New Roman

删除了:(

删除了:),

- Fennel, K., R. Hetland, Y. Feng, and S. Dimarco. 2011. A coupled physical-biological model of the Northern Gulf of Mexico shelf: model description, validation and analysis of phytoplankton variability. *Biogeosciences* **8**: 1881-1899.
- Garcia, H. E., and L. I. Gordon. 1992. Oxygen solubility in seawater: Better fitting equations. *Limnology and Oceanography* **37**: 1307-1312.
- Gattuso, J.-P., M. Frankignoulle, and R. Wollast. 1998. Carbon and carbonate metabolism in coastal aquatic ecosystems. *Annual Review of Ecology, Evolution, and Systematics* **29**: 405-434.
- Geider, R. J., and J. La Roche. 2002. Redfield revisited: variability of C:N:P in marine microalgae and its biochemical basis. *European Journal of Phycology* **37**: 1-17.
- Green, R. E., T. S. Bianchi, M. J. Dagg, N. D. Walker, and G. A. Breed. 2006. An organic carbon budget for the Mississippi River turbidity plume and plume contributions to air-sea CO₂ fluxes and bottom water hypoxia. *Estuaries and Coasts* **29**: 579-597.
- Guo, X., W.-J. Cai, W.-J. Huang, Y. Wang, F. Chen, M. C. Murrell, S. E. Lohrenz, L.-Q. Jiang, M. Dai, J. Hartmann, Q. Lin, and R. Culp. 2012. Carbon dynamics and community production in the Mississippi River plume. *Limnology and Oceanography* **57**: 1-17.
- Hamme, R. C., and S. R. Emerson. 2004. The solubility of neon, nitrogen and argon in distilled water and seawater. *Deep-Sea Research Part I-Oceanographic Research Papers* **51**: 1517-1528.
- Hodur, R. M. 1997. The Naval Research Laboratory's coupled ocean/Atmosphere Mesoscale Prediction System (COAMPS). *Monthly Weather Review* **125**: 1414-1430.
- Huang, W. J., W. J. Cai, R. M. Castelao, Y. C. Wang, and S. E. Lohrenz. 2013. Effects of a wind-driven cross-shelf large river plume on biological production and CO₂ uptake on the Gulf of Mexico during spring. *Limnology and Oceanography* **58**: 1727-1735.
- Huang, W. J., W. J. Cai, R. T. Powell, S. E. Lohrenz, Y. Wang, L. Q. Jiang, and C. S. Hopkinson. 2012. The stoichiometry of inorganic carbon and nutrient removal in the Mississippi River plume and adjacent continental shelf. *Biogeosciences* **9**: 2781-2792.
- Huang, W. J., W. J. Cai, Y. C. Wang, S. E. Lohrenz, and M. C. Murrell. 2015. The carbon dioxide system on the Mississippi River-dominated continental shelf in the northern Gulf of Mexico: 1. Distribution and air-sea CO₂ flux. *Journal of Geophysical Research-Oceans* **120**: 1429-1445.
- Jonsson, B. F., S. C. Doney, J. Dunne, and M. Bender. 2013. Evaluation of the Southern Ocean O₂/Ar-based NCP estimates in a model framework. *Journal of Geophysical Research-Biogeosciences* **118**: 385-399.
- Justić, D., N. N. Rabalais, R. Eugene Turner, and W. J. Wiseman. 1993. Seasonal coupling between riverborne nutrients, net productivity and hypoxia. *Marine Pollution Bulletin* **26**: 184-189.
- Kaiser, J., M. K. Reuer, B. Barnett, and M. L. Bender. 2005. Marine productivity estimates from continuous O₂/Ar ratio measurements by membrane inlet mass spectrometry. *Geophysical Research Letters* **32**.
- Laruelle, G. G., H. H. Durr, C. P. Slomp, and A. V. Borges. 2010. Evaluation of sinks and sources of CO₂ in the global

- coastal ocean using a spatially-explicit typology of estuaries and continental shelves. *Geophysical Research Letters* **37**.
- Laws, E. A. 1991. Photosynthetic quotients, new production and net community production in the open ocean. *Deep-Sea Research Part a-Oceanographic Research Papers* **38**: 143-167.
- Lawson, C. L., and R. J. Hanson. 1974. *Solving Least Squares Problems*. Prentice-Hall, Chapter 23, 161 pp.
- Lehrter, J. C., D. S. Ko, M. C. Murrell, J. D. Hagy, B. A. Schaeffer, R. M. Greene, R. W. Gould, and B. Penta (2013), Nutrient distributions, transports, and budgets on the inner margin of a river-dominated continental shelf, *Journal of Geophysical Research: Oceans*, **118**(10), 4822-4838.
- Lehrter, J. C., M. C. Murrell, and J. C. Kurtz. 2009. Interactions between freshwater input, light, and phytoplankton dynamics on the Louisiana continental shelf. *Continental Shelf Research* **29**: 1861-1872.
- Lohrenz, S. E., W.-J. Cai, F. Chen, X. Chen, and M. Tuel. 2010. Seasonal variability in air-sea fluxes of CO₂ in a river-influenced coastal margin. *Journal of Geophysical Research: Oceans* **115** (C10).
- Lohrenz, S. E., W. J. Cai, S. Chakraborty, K. Gundersen, and M. C. Murrell. 2014. Nutrient and carbon dynamics in a large river-dominated coastal ecosystem: the Mississippi-Atchafalaya River system. *Biogeochemical Dynamics at Major River-Coastal Interfaces: Linkages with Global Change*: 448-472.
- Lohrenz, S. E., M. J. Dagg, and T. E. Whitledge. 1990. Enhanced primary production at the plume oceanic interface of the Mississippi River. *Continental Shelf Research* **10**: 639-664.
- Lohrenz, S. E., G. L. Fahnenstiel, D. G. Redalje, G. A. Lang, X. G. Chen, and M. J. Dagg. 1997. Variations in primary production of northern Gulf of Mexico continental shelf waters linked to nutrient inputs from the Mississippi River. *Marine Ecology Progress Series* **155**: 45-54.
- Lohrenz, S. E., G. L. Fahnenstiel, D. G. Redalje, G. A. Lang, M. J. Dagg, T. E. Whitledge, and Q. Dortch. 1999. Nutrients, irradiance, and mixing as factors regulating primary production in coastal waters impacted by the Mississippi River plume. *Continental Shelf Research* **19**: 1113-1141.
- McKee, B. A., R. C. Aller, M. A. Allison, T. S. Bianchi, and G. C. Kineke. 2004. Transport and transformation of dissolved and particulate materials on continental margins influenced by major rivers: benthic boundary layer and seabed processes. *Continental Shelf Research* **24**: 899-926.
- Muller-Karger, F. E., R. Varela, R. Thunell, R. Luerssen, C. M. Hu, and J. J. Walsh. 2005. The importance of continental margins in the global carbon cycle. *Geophysical Research Letters* **32**(1): L01602.
- [Murrell, M. C., J. G. Campbell, J. D. Hagy III, and J. M. Caffrey. 2009. Effects of irradiance on benthic and water column processes in a Gulf of Mexico estuary: Pensacola Bay, Florida, USA. *Estuarine, Coastal and Shelf Science* 81: 501–512.](#)
- [Murrell, M. C., and J. C. Lehrter. 2011. Sediment and lower water column oxygen consumption in the seasonally hypoxic region of the Louisiana Continental Shelf. *Estuaries and Coasts*, 34, 912-924.](#)
- Murrell, M. C., R. S. Stanley, J. C. Lehrter, and J. D. Hagy. 2013. Plankton community respiration, net ecosystem

删除了: Liss, P. S., and L. Merlivat. 1986. Air-sea gas exchange rates: Introduction and synthesis. *In* P. Buat-Menard [ed.], *The role of air-sea exchange in geochemical cycling*. D. Reidel, Hingham, Mass.

- metabolism, and oxygen dynamics on the Louisiana continental shelf: Implications for hypoxia. *Continental Shelf Research* **52**: 27-38.
- Nicholson, D. P., R. H. R. Stanley, E. Barkan, D. M. Karl, B. Luz, P. D. Quay, and S. C. Doney. 2012. Evaluating triple oxygen isotope estimates of gross primary production at the Hawaii Ocean Time-series and Bermuda Atlantic Time-series Study sites. *Journal of Geophysical Research-Oceans* **117**.
- Ning, X. R., D. Vulot, Z. S. Liu, and Z. L. Liu. 1988. Standing stock and production of phytoplankton in the estuary of the Changjiang (Yangtze River) and the adjacent East China Sea. *Marine Ecology Progress Series* **49**: 141-150.
- Obenour, D. R., D. Scavia, N. N. Rabalais, R. E. Turner, and A. M. Michalak. 2013. Retrospective analysis of midsummer hypoxic area and volume in the Northern Gulf of Mexico, 1985–2011. *Environmental Science & Technology* **47**: 9808-9815.
- Pai, S.-C., G.-C. Gong, and K.-K. Liu. 1993. Determination of dissolved oxygen in seawater by direct spectrophotometry of total iodine. *Marine Chemistry* **41**: 343-351.
- Pierrot, D., E. Lewis, and D. W. R. Wallace (2006), MS Excel program developed for CO₂ system Calculations, ORNL/CDIAC-105a. Carbon Dioxide Information Analysis Center, Oak Ridge National Laboratory, US Department of Energy, Oak Ridge, TN, doi:10.3334/CDIAC/otg.CO2SYS_XLS_CDIAC105a.
- Rabalais, N. N., W. J. Cai, J. Carstensen, D. J. Conley, B. Fry, X. P. Hu, Z. Quinones-Rivera, R. Rosenberg, C. P. Slomp, R. E. Turner, M. Voss, B. Wissel, and J. Zhang. 2014. Eutrophication-driven deoxygenation in the coastal ocean. *Oceanography* **27**: 172-183.
- Rabalais, N. N., R. E. Turner, and W. J. Wiseman. 2002. Gulf of Mexico hypoxia, aka "The dead zone". *Annual Review of Ecology and Systematics* **33**: 235-263.
- Regnier, P., P. Friedlingstein, P. Ciais, F. T. Mackenzie, N. Gruber, I. A. Janssens, G. G. Laruelle, R. Lauerwald, S. Luyssaert, A. J. Andersson, S. Arndt, C. Arnosti, A. V. Borges, A. W. Dale, A. Gallego-Sala, Y. Godderis, N. Goossens, J. Hartmann, C. Heinze, T. Ilyina, F. Joos, D. E. Larowe, J. Leifeld, F. J. R. Meysman, G. Munhoven, P. A. Raymond, R. Spahni, P. Suntharalingam, and M. Thullner. 2013. Anthropogenic perturbation of the carbon fluxes from land to ocean. *Nature Geoscience* **6**: 597-607.
- Reuer, M. K., B. A. Barnett, M. L. Bender, P. G. Falkowski, and M. B. Hendricks. 2007. New estimates of Southern Ocean biological production rates from O₂/Ar ratios and the triple isotope composition of O₂. *Deep-Sea Research Part I-Oceanographic Research Papers* **54**: 951-974.
- Roberts, B. J., and S. M. Doty. 2015. Spatial and temporal patterns of benthic respiration and net nutrient fluxes in the Atchafalaya River Delta Estuary. *Estuaries and Coasts* **38**: 1918-1936.
- Sambrotto, R. N., G. Savidge, C. Robinson, P. Boyd, T. Takahashi, D. M. Karl, C. Langdon, D. Chipman, J. Marra, and L. Codispoti. 1993. Elevated consumption of carbon relative to nitrogen in the surface ocean. *Nature* **363**: 248-250.
- Sarmiento, J. L., and N. Gruber. 2006. *Ocean Biogeochemical Dynamics*. Princeton University Press.
- [Seguro, I., García, C. M., Papaspyrou, S., Gálvez, J. A., García-Robledo, E., Navarro, G., Soria-Piriz, S., Aguilar, V., Lizano,](#)

删除了: Nightingale, P. D., G. Malin, C. S. Law, A. J. Watson, P. S. Liss, M. I. Liddicoat, J. Boutin, and R. C. Upstill-Goddard. 2000. In situ evaluation of air-sea gas exchange parameterizations using novel conservative and volatile tracers. *Global Biogeochemical Cycles* **14**(1): 373-387. .

[O. G., Morales-Ramirez, A., and Corzo, A.: Seasonal changes of the microplankton community along a tropical estuary, *Regional Studies in Marine Science*, **2**, 189-202, 2015.](#)

Shadwick, E. H., B. Tilbrook, N. Cassar, T. W. Trull, and S. R. Rintoul. 2015. Summertime physical and biological controls on O₂ and CO₂ in the Australian Sector of the Southern Ocean. *Journal of Marine Systems* **147**: 21-28.

Sweeney, C., E. Gloor, A. R. Jacobson, R. M. Key, G. Mckinley, J. L. Sarmiento, and R. Wanninkhof. 2007. Constraining global air-sea gas exchange for CO₂ with recent bomb ¹⁴C measurements. *Global Biogeochemical Cycles* **21**(2): GB2015.

[Teeter, L., Hamme, R. C., Ianson, D., and Bianucci, L. \(2018\). *Accurate estimation of net community production from O₂/Ar measurements*, *Global Biogeochemical Cycles*, **32**, 1163–1181. <https://doi.org/10.1029/2017GB005874>](#)

Ternon, J. F., C. Oudot, A. Dessier, and D. Diverres. 2000. A seasonal tropical sink for atmospheric CO₂ in the Atlantic ocean: the role of the Amazon River discharge. *Marine Chemistry* **68**: 183-201.

Turner, R. E., and N. N. Rabalais. 2013. Nitrogen and phosphorus phytoplankton growth limitation in the northern Gulf of Mexico. *Aquatic Microbial Ecology* **68**: 159-169.

Turner, R. E., N. N. Rabalais, and D. Justic. 2012. Predicting summer hypoxia in the northern Gulf of Mexico: Redux. *Marine Pollution Bulletin* **64**: 319-324.

Ulfso, A., N. Cassar, M. Korhonen, S. Van Heuven, M. Hoppema, G. Kattner, and L. G. Anderson. 2014. Late summer net community production in the central Arctic Ocean using multiple approaches. *Global Biogeochemical Cycles* **28**: 1129-1148.

Wallace, R. B., H. Baumann, J. S. Gear, R. C. Aller, and C. J. Gobler. 2014. Coastal ocean acidification: The other eutrophication problem. *Estuarine Coastal and Shelf Science* **148**: 1-13.

[Weiss, R. F. 1974. Carbon dioxide in water and seawater: the solubility of a non-ideal gas, p. 203-215. *Marine Chemistry*.](#)

Wolf-Gladrow, D. A., R. E. Zeebe, C. Klaas, A. Kortzinger, and A. G. Dickson. 2007. Total alkalinity: The explicit conservative expression and its application to biogeochemical processes. *Marine Chemistry* **106**(1-2): 287-300.

Xue, J. H., W. J. Cai, X. P. Hu, W. J. Huang, S. E. Lohrenz, and K. Gundersen. 2015. Temporal variation and stoichiometric ratios of organic matter remineralization in bottom waters of the northern Gulf of Mexico during late spring and summer. *Journal of Geophysical Research-Oceans* **120**: 8304-8326.

Xue, Z., R. He, K. Fennel, W. J. Cai, S. Lohrenz, and C. Hopkinson. 2013. Modeling ocean circulation and biogeochemical variability in the Gulf of Mexico. *Biogeosciences* **10**: 7219-7234.

Xue, Z., R. Y. He, K. Fennel, W. J. Cai, S. Lohrenz, W. J. Huang, H. Q. Tian, W. Ren, and Z. C. Zang. 2016. Modeling pCO₂ variability in the Gulf of Mexico. *Biogeosciences* **13**: 4359-4377.

Yang, X. F., L. Xue, Y. X. Li, P. Han, X. Y. Liu, L. J. Zhang, and W. J. Cai. 2018. Treated wastewater changes the export of dissolved inorganic carbon and its isotopic composition and leads to acidification in coastal oceans. *Environmental Science & Technology* **52**: 5590-5599.

Zeebe, R. E., and D. Wolf-Gladrow (2001), CO₂ in seawater: Equilibrium, kinetics, isotopes., Elsevier, Amsterdam.

删除了:

删除了: Accurate estimation of net community production from O₂/Ar measurements

删除了: Wanninkhof, R. 1992. Relationship between wind-speed and gas-exchange over the ocean. *Journal of Geophysical Research-Oceans* **97**: 7373-7382. .

Zhang, X. Q., R. D. Hetland, M. Marta-Almeida, and S. F. Dimarco. 2012. A numerical investigation of the Mississippi and Atchafalaya freshwater transport, filling and flushing times on the Texas-Louisiana Shelf. *Journal of Geophysical Research-Oceans* **117**(C11).

Table

Table 1 The end member properties used in the three end-member mixing model.

End member	Salinity	TA ($\mu\text{mol kg}^{-1}$)	DIC ($\mu\text{mol kg}^{-1}$)	NO_x ($\mu\text{mol kg}^{-1}$)
Atchafalaya River	0	209	2128	113.14
Mississippi River	0	2314	2312	123.27
Gulf surface seawater	36.15	2407	2076	0.44

Figure

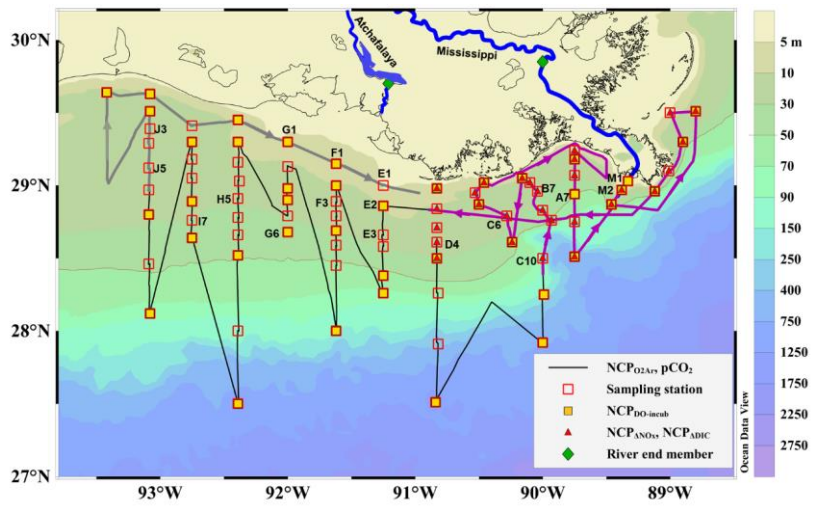


Fig. 1. Map and sampling sites in the northern Gulf of Mexico during the April 2017 cruise. The black dotted line is the cruise track along which the high-resolution underway measurements were made. The track in the Mississippi plume (purple line, 8-11 April) and in the Atchafalaya coastal regions (grey line, 15-17 April) are highlighted. Also shown are the 83 CTD sampling stations (hollow red squares), the 43 stations where light/dark bottle DO incubations were conducted (solid yellow squares), the 30 stations where non-conservative changes in DIC and NO_x were used to estimate NCP rates (solid red triangles), and the 2 stations where the properties of river end members were measured (solid green diamonds). The vertical CTD profiles of the labelled stations were shown in the supplement.

设置了格式: 字体颜色: 自动设置

设置了格式: 字体颜色: 自动设置

删除了: 0.58

删除了: .15

设置了格式: 字体颜色: 自动设置

设置了格式: 字体颜色: 自动设置

设置了格式: 字体颜色: 自动设置

删除了: .43

删除了: .28

设置了格式: 字体颜色: 自动设置

设置了格式: 字体颜色: 自动设置

设置了格式: 字体颜色: 自动设置

删除了: 6.98

设置了格式: 字体颜色: 自动设置

删除了: .34

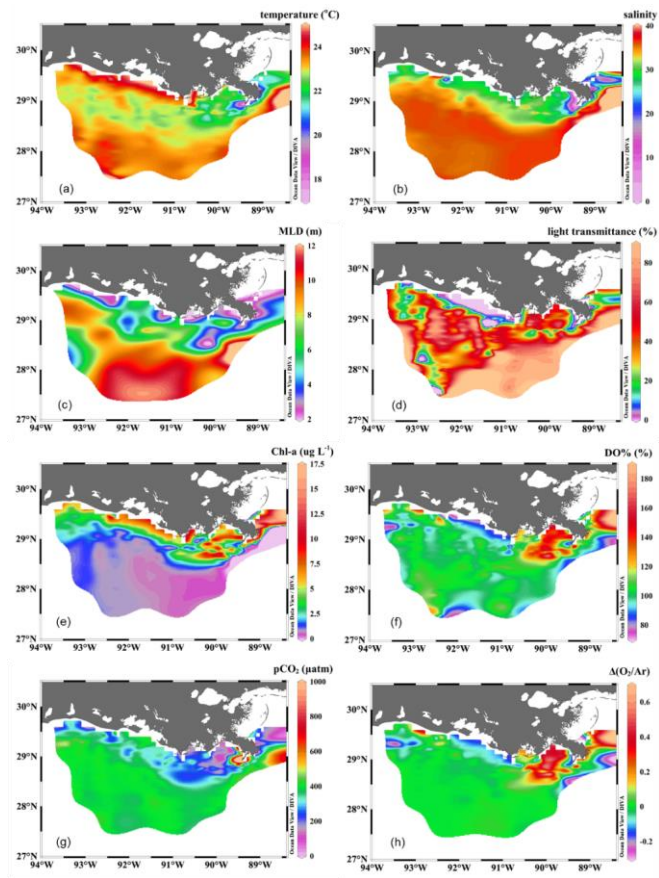


Fig. 2. The distribution of (a) temperature, (b) salinity, (c) mixed layer depth (MLD), (d) light transmittance, (e) chlorophyll-a concentration (Chl-a), (f) oxygen saturation percentage (DO%), (g) partial pressure of CO₂ (pCO₂), and (h) biological-induced oxygen supersaturation ($\Delta O_2/Ar$) in the surface water of the nGOM.

带格式的: 行距: 2 倍行距

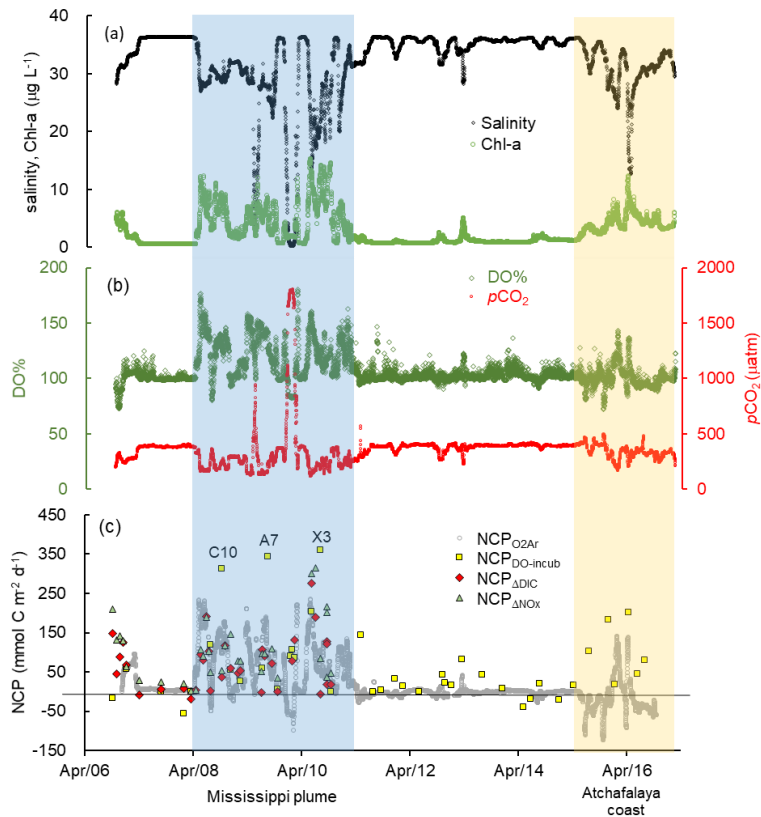


Fig. 3. The underway measurements of (a) salinity and Chl-a, (b) DO% and $p\text{CO}_2$, and (c) NCP rates estimated from the O_2/Ar measurement ($\text{NCP}_{\text{O}_2/\text{Ar}}$, grey circles). Also shown in panel c are the NCP rates estimated from the light/dark DO incubation ($\text{NCP}_{\text{DO-incub}}$, yellow squares), non-conservative changes in DIC ($\text{NCP}_{\Delta\text{DIC}}$, red diamonds) or NO_x ($\text{NCP}_{\Delta\text{NO}_x}$, green triangles). See Figure 1 for the cruise track in the Mississippi plume (8-11 April) and Atchafalaya coast (15-17 April). See Figure 5 for the positions of stations C10, A7, and X3 in the Mississippi plume.

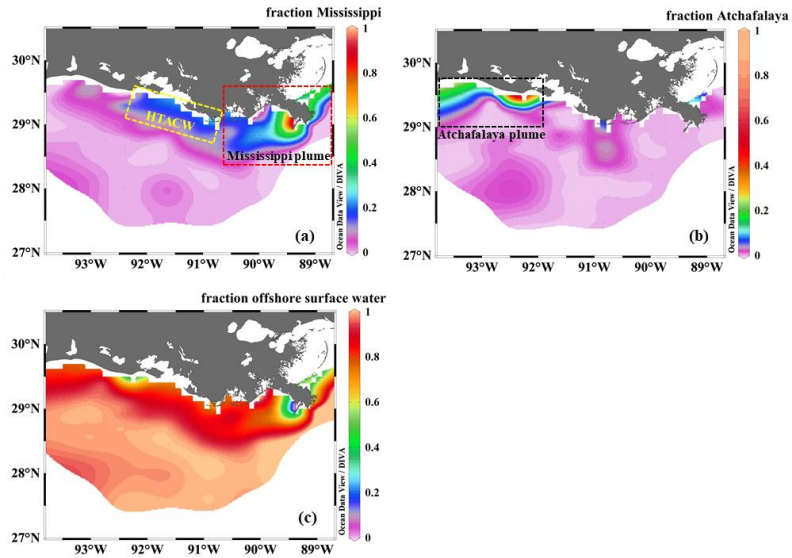


Fig. 4. The fractional contribution of (a) the Mississippi River, (b) the Atchafalaya River, and (c) offshore surface water to the surface water of the nGOM estimated from the three end-member mixing model. The sub-regions shown in panels (a) and (b) are the Mississippi plume, the high-turbidity Atchafalaya coastal water (HTACW), and the Atchafalaya plume.

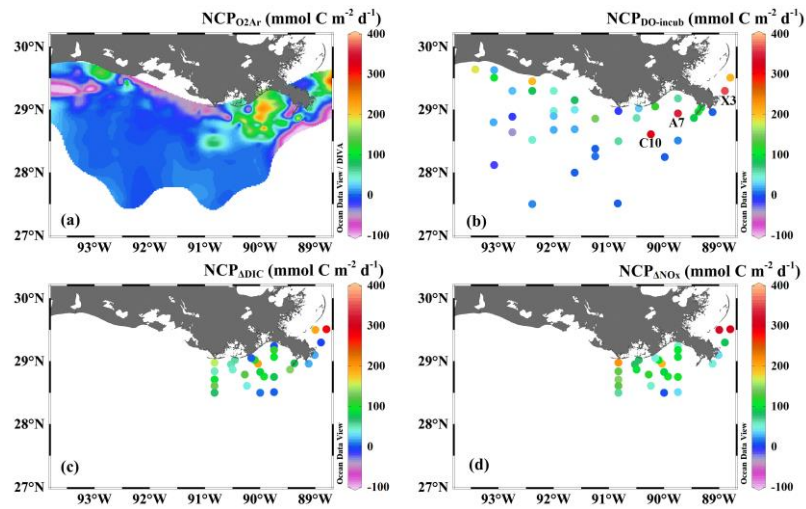


Fig. 5. The spatial variability of (a) $\text{NCP}_{\text{O}_2\text{Ar}}$, (b) $\text{NCP}_{\text{DO-incub}}$, (c) NCP_{ADIC} , and (d) $\text{NCP}_{\text{ANO}_x}$. Noted that NCP_{ADIC} and $\text{NCP}_{\text{ANO}_x}$ were only estimated in the Mississippi plume (panels c, d).

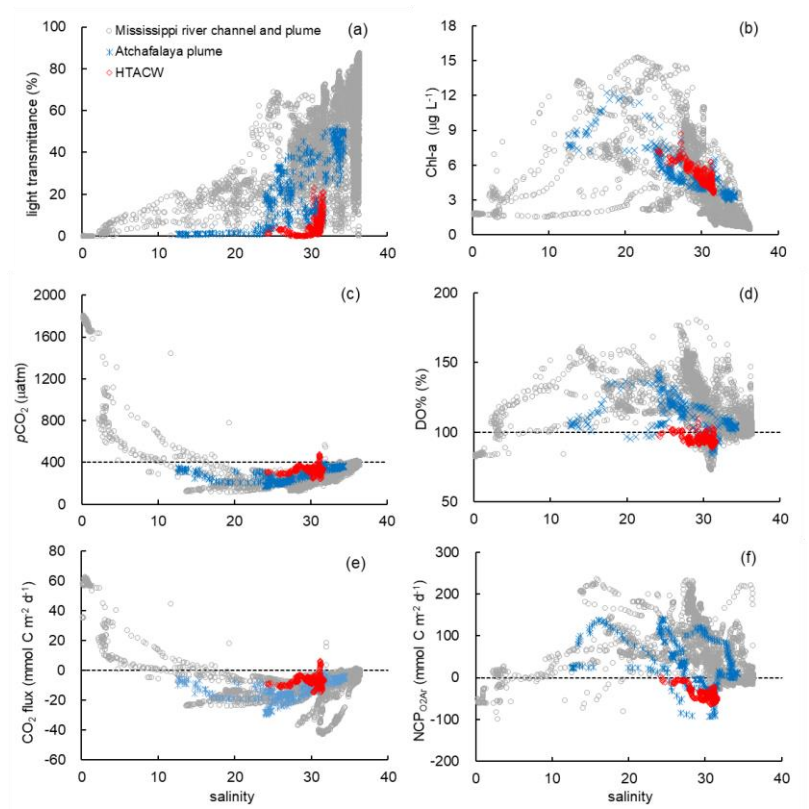


Fig. 6. The distribution of (a) light transmittance, (b) Chl-a, (c) $p\text{CO}_2$, (d) DO%, (e) CO_2 flux, and (f) $\text{NCP}_{\text{O}_2\text{A}_4}$ along the salinity gradient in different sub-regions. The dash lines in panels c to f are the atmospheric $p\text{CO}_2$ (405 μatm), DO% of 100 %, zero CO_2 flux, and zero $\text{NCP}_{\text{O}_2\text{A}_4}$ respectively.

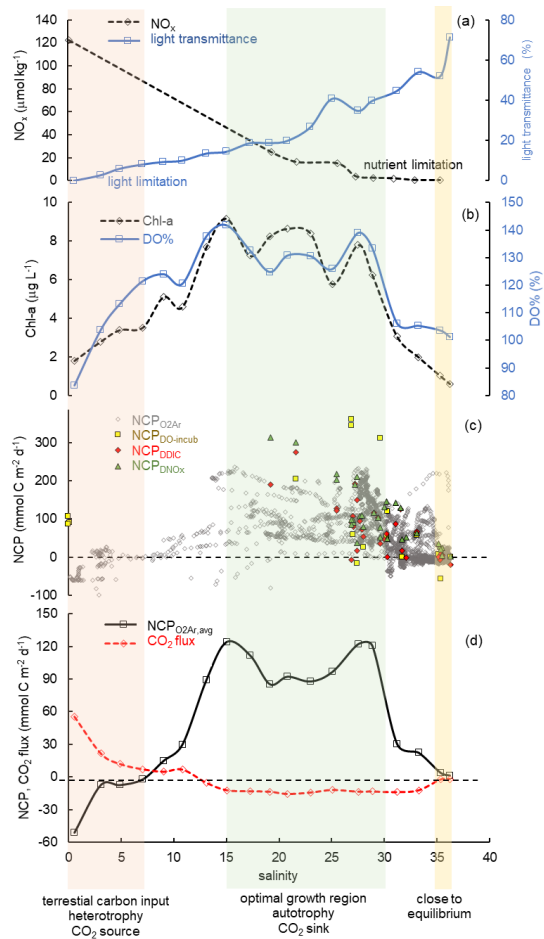


Fig. 7. The distribution of (a) NO₃⁻ and light transmittance, (b) Chl-a and DO%, (c) NCP estimated from various methods, and (d) NCP_{O₂Ar} and CO₂ flux along the salinity gradient in the Mississippi plume. Data in panels (a), (b), and (d) were averaged over increments of two salinity units.

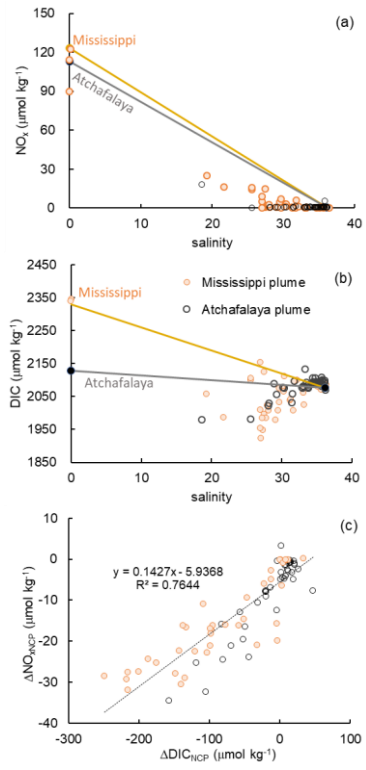


Fig. 8. Scatter plots of (a) DIC and salinity, (b) NO_x and salinity, and (c) the non-conservative changes in DIC ($\Delta\text{DIC}_{\text{NCP}}$) and NO_x ($\Delta\text{NO}_x_{\text{NCP}}$) in the Mississippi and Atchafalaya plumes. The end member concentrations of the Mississippi river, the Atchafalaya River, and offshore gulf surface water are shown in panels (a) and (b) together with the conservative mixing lines.

删除了: NCP

删除了: NCP

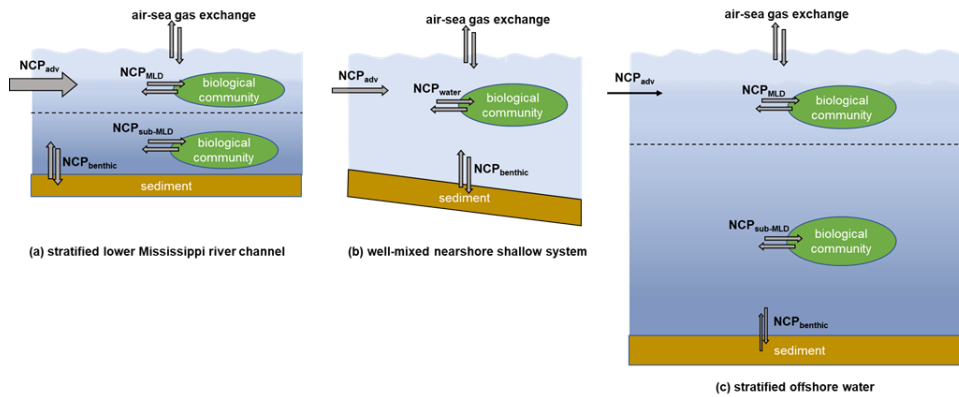


Fig. 9. The differences in water column mixing conditions in the nGOM and their influences on NCP estimation. The dotted lines in panels (a) and (c) indicate the mixed layer depth. In the stratified lower Mississippi River channel (a) and the offshore stratified system (c), $NCP_{DO-incub}$ equals the *in situ* community production in the mixed layer (NCP_{MLD}), while NCP_{O_2Ar} reflects the combined result of the NCP_{MLD} and the influence of lateral advection of the river water (NCP_{adv}). In the nearshore well-mixed shallow system (b), $NCP_{DO-incub}$ equals the water column community production (NCP_{water}), while NCP_{O_2Ar} reflects the combined result of NCP_{water} , $NCP_{benthic}$, and NCP_{adv} . Note that the influence of NCP_{adv} decreases offshore with the increasing water residence time.

设置了格式: 下标

设置了格式: 字体: 小五

设置了格式: 字体: 倾斜

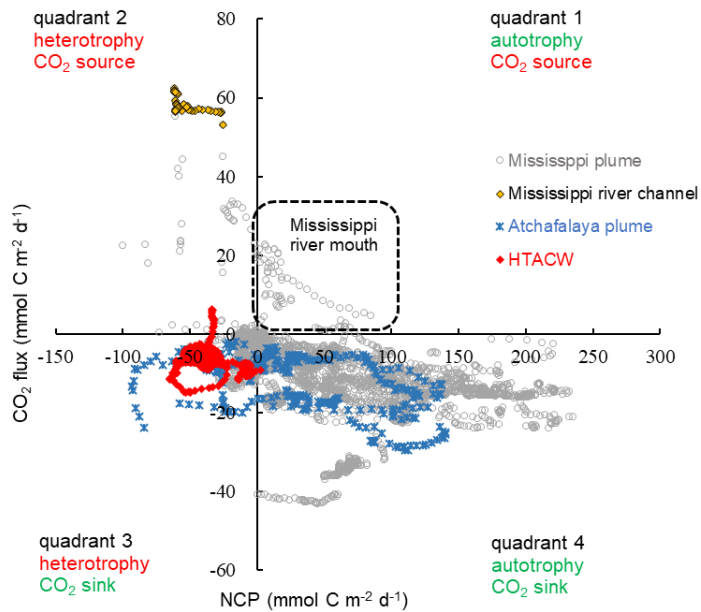


Fig. 10. Scatter plot of $NCP_{O_2A_r}$ and CO_2 flux observed in the surface water of the nGOM. Positive NCP implies net autotrophy and negative CO_2 flux implies net oceanic CO_2 uptake from the atmosphere.

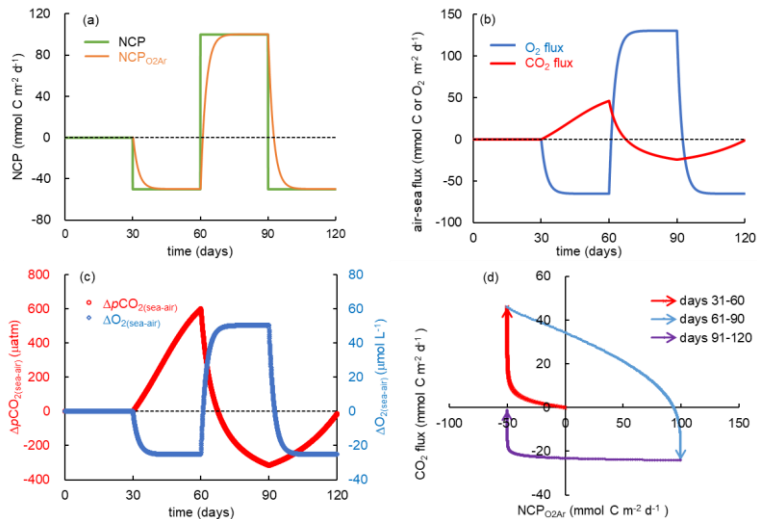
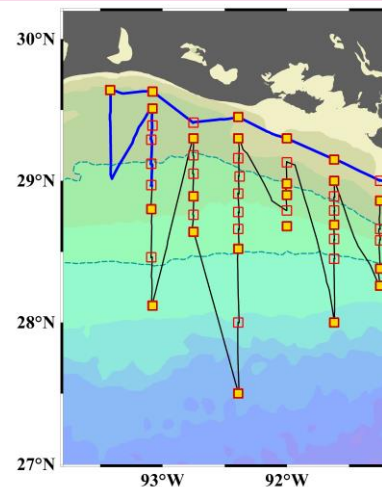


Fig. 11. Simulation of carbon and oxygen dynamics responding to time-dependent varying NCP rates and gas exchange using a 1-D model.

The variations of (a) NCP and exponentially weighted NCP (NCP_{O2Ar}), (b) air-sea CO_2 flux and O_2 flux, and (c) air-sea pCO_2 difference ($\Delta \text{pCO}_2(\text{sea-air})$) and O_2 difference ($\Delta \text{O}_2(\text{sea-air})$). (d) Scatter plot of CO_2 flux and NCP_{O2Ar} . Positive NCP implies net autotrophy and negative O_2 and CO_2 fluxes implies gas influxes into the water. See the text for details.

设置了格式: 下标



删除了:

Figure 1: The underway measurements (black lines), sampling stations (red squares), stations where light/dark bottle DO incubations were conducted (yellow squares), and stations where non-conservative changes in DIC and NO₃ were used to estimate net community production (NCP) rates in the Mississippi plume (red triangles). The 20 m and 50 m isobaths are highlighted, as well as the cruise track in the Mississippi plume (purple, Apr. 8-10) and the Atchafalaya coast (blue, Apr. 15-17).

分页符

设置了格式: 字体颜色: 自动设置

设置了格式: 字体颜色: 自动设置

设置了格式: 字体颜色: 自动设置